

SIMULATING OIL RECOVERY DURING CO<sub>2</sub> SEQUESTRATION  
INTO A MATURE OIL RESERVOIR

A THESIS SUBMITTED TO  
THE GRADUATE SCHOOL OF NATURAL AND APPLIED SCIENCES  
OF  
MIDDLE EAST TECHNICAL UNIVERSITY

BY

YUSUF ZİYA PAMUKÇU

IN PARTIAL FULFILLMENT OF THE REQUIREMENTS  
FOR  
THE DEGREE OF MASTER OF SCIENCE  
IN  
PETROLEUM AND NATURAL GAS ENGINEERING

August 2006

Approval of the Graduate School of Natural and Applied Sciences

---

Prof. Dr. Canan ÖZGEN  
Director

I certify that this thesis satisfies all the requirements as a thesis for the degree of Master of Science.

---

Prof. Dr. Mahmut PARLAKTUNA  
Head of Department

This is to certify that we have read this thesis and that in our opinion it is fully adequate, in scope and quality, as a thesis for the degree of Master of Science.

---

Prof. Dr. Fevzi GÜMRAH  
Supervisor

**Examining Committee Members**

Prof. Dr. Mahmut PARLAKTUNA (METU, PETE) \_\_\_\_\_

Prof. Dr. Fevzi GÜMRAH (METU, PETE) \_\_\_\_\_

Prof. Dr. Nurkan KARAHANOĞLU (METU, GEOE) \_\_\_\_\_

Mrs. İlhan TOPKAYA, MSc. (TPAO) \_\_\_\_\_

Mr. Uğur KARABAKAL, MSc. (TPAO) \_\_\_\_\_

I hereby declare that all information in this document has been obtained and presented in accordance with academic rules and ethical conduct. I also declare that, as required by these rules and conduct, I have fully cited and referenced all material and results that are not original to this work.

Yusuf Ziya PAMUKÇU

# ABSTRACT

SIMULATING OIL RECOVERY DURING CO<sub>2</sub> SEQUESTRATION  
INTO A MATURE OIL RESERVOIR

PAMUKÇU, Yusuf Ziya

M.S., Department of Petroleum and Natural Gas Engineering

Supervisor: Prof. Dr. Fevzi GÜMRAH

August 2006, 102 pages

The continuous rising of anthropogenic emission into the atmosphere as a consequence of industrial growth is becoming uncontrollable, which causes heating up the atmosphere and changes in global climate. Therefore, CO<sub>2</sub> emission becomes a big problem and key issue in environmental concerns.

There are several options discussed for reducing the amount of CO<sub>2</sub> emitted into the atmosphere. CO<sub>2</sub> sequestration is one of these options, which involves the capture of CO<sub>2</sub> from hydrocarbon emission sources, e.g. power plants, the injection and storage of CO<sub>2</sub> into deep geological formations, e.g. depleted oil reservoirs. The complexity in the structure of geological formations and the processes involved in this method necessitates the use of numerical simulations in revealing the potential problems, determining feasibility, storage capacity, and life span credibility.

Field K having 32° API gravity oil in a carbonate formation from southeast Turkey was studied. Field K was put on production in 1982 and produced until 2006, which was very close to its economic lifetime. Thus, it was considered as a candidate for enhanced oil recovery and CO<sub>2</sub> sequestration.

Reservoir rock and fluid data was first interpreted with available well logging, core and drill stem test data. Monte Carlo simulation was used to evaluate the probable reserve that was 7 million STB, original oil in place (OOIP). The data were then merged into CMG/STARS simulator. History matching study was done with production data to verify the results of the simulator with field data. After obtaining a good match, the different scenarios were realized by using the simulator.

From the results of simulation runs, it was realized that CO<sub>2</sub> injection can be applied to increase oil recovery, but sequestering of high amount of CO<sub>2</sub> was found out to be inappropriate for field K. Therefore, it was decided to focus on oil recovery while CO<sub>2</sub> was sequestered within the reservoir. Oil recovery was about 23% of OOIP in 2006 for field K, it reached to 43 % of OOIP by injecting CO<sub>2</sub> after defining production and injection scenarios, properly.

Keywords: Carbon Dioxide (CO<sub>2</sub>), Depleted Oil Reservoir, Sequestration, Enhanced Oil Recovery (EOR), Simulation, CMG/STARS

# ÖZ

## KARBON DİOKSİTİN TÜKETİLMİŞ PETROL REZERVUARINA TECRİDİNDE PETROL ÜRETİMİNİN MODELLENMESİ

PAMUKÇU, Yusuf Ziya

Yüksek Lisans, Petrol ve Doğal Gaz Mühendisliği Bölümü

Tez Yöneticisi: Prof. Dr. Fevzi GÜMRAH

Ağustos 2006, 102 sayfa

Endüstrinin gelişmesiyle birlikte atmosferde oluşan emisyon gazları miktarı kontrol edilemez bir şekilde artmakta ve neticede atmosferin ısınmasına ve küresel iklim değişikliğine sebep olmaktadır. Bundan dolayı, CO<sub>2</sub> emisyonu çevre sorunlarında anahtar konu ve büyük problem durumundadır.

Atmosfere salınan CO<sub>2</sub> miktarını azaltmak için farklı çözümler önerilmiştir. CO<sub>2</sub> tecridi bunlardan birisi olarak, CO<sub>2</sub>'nin termik santraller ve benzeri yerlerde kaynağında tutulması, taşınması ve tükenmiş petrol sahaları gibi derin jeolojik ortamlarda depolanmasını içermektedir. Jeolojik ortamların ve akış proseslerinin kompleks yapıya sahip olması nedeniyle, simülasyon kullanımı depolama kapasitesi, fizibilite çalışmasının yapılması ve problemlerin çözümünde gereklidir.

Bu alıřmada Trkiye'nin gneydoęu blgesinde 32° API gravite ile karbonat formasyonundan petrol reten K sahası ele alındı. K sahası 1982 ile 2006 yılları arasında petrol retmiř ve artık ekonomik mrne ok yakındır. Bu yzden petrol kurtarımı ve CO<sub>2</sub> tecridi iin uygun olabileceęi dřnld.

İlk olarak, sahaya ait kuyu logları, karot ve kuyu testleri deęerlendirilip, rezervuar kaya ve akıřkan verileri elde edildi. Monte Carlo simulasyonu kullanılarak olası rezerv hesabı yapıldı ve yerinde petrol miktarı 7 MMSTB olduęu tahmin edildi. Elde edilen veri, CMG/STARS simlatrne aktarıldı ve retim verileri doęrultusunda tarihsel eřleřtirme yapılarak simlasyon ve saha verisi arasındaki benzerlik ortaya konuldu. Saha verileri ile simulator sonuları arasında bařarılı bir eřleřme saęlandıktan sonra yeni senaryolar geliřtirildi.

Senaryolarda elde edilen sonular K sahasının CO<sub>2</sub> tecridine uygun olmadığını ancak petrol kurtarımı iin elverişli olduęunu gsterdi. Bu nedenle petrol kurtarımı daha detaylı incelendi. 2006 yılına kadar yerinde petrol miktarının %23' retilmiřtir, bu tarihten sonra geliřtirilen retim ve enjeksiyon senaryolarıyla bu oran %43'e ykseltildi.

Anahtar kelimeler: Karbon Dioksit (CO<sub>2</sub>), Tkenmiř Petrol Rezervuarı, Tecrid, Geliřtirilmiř Petrol Kurtarımı (EOR), Modelleme, CMG/STARS.

To My Family

# ACKNOWLEDGEMENTS

I would like to express my sincere gratitude to my supervisor Prof. Dr. Fevzi Gümrah for his guidance, advice, criticism, encouragements and insight throughout the research.

I would like to express my gratitude to my family and my friends for their generous attitude and support.

I would like to express my gratitude to Faculty of Engineering for enrolling me as a research assistant at Middle East Technical University (METU).

I would like to thank National Oil & Gas Company of Turkey (TPAO) for supplementing field data.

I would also like to thank Computer Modelling Group (CMG) for providing the software.

# TABLE OF CONTENTS

Plagiarism .....	iii
Abstract .....	iv
Öz.....	vi
Dedication .....	viii
Acknowledgements.....	ix
List of Tables .....	xiii
List of Figures .....	xv
Abbreviations and Acronyms .....	xxi
Chapters	
Chapter 1: Introduction.....	1
Chapter 2: Literature Review .....	4
2.1 Effects of Greenhouse Gases on Climate Change.....	4
2.2 CO <sub>2</sub> Sequestering in Underground Geological Media.....	10
2.2.1 The Capture and Transportation of CO <sub>2</sub> .....	10
2.2.2 CO <sub>2</sub> Storage Options in Underground Medium .....	12
2.2.2.1 Nonporous Medium.....	12
2.2.2.1.1 Deep Ocean (Hydrates).....	12
2.2.2.1.2 Salt Cavern .....	13
2.2.2.2 Porous Medium.....	14
2.2.2.2.1 Aquifer (deep saline).....	15
2.2.2.2.2 Depleted Oil and Gas Reservoirs .....	16

2.2.2.2.3 Enhanced Coal Bed Methane .....	17
2.2.3 Cost of CO <sub>2</sub> Sequestration .....	17
2.3 Oil Recovery by CO <sub>2</sub> Injection .....	18
2.3.1 Miscible vs. Immiscible CO <sub>2</sub> Flooding .....	19
2.3.2 Carbon Dioxide as a Displacement Fluid .....	21
2.3.3 Oil Recovery Mechanisms by CO <sub>2</sub> Injection .....	24
2.3.4 Ongoing CO <sub>2</sub> projects .....	25
2.3.4.1 Bati Raman Immiscible CO <sub>2</sub> Flooding Project.....	27
Chapter 3: Statement of the Problem .....	28
Chapter 4: Method of Solution .....	29
4.1 Softwares Utilized .....	29
4.1.1 STARS Simulator by CMG .....	29
4.1.2 SURFER by Golden Software .....	31
4.1.3 SAPHIR by Kappa Engineering .....	31
4.1.4 @RISK by Palisade Corporation.....	31
4.2 History Matching .....	32
Chapter 5: Field Description.....	33
Chapter 6: Results and Discussion.....	36
6.1 Evaluation of General Reservoir Characteristics.....	36
6.1.1 Reservoir Pressure and MMP .....	36
6.1.2 Porosity and Water Saturation .....	37
6.1.3 Permeability .....	41
6.1.4 Relative Permeability .....	42
6.2 Reserve Estimation.....	44

6.3 Description of the Reservoir Model .....	46
6.4 Simulation Runs.....	48
6.4.1 Run 1: History Matching .....	51
6.4.2 Run 2: Field Production Continued (Base Run).....	54
6.4.3 Run 3: CO <sub>2</sub> Sequestration (SEQ.).....	57
6.4.4 Run 4: CO <sub>2</sub> EOR/SEQ .....	59
6.4.5 Run 5: CO <sub>2</sub> EOR/SEQ .....	66
6.4.6 Run 6: Field Development & CO <sub>2</sub> EOR/SEQ .....	73
Chapter 7: Conclusions .....	81
References .....	84
Appendices	
Appendix A.....	91
A.1 Drill Stem Test (DST) Results .....	91
A.2 Calculating Minimum Miscibility Pressure (MMP) .....	93
A.3 Well Logging Interpretation Results.....	95
Appendix B.....	99
B.1 Monte Carlo Simulation Results.....	99

## LIST OF TABLES

Table 2.1 World CO <sub>2</sub> emissions (Mtc) by carbon-based fuels in 1990 and 1998 [10] .....	6
Table 2.2 Direct greenhouse gas emissions by sectors between 1990 and 2010 in Turkey (%) [13] .....	9
Table 2.3 Estimated storage capacities of geologic formations (GtCO <sub>2</sub> ) [7] .....	15
Table 2.4 Current and planned carbon capture and storage projects [39] .....	26
Table 5.1 Summary of field properties .....	35
Table 6.1 Summary of well logging interpretation, field K.....	39
Table 6.2 Comparison of reserve estimation methods .....	45
Table 6.3 OOIP results of field K by probabilistic estimation .....	46
Table 6.4 Summary of simulation runs.....	48
Table 6.5 Comparison of simulations, Run 4, CO <sub>2</sub> EOR/SEQ .....	61
Table 6.6 Comparison of simulations, Run 5, CO <sub>2</sub> EOR/SEQ .....	67
Table 6.7 Cumulative oil and gas (CO <sub>2</sub> ) productions, Run5, CO <sub>2</sub> EOR/SEQ .....	67
Table 6.8 Comparison of simulation, Run 6, field development & CO <sub>2</sub> /EOR SEQ.....	74
Table A.1 DST Input Data (1946-1963 m).....	91
Table A.2 Results from DST data by SAPHIR program.....	92
Table B.1 Summary statistics of Monte Carlo simulation.....	102

# LIST OF FIGURES

Figure 2.1 Changes in global mean surface temperatures since 1856 [9].	4
Figure 2.2 Greenhouse gases and their emissions in the U.S. between 1990 and 1998 [8] .....	5
Figure 2.3 Direct greenhouse gas emissions between 1970 and 2010 in Turkey [13] .....	8
Figure 2.4 Phase diagram of CO <sub>2</sub> [37].....	22
Figure 2.5 Variation of CO <sub>2</sub> density as a function of temperature and pressure [38].....	23
Figure 2.6 Variation of CO <sub>2</sub> viscosity as a function of temperature and pressure [38].....	23
Figure 2.7 Location of sites where activities relevant to CO <sub>2</sub> storage are planned or under way [39].....	26
Figure 5.1 Top of formation D structural contour Map of field K.....	34
Figure 6.1 Porosity vs. liquid permeability from core data .....	38
Figure 6.2 Porosity map of zone B .....	40
Figure 6.3 Water Saturation map of zone B .....	40
Figure 6.4 Thickness map of zone B.....	41
Figure 6.5 Permeability map of zone B.....	42
Figure 6.6 Relative permeability curves for oil and water, field K.....	43
Figure 6.7 Relative permeability curves for oil and gas, field K.....	43
Figure 6.8 Probability density function of field K reserve .....	45
Figure 6.9 2D structural map of field K showing boundary conditions and fault locations (subsea depths in m) .....	47
Figure 6.10 3D view of reservoir with well locations .....	47

Figure 6.11 Oil production rates of the wells, Run 1, history matching .....	52
Figure 6.12 Cumulative water production comparison between the field data and simulator results, Run 1, history matching.....	52
Figure 6.13 Well bottom-hole pressures of the wells, Run 1, history matching .....	53
Figure 6.14 Field production summary after primary depletion, Run 1, history matching .....	54
Figure 6.15 Location of production wells, Run2, field production continued .....	55
Figure 6.16 Oil production rates of the wells, Run 2, field production continued .....	55
Figure 6.17 Well bottom-hole pressures of the wells, Run 2, field production continued .....	56
Figure 6.18 Field production summary, Run 2, field production continued .	56
Figure 6.19 Location of injection wells, Run3, CO <sub>2</sub> SEQ .....	58
Figure 6.20 Well bottom hole pressure and CO <sub>2</sub> injection rate of Well K1, Run 3, CO <sub>2</sub> SEQ.....	58
Figure 6.21 Field injection summary, Run 3, CO <sub>2</sub> SEQ.....	59
Figure 6.22 Location of injection and production wells, Run4, CO <sub>2</sub> EOR/SEQ .....	60
Figure 6.23 Oil production rate of the well K2, Run 4a, CO <sub>2</sub> /EOR SEQ .....	61
Figure 6.24 Oil production rate of the well K2, Run 4b, CO <sub>2</sub> /EOR SEQ .....	62
Figure 6.25 Oil production rate of the well K2, Run 4c, CO <sub>2</sub> /EOR SEQ .....	62
Figure 6.26 Well bottom hole pressure and CO <sub>2</sub> injection rate of Well K5, Run 4a, CO <sub>2</sub> EOR/SEQ.....	63
Figure 6.27 Well bottom hole pressure and CO <sub>2</sub> injection rate of Well K5, Run 4b, CO <sub>2</sub> EOR/SEQ.....	63

Figure 6.28 Well bottom hole pressure and CO <sub>2</sub> injection rate of Well K5, Run 4c, CO <sub>2</sub> EOR/SEQ.....	64
Figure 6.29 Field injection and production summary, Run 4a, CO <sub>2</sub> EOR/SEQ .....	64
Figure 6.30 Field injection and production summary, Run 4b, CO <sub>2</sub> EOR/SEQ .....	65
Figure 6.31 Field injection and production summary, Run 4c, CO <sub>2</sub> EOR/SEQ .....	65
Figure 6.32 Location of injection and production wells, Run5, CO <sub>2</sub> EOR/SEQ .....	67
Figure 6.33 Oil recoveries vs. date, Run 5, CO <sub>2</sub> EOR/SEQ.....	68
Figure 6.34 CO <sub>2</sub> produced/CO <sub>2</sub> injected vs. date, Run 5, CO <sub>2</sub> EOR/SEQ ....	68
Figure 6.35 Oil production rate of the well K2, Run 5a, CO <sub>2</sub> /EOR SEQ .....	69
Figure 6.36 Oil production rate of the well K2, Run 5b, CO <sub>2</sub> /EOR SEQ .....	69
Figure 6.37 Oil production rate of the well K2, Run 5c, CO <sub>2</sub> /EOR SEQ .....	70
Figure 6.38 Well bottom hole pressure and CO <sub>2</sub> injection rate of Well K1, Run 5a, CO <sub>2</sub> EOR/SEQ.....	70
Figure 6.39 Well bottom hole pressure and CO <sub>2</sub> injection rate of Well K1, Run 5b, CO <sub>2</sub> EOR/SEQ.....	71
Figure 6.40 Well bottom hole pressure and CO <sub>2</sub> injection rate of Well K1, Run 5c, CO <sub>2</sub> EOR/SEQ.....	71
Figure 6.41 Field injection and production summary, Run5a, CO <sub>2</sub> EOR/SEQ .....	72
Figure 6.42 Field injection and production summary, Run5b, CO <sub>2</sub> EOR/SEQ .....	72
Figure 6.43 Field injection and production summary, Run5c, CO <sub>2</sub> EOR/SEQ .....	73
Figure 6.44 Location of injection and production wells, Run6, CO <sub>2</sub> EOR/SEQ .....	74

Figure 6.45 Oil production rate of the well K2, Run 6, field development & CO <sub>2</sub> /EOR SEQ .....	75
Figure 6.46 Well bottom hole pressure and CO <sub>2</sub> injection rate of Well K1, Run 6, field development & CO <sub>2</sub> EOR/SEQ .....	75
Figure 6.47 Oil production rate of the well KN2, Run 6, field development & CO <sub>2</sub> /EOR SEQ .....	76
Figure 6.48 Well bottom hole pressure and CO <sub>2</sub> injection rate of Well KN3, Run 6, field development & CO <sub>2</sub> EOR/SEQ .....	77
Figure 6.49 Field injection and production summary, Run 6, field development & CO <sub>2</sub> /EOR SEQ .....	78
Figure 6.50 Change in oil viscosity after CO <sub>2</sub> injection, Run 6 field development & CO <sub>2</sub> /EOR SEQ .....	79
Figure 6.51 CO <sub>2</sub> propagation in Zone A, Run 6 field development & CO <sub>2</sub> /EOR SEQ .....	80
Figure 6.52 CO <sub>2</sub> propagation in layers of Zone B, Run 6, field development & CO <sub>2</sub> /EOR SEQ .....	91
Figure A.1 Figure A.1 History plot from DST data .....	91
Figure A.2 Molecular weight vs. Oil gravity [49] .....	93
Figure A.3 Correlation for CO <sub>2</sub> Minimum Pressure as a function of temperature .....	93
Figure A.4 Well K1 porosity vs. depth .....	95
Figure A.5 Well K1 water saturation vs. depth .....	95
Figure A.6 Well K2 porosity vs. depth .....	96
Figure A.7 Well K2 water saturation vs. depth .....	96
Figure A.8 Well K3 porosity vs. depth .....	97
Figure A.9 Well K3 water saturation vs. depth .....	97
Figure A.10 Well K9 porosity vs. depth .....	98
Figure A.11 Well K9 water saturation vs. depth .....	98

Figure B.1 Porosity histogram of zone B.....	99
Figure B.2 Water saturation histogram of zone B .....	100
Figure B.3 Net thickness histogram of zone B.....	100
Figure B.4 Maximum and possible area of field K.....	101
Figure B.5 Area histogram of the field (maximum and minimum) .....	101

## ABBREVIATIONS AND ACRONYMS

CCS	Carbon capture and Storage
CMG	Computer Modelling Group
CO <sub>2</sub>	Carbon Dioxide
COE	Cost of Electricity
DST	Drill Stem Test
ECBM	Enhanced Coalbed Methane
EGR	Enhanced Gas Recovery
EOR	Enhanced Oil Recovery
GHG	Greenhouse gases
IPCC	Intergovernmental Panel on Climate Change
MMP	Minimum Miscibility Pressure
MMSCF	Million Standard Cubic Feet
MMSTB	Million Stock Tank Barrel
Mtc	Million cubic tons
NGCC	Natural Gas Combined Cycles
OECD	Organization for Economic Cooperation and Development Countries

OOIP	Original Oil in Place
PC	Pulverized Coal Fired Single Cycle
UNFCCC	The United Nations Framework Convention on Climate Change

# CHAPTER 1

## INTRODUCTION

Global warming is a term used to describe the observed increases in the average temperature of the Earth's atmosphere and oceans. The average global temperature rose  $0.6 \pm 0.2$  °C over 150 years, and the scientific opinion on climate change is that it is likely that "most of the warming observed over the 20<sup>th</sup> century is attributable to human activities" [1,2].

Factors that may be contributing to global warming are the burning of coal and petroleum products (sources of anthropogenic greenhouse gases (GHG) such as carbon dioxide, methane, nitrous oxide, ozone) and deforestation [3]. It is estimated that the global radiative forcing of anthropogenic carbon dioxide (CO<sub>2</sub>) is approximately 60% of the total due to all anthropogenic greenhouse gases so the climate change is mainly driven by emissions of CO<sub>2</sub> [4].

The United Nations Framework Convention on Climate Change (UNFCCC) was opened for signature in 1992 by a majority of the world's nations in response to global concern over human-induced climate change. A central, and often controversial, issue in these negotiations has been the use of terrestrial carbon sinks (e.g., forests, agricultural soils) to reduce CO<sub>2</sub> emission levels [5]. The 1997 Kyoto Protocol to the UNFCCC included provisions for industrialized nations to manage carbon sinks in order to meet specified emissions-reduction targets. Under the Kyoto Protocol to the UNFCCC, adopted in December 1997, industrialized nations target to

reduce their greenhouse gas emissions of an average of 6 to 8% below 1990 levels between the years 2008-2012 [6].

Deep ocean and geologic sequestration are the only choices to dispose large amount of CO<sub>2</sub> by safely and economically for long term periods. Geologic sequestration, a prospective technology to reduce large amount of CO<sub>2</sub> released into the atmosphere, involves the capture of CO<sub>2</sub> from hydrocarbon emissions, transportation of compressed CO<sub>2</sub> from the source to the field, and injection and storage of CO<sub>2</sub> into the subsurface.

Sequestration into depleted oil reservoirs, which are very close to their economic lifetime, has advantages when compared with other familiar projects. First of all, a structural trap has already been available in the reservoir to hold the injected CO<sub>2</sub>. Secondly, reservoir is well characterized in terms of porosity, permeability, faults and rock integrity. Usually the presence of core sample and seismic data with many others make easy to decide the capability of CO<sub>2</sub> sequestration in a storage site. Thirdly, CO<sub>2</sub> injection can be made through existing wells with very low economical burden. Some other wells may be used for monitoring the ongoing injection process. And generally, no additional cost is required to drill new wells. Finally and most importantly, there is an invaluable experience since the CO<sub>2</sub> injection into oil reservoirs has been in practice for enhanced oil recovery (EOR) for more than 35 years [7].

Because oil reservoirs have known seal and because there is a regularity structure that has experience in permitting gas-injection operations, existing oil fields are likely to be first places for CO<sub>2</sub> sequestration if is to be done at large scale [7]. Therefore; utilizing CO<sub>2</sub> for EOR and sequestration processes not only reduces greenhouse emissions but also awards economical benefits. Here, it is important to realize that in CO<sub>2</sub>-EOR the

main purpose is to maximize oil recovery with the minimum quantity of CO<sub>2</sub> while a maximum amount of CO<sub>2</sub> is aimed to store in a sequestration.

Thus, enhancing oil recovery in a sequestration is an optimization process that requires careful analysis.

In this study, the compositional simulator (STARS) of CMG software was used to study the recovery and the ability of the selected oil field to accept and retain maximum amount of injected CO<sub>2</sub> in a supercritical state for long periods of time within the reservoir.

# CHAPTER 2

## LITERATURE REVIEW

### 2.1 Effects of Greenhouse Gases on Climate Change

Observations (Figure 2.1) show that global temperatures have risen by roughly 0.6 °C over the 20th century and most of the observed warming over the last 50 years is attributable to human activities. Moreover, sensitivity studies and climate models referenced by the Intergovernmental Panel on Climate Change (IPCC) predict that global temperatures may increase by between 1.4 and 5.8 °C between 1990 and 2100 [9].

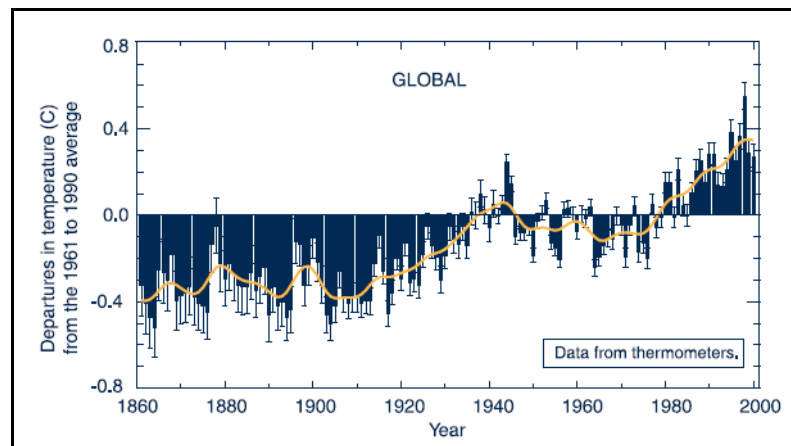
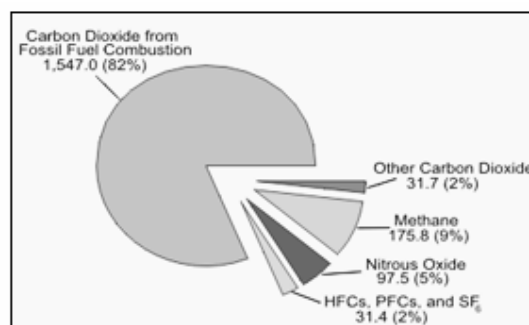


Figure 2.1 Changes in global mean surface temperatures since 1856 [9]

Water vapour, carbon dioxide, ozone, methane, nitrous oxide, and halocarbons and other industrial gases are the most important greenhouse gases affecting the global warming. Among these GHGs, the most prevalent of them is CO<sub>2</sub>. For instance, CO<sub>2</sub> accounted for 82% of total U.S. GHG emissions from 1991 to 2000[8, 9]. Figure 2.2 indicates major greenhouse gases and their contribution to emission ratios in the U.S. in 1990 and 1998 [8].



**Figure 2.2 Greenhouse gases and their emissions in the U.S. between 1990 and 1998 [8]**

Table 2.1 gives CO<sub>2</sub> emissions from the burning of the three principal carbon-based fossil fuels in different regions of the world in 1990 and 1998. It is obvious that emissions of carbon from the burning of fossil fuels increased by over 20% between 1990 and 1998, almost doubled in the Middle East and Far East/Oceania regions and significantly increased in U.S. It should be noticed that CO<sub>2</sub> emissions from natural gas have been increasing since its usage have notably enhanced during last decades [10, 11].

**Table 2.1 World CO<sub>2</sub> emissions (Mtc) by carbon-based fuels in 1990 and 1998 [10]**

Region	Natural Gas		Oil		Coal	
	1990	1998	1990	1998	1990	1998
North America	339	384	732	771	414	574
Central/South America	22	57	141	180	11	19
Western Europe	116	206	572	550	335	241
Eastern/Central Europe	209	323	415	193	488	284
Middle East	53	102	83	159	1	7
Far East/Oceania	43	144	431	706	503	985
<b>Total</b>	812	1264	2432	2658	1807	2202

The increase in global temperatures is expected to result in other changes, including rises in sea level and changes in the amount and pattern of precipitation. These changes may increase the frequency and intensity of extreme weather events, such as floods, droughts, heat waves, and hurricanes. It may cause higher or lower agricultural yields, glacier retreat, reduced summer stream flows, and contribute to biological extinctions. Tide gauge data show that global average sea level rose between 0.1 and 0.2 meters during the 20th century and global ocean heat content has increased since the late 1950s [5, 8].

The international community is working together to minimize these risks. Kyoto Protocol is the world's primary international agreement on combating climate change. Under the Kyoto Protocol to the UNFCCC, ratified in December 1997, Annex I parties (mostly Organization for Economic Cooperation and Development Countries) are to reduce their greenhouse gas emissions at least 5% below the 1990 level by the period of 2008-2012. Such commitments are important first steps, but they will make only a small contribution towards the ultimate goal of stabilizing greenhouse gas concentrations in the atmosphere. Stabilizing carbon

dioxide concentrations at 450 ppm (some 23% above current levels) would require global emissions to drop below 1990 levels within a few decades. Stabilizing CO<sub>2</sub> at 650 ppm or 1,000 ppm would require the same emissions decline within about one century or two centuries [5, 12].

Although Turkey has not already ratified to the convention and Kyoto Protocol, Turkey has also accepted the objectives of protocol. Thus, Turkey is responsible for the stabilization of greenhouse gases at 1990 level and provides technical and financial support to the developing countries since it is a member of OECD where it is placed in Annex I countries [13, 14].

IPCC defines carbon dioxide (CO<sub>2</sub>), methane (CH<sub>4</sub>) and nitrous oxide (N<sub>2</sub>O) as direct greenhouse gases and nitrogen oxides (NO<sub>x</sub>), carbon monoxides (CO), nonmethane volatile organic compound (NMVOC), hydrofluoro carbons (HFCs), perfluorocarbons (PFCs), sulphur hexafluoride (SF<sub>6</sub>) and sulphur dioxide (SO<sub>2</sub>) as indirect greenhouse gases. Direct greenhouse gas emissions as CO<sub>2</sub> equivalents were estimated as 68.25 million tonnes in 1970, as 200.7 million tonnes in 1990 and as 271.2 million tonnes in 1997 and in 2010 direct greenhouse gas emissions will be estimated to reach 567 million tonnes in Turkey (Figure 2.3) [13].

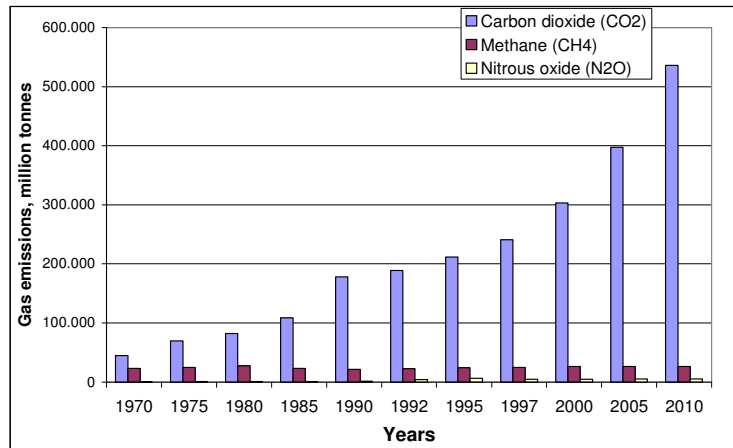


**Figure 2.3 Direct greenhouse gas emissions between 1970 and 2010 in Turkey [13]**

It is obvious that CO<sub>2</sub> is the main contributor of the greenhouse effect. In 1990, 88.7 % of total greenhouse gas emissions were CO<sub>2</sub> and the ratio of CO<sub>2</sub> emissions among the total direct greenhouse gas emissions has a tendency to increase to 94.5 % in 2010 (Table 2.2) [13].

**Table 2.2 Direct greenhouse gas emissions by sectors between 1990 and 2010 in Turkey (%)**

[13]

Greenhouse gases	Years				
	1990	1995	2000	2005	2010
Total direct greenhouse gases (Gg)	200,720	241,717	333,320	427,739	567,000
CO <sub>2</sub> (%)	88.67	87.42	90.93	92.9	94.53
CH <sub>4</sub> (%)	10.77	10.05	7.68	5.97	4.52
N <sub>2</sub> O (%)	0.56	2.53	1.40	1.14	0.95
<b>Emission fractions generated from fuel consumption</b>					
Direct greenhouse gases (Gg)	146,735	172,933	258,314	352,733	491,995
CO <sub>2</sub> (%)	97.3	97.8	98.2	98.6	98.9
CH <sub>4</sub> (%)	2.1	1.6	1.4	1.0	0.7
N <sub>2</sub> O (%)	0.6	0.5	0.4	0.4	0.4
<b>Emission fractions generated from industrial processes</b>					
Direct greenhouse gases (Gg)	35,424	47,251	52,929	52,929	52,929
CO <sub>2</sub> (%)	99.5	89.1	93.5	93.5	93.5
CH <sub>4</sub> (%)	0.1	0.1	0.1	0.1	0.1
N <sub>2</sub> O (%)	0.4	10.8	6.4	6.4	6.4

In conclusion, a better mitigation of global warming, thus, include effectively usage of energy, changing energy scheme from carbon-based fossil fuels to alternative energy sources and carbon capture and storage for sequestration.

## **2.2 CO<sub>2</sub> Sequestering in Underground Geological Media**

Geological sequestration is a way to reduce large amount of CO<sub>2</sub> released into the atmosphere from petroleum developments as well as other stationary sources including fossil-fired power plants. Sequestration process is composed of separating CO<sub>2</sub> by chemical and physical absorption, cryogenic or membrane methods, dehydrating, compressing, transporting and injecting into well. In order to predict the movement of CO<sub>2</sub> in the reservoir (depleted oil and gas fields, aquifers and coal beds) and to ensure that CO<sub>2</sub> is retained there, reservoir simulations and geophysics studies are done [15].

### **2.2.1 The Capture and Transportation of CO<sub>2</sub>**

The key issue Under the Kyoto Protocol is the capturing of CO<sub>2</sub>. Although technologies for capture of CO<sub>2</sub> exist already today, there are neither developed nor optimized for these purposes and they are expensive [16]. CO<sub>2</sub> can be removed from gas streams by physical or chemical absorption.

Chemical absorption is chosen for low to moderate CO<sub>2</sub> partial pressures. Because CO<sub>2</sub> is an acid gas, chemical absorption of CO<sub>2</sub> from gaseous streams such as flue gases depends on acid base neutralization reactions using basic solvents. Most common among the solvents in commercial use for neutralizing CO<sub>2</sub> are alkanolamines such as monoethanolamine (MEA), diethanolamine (DEA), and methyldiethanolamine (MDEA). Other chemical solvents in use are ammonia and hot potassium carbonate. CO<sub>2</sub> reacts with chemical solvent to form a weakly bonded intermediate compounds, which are then broken down by the application of heat,

regenerating the original solvent for reuse and producing a CO<sub>2</sub> stream. This process is called separation of CO<sub>2</sub> by chemical absorption [17].

CO<sub>2</sub> is physically absorbed in a solvent according to Henry's law (i.e., they are temperature and pressure dependent with absorption occurring at high pressures and low temperatures) and then regenerated using either or both heat or pressure reduction in which little or no energy is required. Physical absorption are used when the concentration (i.e., partial pressure of CO<sub>2</sub>) is high (>525 kPa)[17].

On the other hand, cryogenic technologies are high pressure but low temperature physical approach in which CO<sub>2</sub> is separated directly by condensing or by using a solvent such as a C4 hydrocarbon. This technique is advantageous since geological disposal requires CO<sub>2</sub> to be at high pressure [15].

CO<sub>2</sub> can be transported to the injection site by pipelines or tanks.

In pipeline transportation, the best working condition is to retain CO<sub>2</sub> at pressure higher than its critical pressure that is 7.4 MPa therefore CO<sub>2</sub> pipeline is usually operated at pressure between 8 and 17 MPa. In order to transport CO<sub>2</sub> in a pipeline it must be compressed at pressures above 8 MPa to achieve a single phase flow. By running the system with CO<sub>2</sub> in this situation problems associated with the two phase flow are prevented in the subsequent pipeline and injecting stages [15]. Suitable operating pressure and temperature lies in between 8,619 kPa at 4 °C and 15,300 kPa at 38 °C. These limits are set by the ASME-ANSI 900# flange rating and ambient condition coupled with the phase behavior of CO<sub>2</sub> [18].

Transporting CO<sub>2</sub> in the tanks by both truck and rail was used to be considered more expensive than pipeline. However, according a recent study shipping CO<sub>2</sub> by customized LPG gas vessels is more flexible and less costly [19]. LPG is carried from offshore oilfield to the onshore terminal. Vessels are unloaded and replaced with industrial exhausted CO<sub>2</sub>. After returning to the offshore field, CO<sub>2</sub> is injected and stored in the geological reservoirs [15]. Another point is that, tankers carrying dry ice or supercritical liquid carbon dioxide may be more economic than pipelines for ocean disposal at distances greater than about 300 km from shore, as pipelines require depressurization at regular intervals. The distance that the carbon dioxide is to be carried does not considerably affect the costs of transporting CO<sub>2</sub> by tanker [20].

## **2.2.2 CO<sub>2</sub> Storage options in Underground Medium**

After recovering CO<sub>2</sub> in an energy conversation process, it should be stored in such a way that emission into atmosphere is not possible or at least greatly delayed. Other than storing in algae and deep oceans, considering underground storage, rock and salt cavities, aquifers, depleted natural gas and oil fields and coal beds can be mentioned as storage places [21].

### **2.2.2.1 Nonporous Medium**

#### **2.2.2.1.1 Deep Ocean (Hydrates)**

Oceans are the largest sinks available for carbon dioxide since they cover approximately 70% of the Earth's surface. Ocean disposal is the interest for the countries which are with coastal zones and access to ocean

depths of greater than 3000 m since transportation costs rise with distance traveled [20].

Disposal of carbon dioxide to ocean is involved as the following [22]:

- Dry ice is discharged to the ocean surface from a ship.
- Then, liquid CO<sub>2</sub> is injected at a depth of about 1000 m via a pipe towed by a moving ship and forming a rising droplet plume.
- Liquid carbon dioxide is injected at a depth of about 1000 m from a manifold lying on the ocean bottom and forming a rising droplet plume.
- To form sinking bottom gravity current, a dense carbon dioxide-seawater mixture is created at a depth of between 500 and 1000 m.
- Introducing liquid carbon dioxide to a sea floor depression, it forms a stable 'deep lake' at a depth of about 4000 m.

#### **2.2.2.1.2 Salt Cavern**

Salt caverns are appropriate for storing CO<sub>2</sub> permanently (more than 1000 years) or temporarily (decades) even though it has low priority among carbon sequestration techniques. Regardless of the cost and other potential environmental issues related to cavern mining, advantages of storing into salt caverns are [23]:

- The rate of filling or emptying of salt caverns is not limited by porous media flow capabilities.
- Storage sites where other appropriate unfractured geological sites are not easily found can be provided by salt strata.

- Storing CO<sub>2</sub> in shallow, cool salt caverns in supercritical form provides more storage capacity than storing CO<sub>2</sub> in solution, as a free gas, or through adsorption onto coal or oil shale.
- The accessibility and availability in pure form at any future time.

#### **2.2.2.2 Porous Medium**

Aquifers, depleted oil or gas reservoirs and coal beds are considered as geological structures for CO<sub>2</sub> to be stored. Underground storage follows three major steps independent of the choice of host formation [16]:

- The injected CO<sub>2</sub> dissolves and diffuses in oil and water and flows according to the existing pressure gradient in the porous medium (hydrodynamic trapping).
- Later, CO<sub>2</sub> reaches thermal equilibrium in all fluid phases (gas, water and gas) depending on fluid, pressure and temperature conditions (solution trapping).
- Then the dissolved CO<sub>2</sub> reacts with the minerals within the formation and induces dissolution/precipitation reactions (mineral trapping).

The capacity of a reservoir to store CO<sub>2</sub> depends on the parameters such as size of the reservoir, effective porosity, the net fraction of the reservoir that can be filled, and the density of the CO<sub>2</sub>. The storing capacity in aquifers is more equally spread over the world whereas in natural gas fields and oil fields are not [21].

World subsurface estimates of CO<sub>2</sub> storage capacities are given in Table 2.3. Estimates are large enough to suggest that there is sufficient capacity to store a major fraction of expected CO<sub>2</sub> emissions through 2030 and beyond. CO<sub>2</sub> emissions are currently about 24 GtCO<sub>2</sub>/yr (1 GtCO<sub>2</sub>= 1 billion metric tons of CO<sub>2</sub>), and if the rise in emission were roughly linear, then the total emissions would be about 1300 GtCO<sub>2</sub> for the period from 2000 to 2030. Therefore, the capacity of geologic formations is sufficient to store CO<sub>2</sub> at significant level [7].

**Table 2.3 Estimated storage capacities of geologic formations (GtCO<sub>2</sub>) [7]**

<b>Storage Environment</b>	<b>Parson &amp; Keith [24], 1998</b>	<b>Gale [25], 2003</b>
Oil and Gas Reservoirs	740-1850	920
Deep Saline Aquifers	370-3700	400-10,000
Coal Beds	370-1100	40

#### **2.2.2.2.1 Aquifer (deep saline)**

Since aquifers are considered to be most widely available, there is high potential to find a suitable aquifer with large capacity or close to CO<sub>2</sub> source. The structure and the interconnection of the pores provide flow of gases or fluids through the bed. An aquifer is suited for underground storage of gases or liquids since it is a reservoir with porosity, permeability and a sealing cap rock [21].

Without raising aquifer pressure to a large extent, CO<sub>2</sub> can be injected to aquifers with large volumes. After the injection, CO<sub>2</sub> will dissolve in the brine and cause brine/CO<sub>2</sub> mixture denser than the brine alone. Dissolving furthermore, fresh brine is brought in contact with the CO<sub>2</sub> phase. It is

estimated that hundreds to thousands of years will be required to dissolve all the CO<sub>2</sub>, trapping much of the CO<sub>2</sub> [26].

#### **2.2.2.2.2 Depleted Oil and Gas Reservoirs**

Presently, policy for reducing the amount of CO<sub>2</sub> in the atmosphere is sequestration of carbon dioxide in depleted oil reservoir. On the other hand, CO<sub>2</sub> sequestration in oil reservoirs is a complex issue covering a broad scope of scientific, technological, economic, safety, and regularity issue [27].

The reasons why oil and gas reservoirs are attractive targets for CO<sub>2</sub> sequestration can be listed as:

- Structural traps which have contained the oil or gas over geological timescales should be able to contain carbon dioxide, assuming increased pressure does not create any new pathways to the surface or through the extraction process.
- The geologic structure and physical properties of most oil and gas fields have been significantly described.
- Computer models have been utilized in order to forecast the displacement behavior and trapping of CO<sub>2</sub> for EOR [20].
- The reservoir will not be environmentally degraded by the CO<sub>2</sub>, as the reservoir has already contained hydrocarbons.
- While some production wells may be converted to gas injection wells, the others may be used to monitor the behavior of the CO<sub>2</sub> within the reservoir. CO<sub>2</sub> sequestration plan can be adopted for to improve oil production, if the field is still producing [16].

### **2.2.2.2.3 Enhanced Coal Bed Methane (ECBM)**

By adsorbing, a coal stores CO<sub>2</sub> while desorbing the methane as free gas for recovery. Volume of CO<sub>2</sub> adsorbed by coal is twice as much as methane. Since permeability of coal bed is low, CO<sub>2</sub> injectivity is generally low. Consequently it requires both reservoir treatment and larger number of wells [15].

Unlike in oil, gas reservoirs and aquifers, deep unmineable coal beds offer a different storage mechanism, the same mechanism that is the source of coal bed methane. CH<sub>4</sub> or CO<sub>2</sub> are adsorbed on the surfaces of coal particles at high pressure. According to the adsorption curve hysteresis, once CO<sub>2</sub> is adsorbed, a large amount of it will remain as adsorbed even if the pressure is reduced later. CO<sub>2</sub> can be used to enhance CH<sub>4</sub> recovery since the flow in coal beds occur primarily in the fracture network, diffusing into matrix blocks and replacing adsorbed CH<sub>4</sub> [28-29].

### **2.2.3 Cost of CO<sub>2</sub> Sequestration**

CO<sub>2</sub> sequestration economy includes three distinct phases: capture of the CO<sub>2</sub> from the source followed by dehydration and compression, transportation to the storage site and injection and storage of the CO<sub>2</sub> in the geological reservoir.

CO<sub>2</sub> capture costs are relatively high. Typical cost ranges for CO<sub>2</sub> removal from the exhaust gas of power plants with amines are in the range of 40–60 \$/tCO<sub>2</sub> avoided for pulverized coal fired single cycle (PC) and 30–70 \$/tCO<sub>2</sub> avoided for natural gas combined cycles (NGCC). However, capture costs can be minimized by utilizing exhaust gas streams with high-purity CO<sub>2</sub>, which are emitted by several industrial processes [30].

The cost of transport is low compared to other costs. Transport costs vary between 1 and 3 \$/tCO<sub>2</sub> per 100 km of pipeline [28]. Transportation costs can be minimized if the reservoir is close to the carbon emission sources.

Geologic storage costs depend on the reservoir type and local geological conditions. For aquifers and gas reservoirs (on- and offshore) storage costs vary between approximately 1 and 15 \$/tCO<sub>2</sub>. If oil and gas recovery is enhanced by the injection of CO<sub>2</sub> into oil/gas reservoirs or deep unminable coal seams, storage costs can be decreased to small (or even negative) by generating oil/gas revenues [31].

### **2.3 Oil Recovery by CO<sub>2</sub> Injection**

CO<sub>2</sub> injection into oil reservoirs which are close to the end of their economic lifetime, to enhance oil recovery (CO<sub>2</sub>-EOR) is successfully applied in several ongoing commercial projects in the world. CO<sub>2</sub> is sequestered through the injection well into immobile oil and empty pores and oil, water and CO<sub>2</sub> are produced at the production well. These components are separated and the CO<sub>2</sub> is compressed and recycled to the injection well. It is important to realize that in a CO<sub>2</sub>-EOR project, the ultimate goal is to maximize oil recovery with a minimum injection quantity of CO<sub>2</sub>, which might be contradictory with the purpose to maximize CO<sub>2</sub> sequestration.

About 84 commercial CO<sub>2</sub>-EOR operations are ongoing in the USA, Canada, Hungary, Turkey and Trinidad. 200,000 barrels (bbl) of oil per day is produced, a small but significant fraction (0.3%) of the 67.2 million bbl per day total of world-wide oil production in 2004 [30].

### 2.3.1 Miscible vs. Immiscible CO<sub>2</sub> Flooding

CO<sub>2</sub> sequestration can be achieved within producing oil reservoirs by miscible and immiscible gas displacement during EOR projects.

Two fluids are miscible when they can be mixed together in all proportions and all mixtures remain single phase [32]. For miscible flooding to be a competitive process in a given reservoir, several conditions must be satisfied: an adequate volume of CO<sub>2</sub> must be available at a rate and cost that will allow favorable economics, the reservoir pressure required for miscibility between the solvent and oil in question must be attainable, and incremental oil recovery must be sufficiently large and timely for project economics to withstand the added cost.

The miscibility of CO<sub>2</sub> in the oil phase is the key factor that determines the efficiency of EOR with CO<sub>2</sub> injection. At pressures greater than the minimum miscibility pressure (MMP), oil and CO<sub>2</sub> are mutually soluble. The dissolved CO<sub>2</sub> reduces the viscosity of the oil and also causes swelling of the oil phase. Thus, CO<sub>2</sub> injection projects are preferred for oil with density ranging from 29° to 48° API (882–788kg/m<sup>3</sup>) and reservoir depths from 760 to 3700m [33]. Although injected CO<sub>2</sub> is not first-contact miscible with the oil, as CO<sub>2</sub> flows, it extracts certain hydrocarbon components from the oil such that the enriched CO<sub>2</sub> may become miscible in the oil (multi-contact miscibility).

Holm and Josendal [34] reached the following conclusions from an experimental study of factors affecting CO<sub>2</sub> miscibility pressure:

- Dynamic miscibility occurs when the CO<sub>2</sub> density is sufficiently great that the dense gas CO<sub>2</sub> or liquid gas CO<sub>2</sub> solubilizes the C<sub>5</sub>-through-C<sub>30</sub> hydrocarbons contained in the reservoir oil.

- Reservoir temperature is an important variable affecting MMP. A higher temperature results in a higher miscibility pressure requirement, if the other factors are remaining equal.
- MMP is affected by the molecular weight distribution of the individual C<sub>5</sub>-through-C<sub>30</sub> hydrocarbons in the reservoir oil.
- MMP also is affected but to a much lesser degree by the type of hydrocarbons present in the C<sub>5</sub>-through-C<sub>30</sub> fraction. For example, aromatics result in lower miscibility pressure.
- The presence of methane in the reservoir oil does not change the MMP appreciably.

Many MMP correlations are proposed for gas-injection processes, but a simple estimate of the miscibility pressure as a function of reservoir temperature, molecular weight of the crude oil and mole percentage of methane and nitrogen is as follows [35].

$$P_{\text{mdmp}} = 15.988 (T_{\text{res}})^{0.744206+0.0011038(\text{MWC5}^+)+0.0015279(Y_{\text{C1}})} \quad 2.1$$

where;

$P_{\text{mdmp}}$  : predicted minimum dynamic miscibility pressure, psia

$T_{\text{res}}$  : reservoir temperature, °F

$\text{MWC5}^+$  : molecular weight pentanes and heavier fractions

$Y_{\text{C1}}$  : mole percentage of methane and nitrogen

### 2.3.2 Carbon Dioxide as a Displacement Fluid

Oil displacement strongly depends on factors, which are related to the phase behavior of CO<sub>2</sub> – crude oil mixtures.

CO<sub>2</sub> is compressed to a supercritical state in order to avoid the separation of CO<sub>2</sub> into gas and liquid phases during transportation and injection processes. At normal atmospheric conditions, CO<sub>2</sub> is a thermodynamically very stable gas with a 50% greater density than air. The phase diagram of pure CO<sub>2</sub> shows a critical temperature of 31°C and a critical pressure of 7.4 MPa (1074 psi) (Figure 2.4). Below this temperature and/or pressure the CO<sub>2</sub> is either in a liquid or vapor phase and above the critical values the pure CO<sub>2</sub> is in supercritical state. At these pressure and temperature conditions, CO<sub>2</sub> behaves still like a gas by filling all the available volume, but has a 'liquid' density that increases, depending on pressure and temperature, from 200 to 900 kg/m<sup>3</sup> (Figure 2.5). This is related with the phase change from gas to supercritical fluid. Consequently, CO<sub>2</sub> occupies much less space in the subsurface than at the surface. One tonne of CO<sub>2</sub> at a density of 700 kg/m<sup>3</sup> occupies 1.43 m<sup>3</sup>, or less than 6 m<sup>3</sup> of rock with 30% porosity if 80% of the water in the pore space could be displaced. At 0 °C and 1 atm, 1 tonne of CO<sub>2</sub> occupies 509 m<sup>3</sup> [36].

The viscosity of CO<sub>2</sub> (Figure 2.6) is a strong function of pressure and temperature. As pressure increases at a constant reservoir temperature, gas viscosity increases. So CO<sub>2</sub> has considerably stronger sweep efficiency [38].

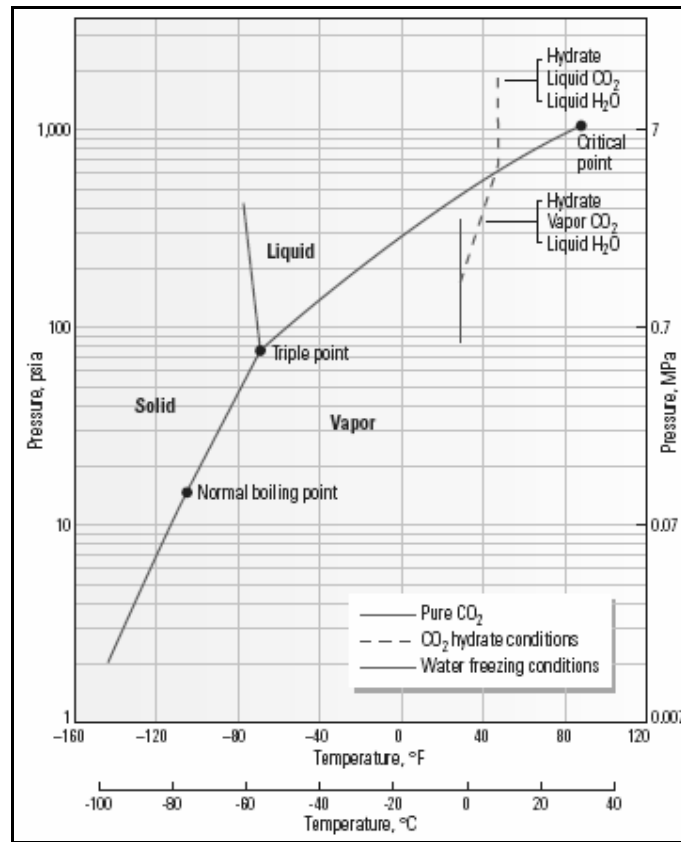


Figure 2.4 Phase diagram of CO<sub>2</sub> [37]

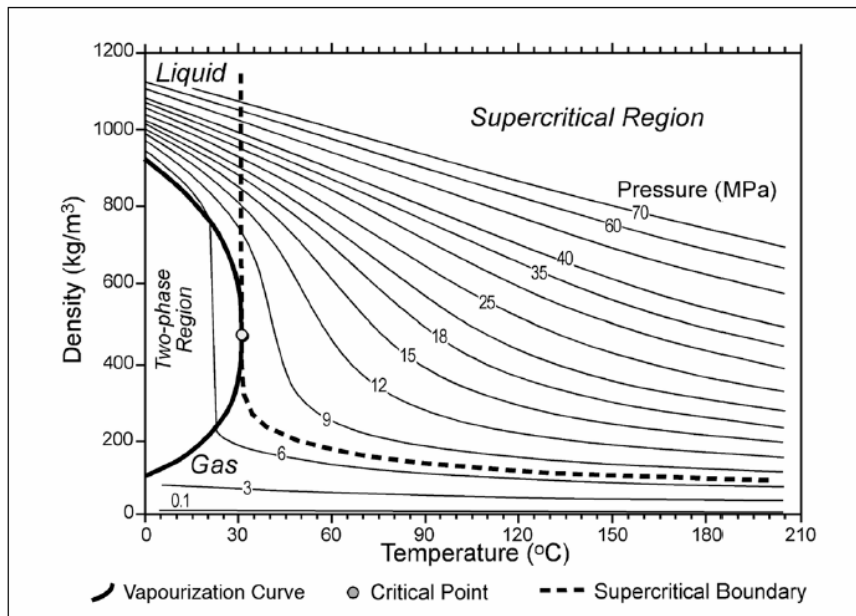


Figure 2.5 Variation of CO<sub>2</sub> density as a function of temperature and pressure [38]

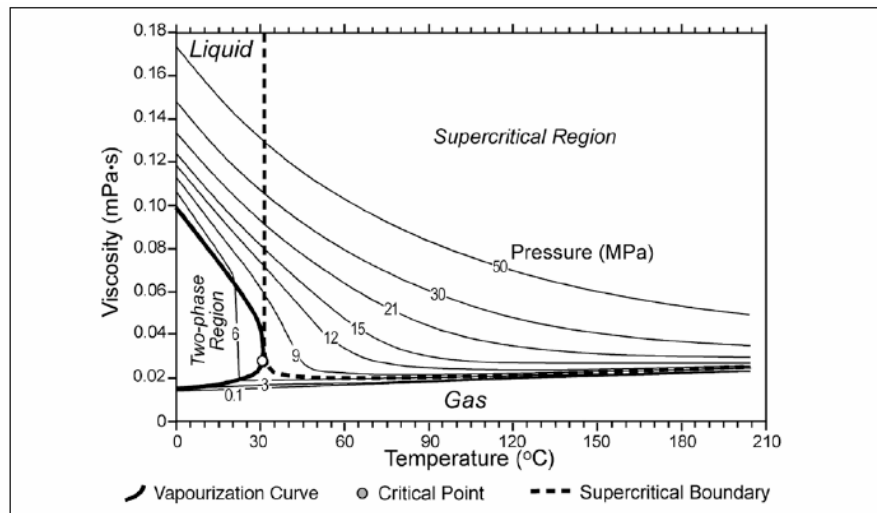


Figure 2.6 Variation of CO<sub>2</sub> viscosity as a function of temperature and pressure [38]

### 2.3.3 Oil Recovery Mechanisms by CO<sub>2</sub> Injection

Whether it can be carried out as a miscible or as an immiscible gas displacement and regardless of how it is applied in the field, following mechanisms play a role in the oil recovery by CO<sub>2</sub> flooding [34]:

- Reduction of oil viscosity: A large reduction in the viscosity of crude oils occurs as they become saturated with CO<sub>2</sub> at increasing pressures. As pointed out in the literature, a larger percentage reduction occurs in the viscosity of the more viscous crude so the mobility ratio increases.
- Oil swelling: CO<sub>2</sub> promotes swelling. The high solubility of CO<sub>2</sub> in hydrocarbon oil causes these oils to swell. However, the difference between the solubility of CO<sub>2</sub> in gas saturated reservoir oil and in stock-tank oil, with the subsequent difference in the degree to which the resultant oils to swell, has received less attention.
- Increase in oil density: CO<sub>2</sub> has an effect on the water or brine that is present in the reservoir when displacement processes are in operation. There is some expansion of water when CO<sub>2</sub> is injected; the densities of the oil and water become closer to each other, which lessen the chances for gravity segregation of these fluids and the resultant overriding of the CO<sub>2</sub>-water mixture.
- Extraction and vaporization of oil: CO<sub>2</sub> can vaporize and extract portions of crude oil. This occurs at low temperatures where CO<sub>2</sub> is a liquid, as well as at higher temperatures above the critical, 89 °F.
- Miscibility effects: CO<sub>2</sub> is highly soluble in water and in hydrocarbon oils.

- CO<sub>2</sub> reduces the interfacial tension between water and oil.
- Increase in the injectivity (acidic effect): the acidic effect of CO<sub>2</sub> on the rock has been shown to increase the injectivity of water by direct action on carbonate portions of the rock and by stabilizing action on clays in the rock.

The mechanisms, which have been listed above, are more or less important depending on whether the CO<sub>2</sub> displacement is miscible or immiscible. For example, the vaporization of crude oil, development of miscibility, and reduction of interfacial tension are very important with the miscible CO<sub>2</sub> process, whereas reduction of crude oil viscosity and its swelling are more important effects with the immiscible CO<sub>2</sub> displacement [34].

### **2.3.4 Ongoing CO<sub>2</sub> projects**

There exists numbers of commercial and research CO<sub>2</sub> storage projects (Figure 2.7). Industrial scale projects (projects in the order of 1 MtCO<sub>2</sub> yr<sup>-1</sup> or more) are the Sleipner project in the North Sea, the Weyburn project in Canada and the In Salah project in Algeria. About 3–4 MtCO<sub>2</sub> that would otherwise be released to the atmosphere is captured and stored annually in geological formations. Additional projects are listed in Table 2.4. In addition to the Carbon Capture and Storage (CCS) projects currently in place, 30 MtCO<sub>2</sub> is injected annually for EOR, mostly in Texas, USA, where EOR commenced in the early 1970s. Most of this CO<sub>2</sub> is obtained from natural CO<sub>2</sub> reservoirs found in western regions of the US, with some coming from anthropogenic sources such as natural gas processing. Much of the CO<sub>2</sub> injected for EOR is produced with the oil, from which it is separated and then reinjected. At the end of the oil recovery, the CO<sub>2</sub>

can be retained for the purpose of climate change mitigation, rather than vented to the atmosphere. This is planned for the Weyburn project [39].

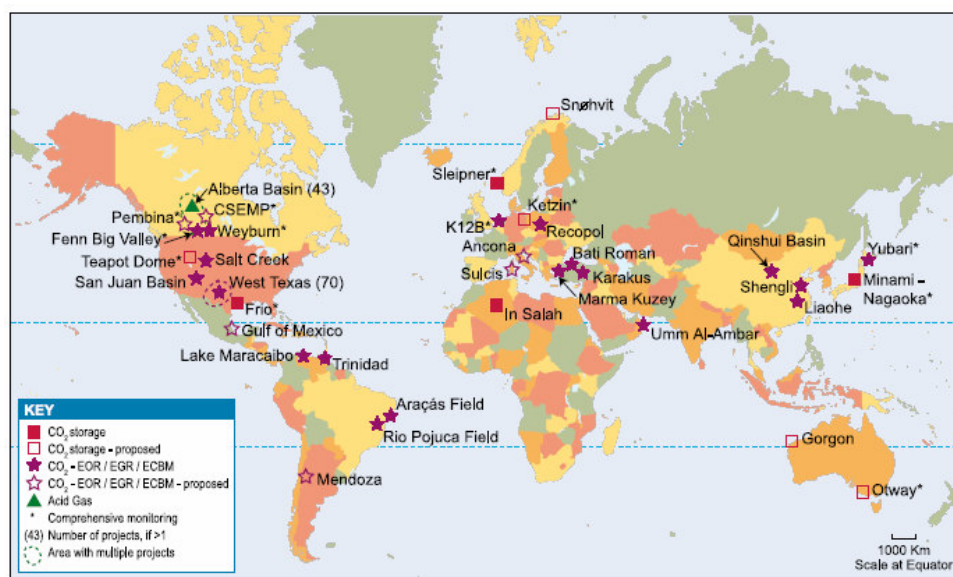


Figure 2.7 Location of sites where activities relevant to CO<sub>2</sub> storage are planned or under way [39]

Table 2.4 Current and planned carbon capture and storage projects [39]

Project	Country	Injection start (year)	Average daily injection rate (tCO <sub>2</sub> /day)	Total (planned) storage (tCO <sub>2</sub> )	Storage Type	Lithology
Weyburn	Canada	2000	3,000-5,000	20,000,000	CO <sub>2</sub> -EOR	Carbonate
In Salah	Algeria	2004	3,000-4,000	17,000,000	Depleted hydrocarbon reservoir	Sandstone
Sleipner	Norway	1996	3,000	20,000,000	Aquifer	Sandstone
K12B	Netherlands	2004	100	8,000,000	CO <sub>2</sub> -EGR	Sandstone
Frio	U.S.A	2004	177	1600	Saline formation	Brine-bearing sandstone shale
Fenn Big Valley	Canada	1998	50	200	CO <sub>2</sub> -ECBM	Coal
Qingshui Basin	China	2003	30	150	CO <sub>2</sub> -ECBM	Coal
Yubari	Japan	2004	10	200	CO <sub>2</sub> -ECBM	Coal
Recopol	Poland	2003	1	10	CO <sub>2</sub> -ECBM	Coal
Gorgon(planned)	Austria	2009	10,000	unknown	Saline formation	Massive sandstone with shale seal
Snøhvit	Norway	2006	2,000	unknown	Saline formation	Sandstone

#### **2.3.4.1 Batı Raman Immiscible CO<sub>2</sub> Flooding Project**

There exists few numbers of immiscible displacement projects. Batı Raman oilfield, in southeast Turkey, is the only large-scale project that uses immiscible flooding. The oilfield contains heavy oil with very low gravity of 12° API and high viscosity of 592 cp. Primary oil recovery was 2% of the OOIP. With the injection of CO<sub>2</sub> coming from a nearby natural reservoir (Dodan), commenced in 1986, 6000 barrels of oil per day are produced. Moreover, it has been estimated that 12% of OOIP will be recovered by EOR. By the end of 2003, Batı Raman cumulative oil production was 86,8 million barrels, where 50,8 million barrels came from CO<sub>2</sub> injection secondary recovery process. In 2003, 470,9 million m<sup>3</sup> CO<sub>2</sub> was injected, 378,6 million m<sup>3</sup> of this amount was produced back, and 171,3 million m<sup>3</sup> of this produced gas was re-injected into the reservoir [40-41].

## CHAPTER 3

### STATEMENT OF THE PROBLEM

The increase in atmospheric carbon dioxide (CO<sub>2</sub>) concentration resulting from anthropogenic sources is an important environmental issue. Sequestration in geological formations is one of the proposed solutions for removing greenhouse emissions from the atmosphere and in most of the cases CO<sub>2</sub> forms a considerable percentage of these greenhouse gases.

The presence of abundant well data and economic benefits through enhanced oil recovery (EOR) make it easy to decide the capability of CO<sub>2</sub> sequestration in depleted oil reservoirs.

In Turkey, TPAO has an experience on CO<sub>2</sub> injection for oil recovery. But the sequestration of CO<sub>2</sub> has not been planned yet. Turkey is a growing country and becoming industrialized one in near future. Turkey has accepted the objectives of Kyoto protocol, thus, Turkey is responsible for stabilizing of greenhouse gases below 1990 levels.

From this point of view, in order to develop a CO<sub>2</sub> sequestration project, the compositional simulator (STARS) of CMG software will be used to investigate CO<sub>2</sub> storage and flooding potential of a depleted oil reservoir located in the southeast of Turkey. History matching will be utilized to verify simulation data with the actual field one. Different scenarios will be developed to maximize amount of CO<sub>2</sub> stored while obtaining ultimate oil recovery at the same time.

# CHAPTER 4

## METHOD OF SOLUTION

Carbon dioxide injection into the subsurface is a multiphase multi-component flow process. Since the structure of the geological formations are highly complex , numerical simulations are needed to predict the movement of CO<sub>2</sub> in the reservoir, the storage capacity of the reservoir, and to ensure that CO<sub>2</sub> is retained within the reservoir during CO<sub>2</sub> sequestration. Therefore, CO<sub>2</sub> injection into the Field K was modeled by using Computer Modeling Group's STARS simulator. SURFER provided by Golden software was used to obtain porosity, saturation and thickness maps. Drill stem test (DST) data was interpreted by the help of SAPHIR software to acquire initial reservoir properties. Probabilistic reserve calculations were done by @RISK simulator. History matching was done to validate the simulator data at the end of data preparation for STARS simulator.

### 4.1 Softwares Utilized

#### 4.1.1 STARS Simulator by CMG

STARS, CMG's full featured advanced processes reservoir simulator, models the flow of three-phase, multi-component fluids. It models in one, two, or three dimensions, including complex heterogeneous faulted structures. STARS is a comprehensive numerical reservoir simulation tool that models steam flood, steam cycling, steam-with-additives, dry and

wet combustion, along with many types of chemical additive processes, using a wide range of grid and porosity models in both field and laboratory scale [42].

STARS incorporates CMG's advanced Well/Production Management module, as well as specialized well features to model complex reservoirs. These features account for wellbore cross flow and/or multi-lateral horizontal wells. STARS couples directly to a sophisticated surface facilities program, to model dry or wet gas flow from the reservoir, through a complex surface network facility, to the gas plant [42].

STARS models multiple PVT and equilibrium regions as well as multiple rock types and has flexible relative permeability choices. Regardless of the size or complexity of your reservoir problem, STARS is an effective tool for a broad range of reservoir management issues including [42]:

- Primary depletion and EOR predictions of undersaturated and saturated reservoirs performing below bubble point,
- Coning studies,
- Reservoir performance under surface constraints,
- Secondary recovery; water flood and gas injection,
- Enhanced recovery; miscible and pseudo-miscible injection and WAG) processes,
- Gas deliverability and forecasting,
- In-situ generation and flow of emulsions and foams (including foamy oils) and in-situ precipitation of waxes and asphaltenes.

#### **4.1.2 SURFER by Golden Software**

Surfer software is used to interpolate reservoir physical properties over the field using gridding methods. Surfer is a contouring and 3D surface mapping and plotting program that runs under Microsoft Windows. Surfer quickly and easily converts your data into outstanding contour maps and surface plots. And with all the options available in Surfer, the maps can be customized to produce exactly the presentation you want [43].

While processing data that has been inputted, the software uses many gridding methods: Inverse Distance to a Power, Krigging, Minimum Curvature, Nearest Neighbor, Polynomial Regression, Radial Basis Functions, Shepard's Method, Triangulation w/Linear Interpolation. Among those many methods, the Krigging method was used in the reservoir characterization process [43].

#### **4.1.3 SAPHIR by Kappa Engineering**

Saphir, a well test interpretation software, is known for the ease of use, advanced features and fast, helpful technical support. Saphir provides users with very important data from well tests (buildup or drawdown) like permeability, initial pressure, and skin factor [44].

#### **4.1.4 @RISK by Palisade Corporation**

@RISK is the Risk Analysis and Simulation add-in for Microsoft Excel. As an add-in, @RISK becomes seamlessly integrated - via a new toolbar and functions - with your spreadsheet, adding Risk Analysis to your existing models. @RISK uses a technique known as Monte Carlo simulation to allow you to take all possible outcomes into account. Simply replace uncertain

values in your spreadsheet model with @RISK functions to represent a range of possible values [45].

## **4.2 History Matching**

History matching is a way of verifying the accuracy of prepared simulation data with the actual field data. It is necessary to acquire model input data, especially the history of field performance. One of the essential tasks of the data verification stage is to determine which data should be matched during the history matching process. If a gas-water reservoir is being modeled, gas rate is usually specified and water production is matched. By contrast, if an oil reservoir is being modeled, oil rate is specified and water and gas production are matched. Data acquisition is an essential part of model initialization. Model initialization is the stage when the data is prepared in a form that can be used by the simulator. The model is considered initialized when it has all the data it needs to calculate fluids in place [46].

## CHAPTER 5

### FIELD DESCRIPTION

Field K, shown in Figure 5.1, is located in Southeast Turkey. The alternating layers of sands and shales deposited in deltaic and marine carbonates form a faulted anticline structure extending over an area of 2.70 km by 0.75 km. It has been on production since 1982. The light crude is produced from the carbonate formation D at an average depth of 1930 m to 1950 m with an average thickness of 25 m to 155 m. Primary drive mechanism is water drive. The reservoir zones contain 7 MMSTB (1,112,911  $\text{m}^3$ ) of OOIP. Approximately 25% of the initial oil in place has been produced with the support of water drive and its natural aquifer. The average reservoir permeability is approximately 60 md with tighter zones at the top and the bottom. The average reservoir porosity is approximately 25% and water saturation is 25%. The reservoir crude oil gravity is 32° API, with an average solution gas/oil ratio of 13 scf/stb. The original reservoir pressure was 2520 psi (17375 kPa) and temperature 64 °C (148 °F) at 1950 m. The current reservoir pressure of 1740 psi is above the bubble point pressure of 50 psi. Original oil formation volume factor is 1.030 bbl/stb and the average oil viscosity is approximately 5 cp. Sulfur content of the mixture is 1.1 wt%. Table 5.1 summarizes general reservoir rock and fluid properties [41].

Following the first discovery in 1982, 8 additional wells were drilled. But 6 wells are abandoned due to high water production. Higher water production and water cut values show an active aquifer system which lies at the bottom of the reservoir with an average 18% porosity and 22 md permeability [41].

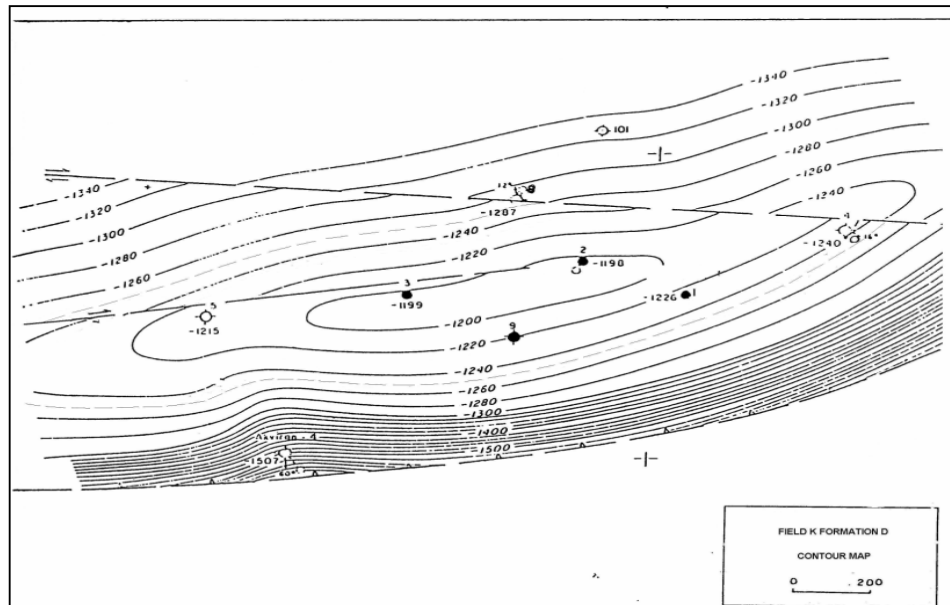


Figure 5.1 Top of formation D structural contour map of field K

**Table 5.1 Summary of field properties**

Field K General Reservoir Properties	
<b>Field Discovery, Year</b>	: 1982
<b>Location</b>	: Southeast of Turkey
<b>Original Oil in Place, MMSTB</b>	: 7
<b>Reservoir Pressure, psi</b>	: 2520
<b>Temperature, °F</b>	: 148
<b>Porosity, %</b>	: 25
<b>Water Saturation, %</b>	: 25
<b>Permeability, md</b>	: 60
<b>Net Thickness, m</b>	: 9
<b>Water Oil Contact Depth (subsea), m</b>	: 1250
Field K PVT Properties	
<b>API Gravity</b>	: 32
<b>Specific Gravity</b>	: 0.865
<b>Viscosity, cp</b>	: 5.00
<b>Bubble Point Pressure, psi</b>	: 50
<b>Gas Oil Ratio (GOR), scf/stb</b>	: 13
<b>Original Oil Formation Volume Factor, bbl/stb</b>	: 1.030
<b>Formation Water Salinity, ppm</b>	: 5,000-12,000
<b>Formation Water Resistivity, ohm-m</b>	: 0.600-0.260
<b>Compressibility of Oil, 1/psi</b>	: 5.30E-06
<b>Compressibility of Water, 1/psi</b>	: 3.30E-06
<b>Compressibility of Rock, 1/psi</b>	: 3.90E-06
<b>Total Compressibility, 1/psi</b>	: 8.70E-06
<b>Sulfur Content, % weight</b>	: 1.1
<b>Freezing Point, °F</b>	: 9
<b>Flash Point, °F</b>	: 28

## CHAPTER 6

### RESULTS AND DISCUSSION

#### 6.1 Evaluation of General Reservoir Characteristics

##### 6.1.1 Reservoir Pressure and MMP

Pressure is one of the most important factors in determining CO<sub>2</sub> miscibility in oil. Initial reservoir pressure of Field K was obtained by analyzing the drill stem test (DST) taken at the depth of reservoir zone. A drill stem test (DST) provides a means of estimating formation and fluid properties. DST data was interpreted by using SAPHIR program. Static reservoir pressure was calculated as 2520 psi (17375 kPa) at the depth of 1230 m (subsea) (Appendix A.1).

CO<sub>2</sub> is not first-contact miscible fluid with oil, but as CO<sub>2</sub> flows through the deeper parts of the reservoir, it extracts certain light hydrocarbon components from the oil such that the enriched CO<sub>2</sub> may become miscible in the oil, called as multi-contact miscibility. The minimum miscibility pressure (MMP) is highly dependent on depth, temperature, and crude oil composition. The minimum miscibility pressure was determined by conducting slim tube experiments, but due to absence of laboratory analysis, correlations were utilized to estimate MMP of Field K. MMP of CO<sub>2</sub> for Field K was found as 2150 psi (13690 kPa) (Appendix A.2). After primary depletion of Field K, the current reservoir pressure is 1770 psi (12200 kPa), which is below the MMP. But with the injection of CO<sub>2</sub> multi-

contact miscibility can be achieved while the reservoir is repressurizing with time.

### **6.1.2 Porosity and Water Saturation**

Porosity, the void space within rock that can hold fluid, is the fundamental contributor to reservoir storage capacity so it is a critical parameter in a CO<sub>2</sub> sequestration project. On the other hand, knowing the saturation profile within the reservoir is an important data for the application of oil recovery techniques. Well logging is a well-known technique used to evaluate formations in the oil and gas industry. Rock and fluid properties of the formation are recorded to find hydrocarbon zones in the geological formations by a wireline lowered into the well. An interpretation of these measurements is then made to locate and quantify potential depth zones containing hydrocarbons [47].

Core data was first used to get porosity-cut off value of the field. This value was found out to be 7% by interpreting the graph of liquid permeability vs. porosity (Figure 6.1). Effective water saturation cut-off value was taken from TPAO as 50%.

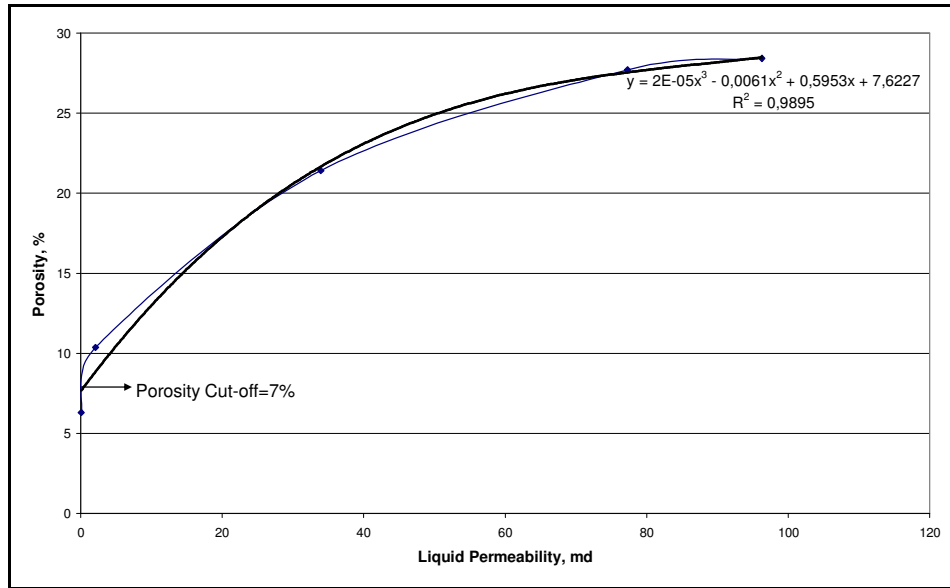


**Figure 6.1 Porosity vs. liquid permeability from core data**

Available gamma ray, sonic, density neutron and resistivity logs from wells were interpreted to evaluate the formation properties of Field K. Using gamma ray log records, formation clay type and boundaries of each zone were found. Using sonic log data together with neutron and density logs, effective porosities and lithology of formations for each well were determined. Resistivity logs were interpreted to find oil and water saturations so that the hydrocarbon bearing zones are located.

Lithology and rock properties of each zone are tabulated below (Table 6.1). Zone B is the only productive zone when taking porosity and water saturation values into account. Average reservoir porosity and water saturation are both found as 25%. Zone C can be regarded as the aquifer region since it has high water saturation. Appendix A.3 gives details of well logging interpretation results.

**Table 6.1 Summary of well logging interpretation, field K**

<b>Well K1</b>						
	<b>Lithology</b>	<b>Elevation Interval, m</b>	<b>Depth Interval, m</b>	<b>Thickness, m</b>	<b>Porosity Average, %</b>	<b>Sw Average, %</b>
<b>Zone A</b>	Limestone	1226-1237	1948-1959	12	5,2	89,4
<b>Zone B</b>	Dolomite	1238-1245	1960-1967	8	22,5	23,4
<b>Zone C</b>	Dolomite	1246-1254	1968-1976	9	13,2	70,4
<b>Zone D</b>	Limestone	1255-1268	1978-1991	14	1,3	100,0
<b>Well K2</b>						
	<b>Lithology</b>	<b>Elevation Interval, m</b>	<b>Depth Interval, m</b>	<b>Thickness, m</b>	<b>Porosity Average, %</b>	<b>Sw Average, %</b>
<b>Zone A</b>	Limestone	1199-1210	1928-1939	12	5,7	82,8
<b>Zone B</b>	Dolomite	1211-1220	1940-1949	10	26,0	18,5
<b>Zone C</b>	Dolomite	1221-1231	1950-1960	11	18,3	59,4
<b>Zone D</b>	Limestone	1232-1248	1961-1977	17	7,4	99,3
<b>Well K3</b>						
	<b>Lithology</b>	<b>Elevation Interval, m</b>	<b>Depth Interval, m</b>	<b>Thickness, m</b>	<b>Porosity Average, %</b>	<b>Sw Average, %</b>
<b>Zone A</b>	Limestone	1199-1210	1953-1964	12	5,5	82,1
<b>Zone B</b>	Dolomite	1211-1219	1965-1973	9	27,3	19,8
<b>Zone C</b>	Dolomite	1220-1231	1974-1985	12	18,3	77,3
<b>Zone D</b>	Limestone	1232-1248	1986-2002	17	5,2	99,3
<b>Well K9</b>						
	<b>Lithology</b>	<b>Elevation Interval, m</b>	<b>Depth Interval, m</b>	<b>Thickness, m</b>	<b>Porosity Average, %</b>	<b>Sw Average, %</b>
<b>Zone A</b>	Limestone	1220-1227	1948-1955	8	2,9	92,6
<b>Zone B</b>	Dolomite	1228-1235	1956-1963	8	23,8	28,1
<b>Zone C</b>	Dolomite	1236-1247	1964-1975	12	16,6	56,8

These calculated values were then distributed throughout the reservoir by the help of SURFER program with the option of krigging method (Figure 6.2, 6.3 and 6.4).

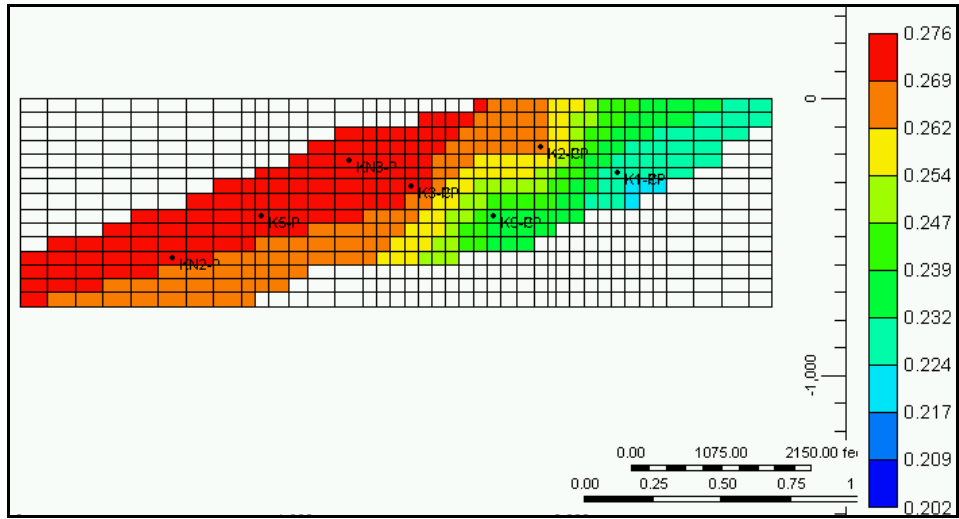


Figure 6.2 Porosity map of zone B, fraction

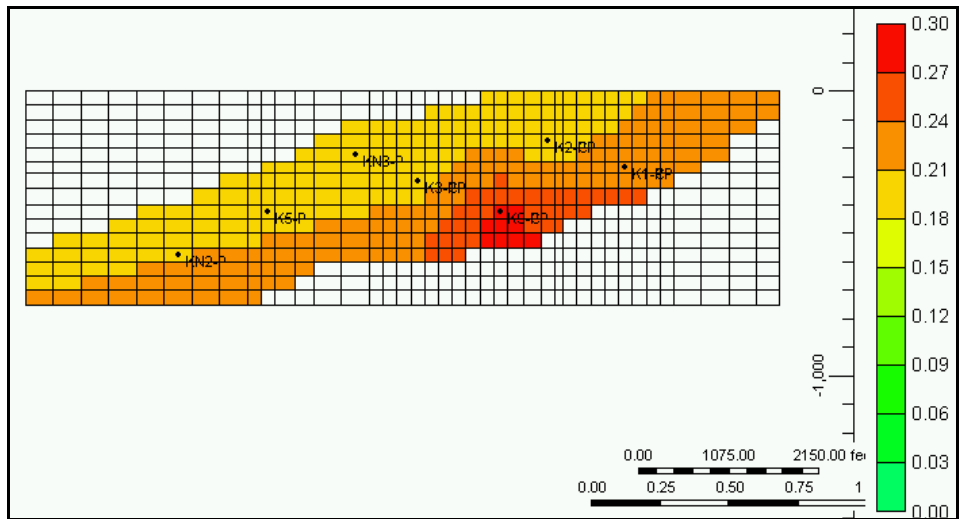
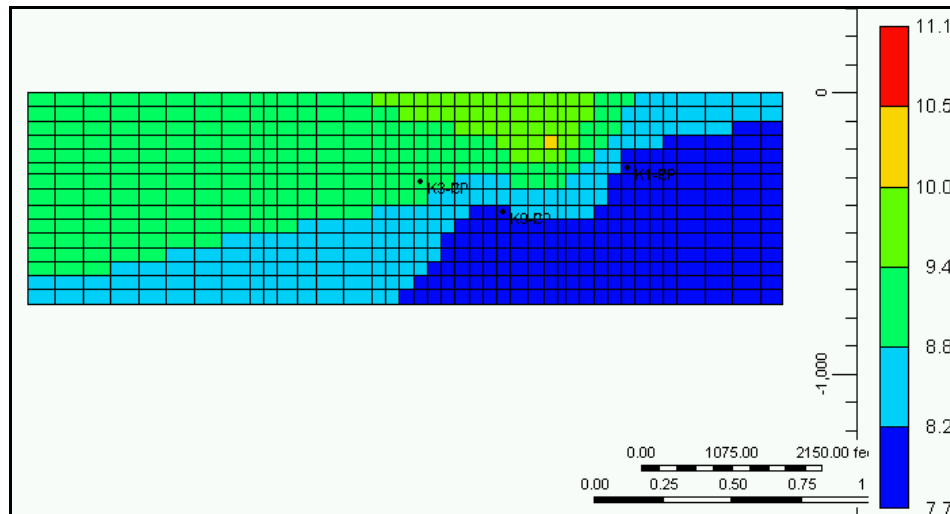


Figure 6.3 Water saturation map zone B, fraction



**Figure 6.4 Thickness map of zone B, m**

### 6.1.3 Permeability

Permeability, the ease at which fluid flows through a rock, determines the fluid dynamics of the reservoir. High permeability will allow high injection rates for CO<sub>2</sub> into a single well. High permeability will also allow CO<sub>2</sub> to move out more quickly within the reservoir, which is also favorable to sequestration.

Core data and DST results were two options to obtain the permeability of the reservoir rock. DST analysis was done by the help of SAPHIR program and permeability was calculated as 56 md for zone B (Appendix A.1). Permeability of zone B was also obtained from core data as 60 md. Both DST and core data gave similar results. Since the core data is more reliable and it was taken from the different locations of the field, permeability map data of the field was generated by the relation (Figure 6.1) between porosity and liquid permeability acquired from core data and with the help of SURFER program (Figure 6.5).

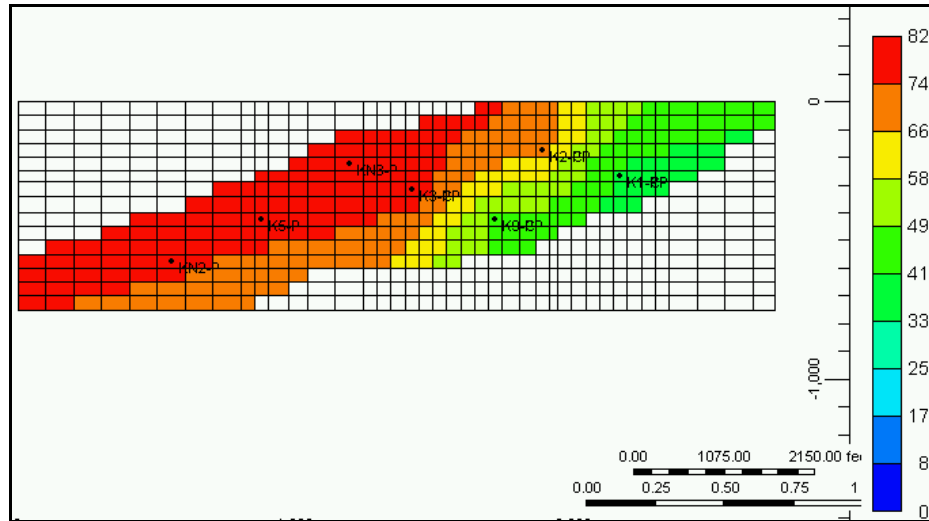


Figure 6.5 Permeability map of zone B, md

#### 6.1.4 Relative Permeability

Relative permeability is defined as the permeability of one phase relative to another when two or more fluids flowing together. It is an important factor since it determines the mobility ratio and the injectivity of the CO<sub>2</sub> in a CO<sub>2</sub> sequestration process.

The relative permeability for simultaneous flow of oil and water as well as liquid and gas should be defined carefully. Relative permeability of oil and water, already obtained from the core analysis, was correlated during history matching run by trial-and-error approach. Unfortunately, there was no liquid and gas relative permeability data. Thus, gas relative permeability curve was generated by CMG/STARS's corresponding relative permeability correlation tools. It is assumed that the curves are the same for drainage and imbibitions. The capillary pressure among the oil, water and CO<sub>2</sub> are neglected for this study. Figures 6.6 and 6.7 are water and gas relative permeability curves, respectively.

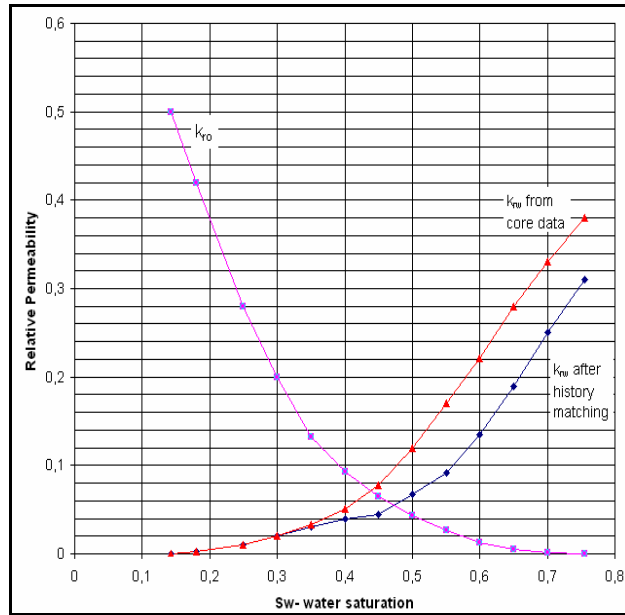


Figure 6.6 Relative permeability curves for oil and water, field K

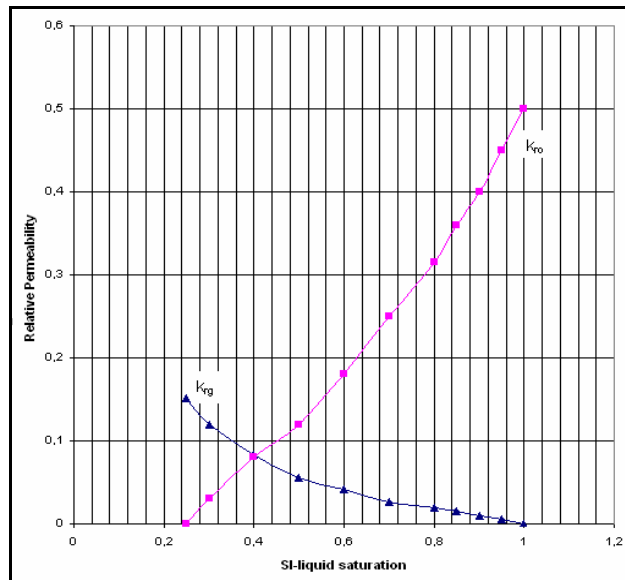


Figure 6.7 Relative permeability curves for oil and gas

## 6.2 Reserve Estimation

After obtaining reservoir rock and fluid properties, the next stage was the reserve estimation of the field. Reserve estimation can be done by volumetric and probabilistic approach. Original oil in place (OOIP) by volumetric method is calculated by the following formula;

$$OOIP = A * h * \varnothing * (1 - S_{wi}) / (B_{oi} * 5.615) \quad 6.1$$

where;

A : area, ft<sup>2</sup>

h : net thickness, ft

$\varnothing$  : porosity, fraction

S<sub>wi</sub> : initial water saturation, fraction

B<sub>oi</sub> : initial formation volume factor of oil, bbl/STB

The area encompassed by water oil contact was planimetered as 10,062,360 ft<sup>2</sup> from the structural map. Net thickness of the reservoir zone is 23 ft. Average porosity and initial water saturation are both 0.25. Thus, OOIP of the field K was calculated as 7,5 MMSTB by volumetric method.

Pertophysical parameters porosity, saturation and thickness have some sort of vagueness due to their characteristics and measurement shortcomings [48]. At this point, probabilistic techniques are used to estimate and classify reserves. Monte Carlo simulation, which is one of these techniques, considers entire ranges of the variables of original oil in place (OOIP) formula.

Probabilistic reserve calculation is done by @Risk software program that is used for implementing Monte Carlo method. Log data for the reservoir was considered as the sample set for the simulation. Outcomes of Monte Carlo simulation were given in Appendix B.1. At the end of simulation it was found that Field K has P50 reserves as 7 MMSTB which is close to volumetric approach (Table 6.2). Probable and Possible Reserves are given below (Figure 6.8 and Table 6.3).

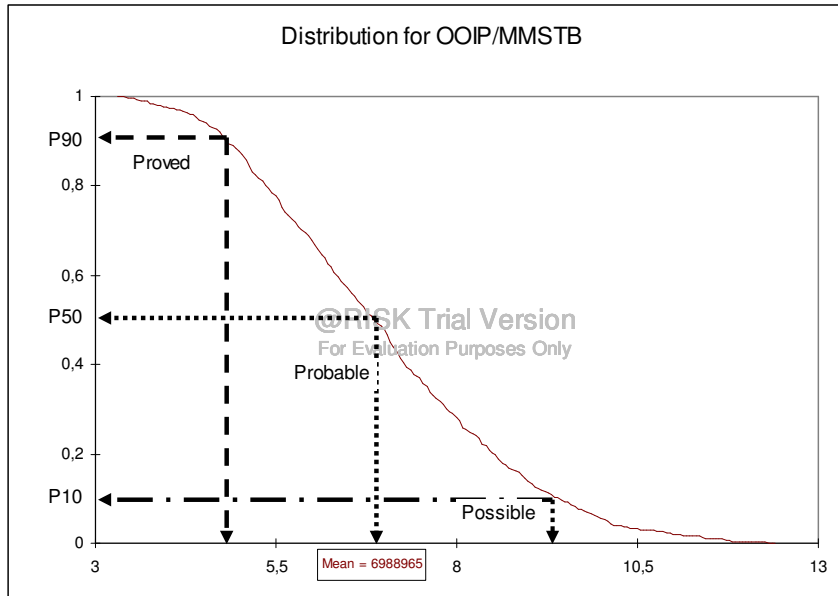


Figure 6.8 Probability density function of field K reserve

Table 6.2 Comparison of reserve estimation methods

	Reserve (OOIP)
Deterministic Method	7.5 Million STB
Probabilistic Method	7.0 Million STB

**Table 6.3 OOIP results of field K by probabilistic estimation**

<b>Possible Reserve (90%)</b>	9.4 Million STB
<b>Probable Reserve (50%)</b>	7.0 Million STB
<b>Proven Reserve (10%)</b>	4.8 Million STB

TPAO also calculated the volumetric OOIP as 7.5 MMSTB [41]

### **6.3 Description of the Reservoir Model**

The reservoir modeled in this study is a heterogeneous reef composed of two distinct carbonate formations. The upper formation is limestone (zone A) with an average thickness of 11 m. It is tight and it has an average porosity of 0.05 and average permeability of 0.06 md. The lower formation (zone B) is dolomite with an average thickness of 9 ft, average porosity of 0.25, and average permeability of 60 md. Vertical to horizontal permeability was assumed as 0.3. The reservoir shape is anticline, and it is bounded by faults and underlain by an aquifer (zone C) (Figure 6.9). Oil, which is produced from the lower formation, has a viscosity of 5 cp and gravity of 32° API. The average reservoir depth is 1950 m (1230 m subsea depth) with an initial pressure and temperature of 2520 psi and 148 °F, respectively. Interpreted rock and fluid data were merged into the CMG/STARS numerical simulator, which was used for simulation studies. The reservoir model (Figure 6.10) was divided into grids in cartesian coordinates which contains a total of 2400 blocks (40x15x4) of which 668 are inactive blocks. Although the reservoir contains two distinct layers (upper and lower formations), the lower one (zone B) was divided into 3 equal grid layers with the same properties to observe the vertical movements of CO<sub>2</sub> since it was injected from the most bottom layer (Zone B3) for all simulation runs of this study.

There was an aquifer (zone C) at the bottom of Zone B. This was implemented by using the data related to aquifer system into CMG simulator. No flow boundary condition was assumed at the boundaries surrounding the reservoir. The edges of the reservoir could also be considered as a constant pressure boundary. But there was no information along the boundaries of the reservoir.

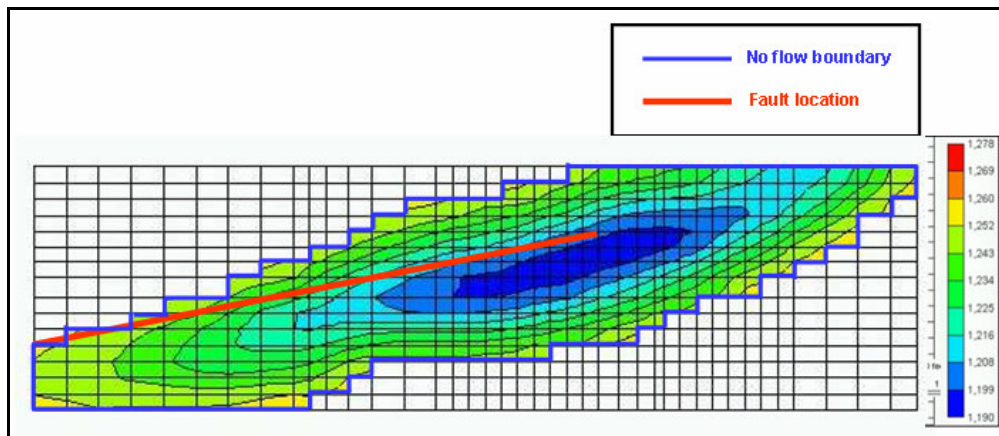


**Figure 6.9 2D structural map of field K showing boundary conditions and fault locations (subsea depths in m)**

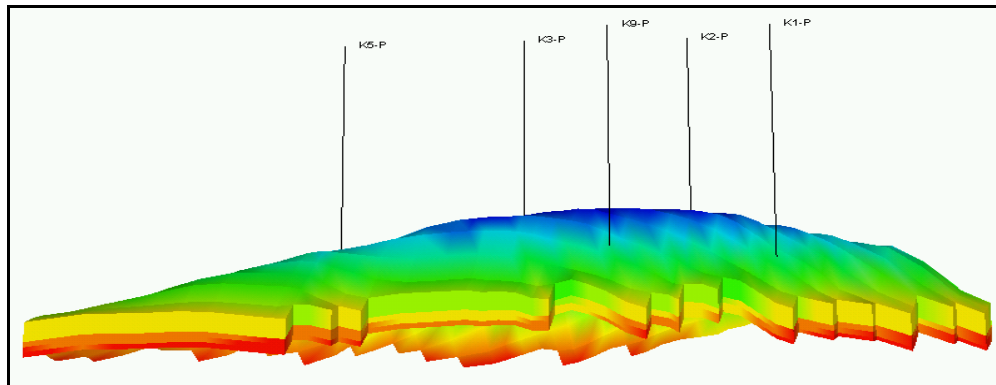


**Figure 6.10 3D view of reservoir with well locations**

## 6.4 Simulation Runs

Oil recovery behavior and CO<sub>2</sub> sequestration capacity of the Field K were examined in different simulation scenarios (Table 6.4). Different scenarios were analyzed to determine highest oil recovery and highest CO<sub>2</sub> storage strategies.

**Table 6.4 Summary of simulation runs**

SIMULATION RUNS				
<b>Run 1: History Matching</b>				
Wells in Production/Date	Wells in Injection/Date	CO <sub>2</sub> Injection Rate, m <sup>3</sup> /day/well	Constraints	Comments
K1/20.08.1982 - 01.06.1986 (abandoned) K1/01.01.1987 (reproduction) - 01.02.2006 K2/15.11.1982 - 01.02.2006 K3/15.02.1983 - 01.02.2006 K9/01.08.1986 - 01.06.1988 (abandoned)				• TPAO data was matched with simulation data.
<b>Run 2: Base Run</b>				
Wells in Production/Date	Wells in Injection/Date	CO <sub>2</sub> Injection Rate, m <sup>3</sup> /day/well	Constraints	Comments
K1/20.08.1982 - 01.06.1986 (abandoned) K1/01.01.1987 (reproduction) - 01.02.2036 K2/15.11.1982 - 01.02.2006 K3/15.02.1983 - 01.02.2006 K9/01.08.1986 - 01.06.1988 (abandoned) + K1/01.03.2006 - 01.03.2036 K2/01.03.2006 - 01.03.2036 K3/01.03.2006 - 01.03.2036			• Minimum Surface Oil Production Rate for all producing wells were 1 m <sup>3</sup> /day (6.290 barrel/day).  • Well bottomhole flowing pressure for all producing wells were kept at 10000 kPa (1450 psi) after 01.03.2006.	• TPAO current production scenario was pursued for 30 years.
<b>Run 3: CO<sub>2</sub> SEQ.</b>				
Wells in Production/Date	Wells in Injection/Date	CO <sub>2</sub> Injection Rate, m <sup>3</sup> /day/well	Constraints	Comments
K1/20.08.1982 - 01.06.1986 (abandoned) K1/01.01.1987 (reproduction) - 01.02.2036 K2/15.11.1982 - 01.02.2006 K3/15.02.1983 - 01.02.2006 K9/01.08.1986 - 01.06.1988 (abandoned)	K1/01.03.2006 - 01.03.2036 K2/01.03.2006 - 01.03.2036 K3/01.03.2006 - 01.03.2036 K5/01.03.2006 - 01.03.2036 K9/01.03.2006 - 01.03.2036	6000 6000 6000 6000 6000	• CO <sub>2</sub> was injected at 17500 kPa (2537 psi) (close to initial reservoir pressure).  • The wells were shut when pressure reaches to 20000 kPa (2900 psi).	• CO <sub>2</sub> was only injected for sequestration purpose after 2006.

Table 6.4 (continued)

Run 4a: CO <sub>2</sub> EOR/SEQ.				
Wells in Production/Date	Wells in Injection/Date	CO <sub>2</sub> Injection Rate, m <sup>3</sup> /day/well	Constrains	Comments
K1/20.08.1982 - 01.06.1986 (abandoned) K1/01.01.1987 (reproduction) - 01.02.2036 K2/15.11.1982 - 01.02.2006 K3/15.02.1983 - 01.02.2006 K9/01.08.1986 - 01.06.1988 (abandoned) + K1/01.03.2006 - 01.03.2036 K2/01.03.2006 - 01.03.2036 K3/01.03.2006 - 01.03.2036	K5/01.03.2006 - 01.03.2036 K9/01.03.2006 - 01.03.2036	6000 6000	<ul style="list-style-type: none"> <li>• Minimum Surface Oil Production Rate for all producing wells were 1 m<sup>3</sup>/day</li> <li>• Well bottomhole flowing pressure for all producing wells were kept at 10000 kPa (1450 psi) after 01.03.2006.</li> <li>• CO<sub>2</sub> was injected at 17500 kPa (2537 psi) (close to initial reservoir pressure).</li> <li>• The wells were shut when pressure reaches to 20000 kPa (2900 psi).</li> <li>• <b>No gas oil ratio (GOR) constraint was defined.</b></li> </ul>	<ul style="list-style-type: none"> <li>• CO<sub>2</sub> was injected for EOR and sequestration puposes with existing TPAO wells.</li> <li>• CO<sub>2</sub> was injected into the abandoned wells.</li> <li>• Injection and production was immediately started 2006.</li> </ul>
Run 4b: CO <sub>2</sub> EOR/SEQ.				
Wells in Production/Date	Wells in Injection/Date	CO <sub>2</sub> Injection Rate, m <sup>3</sup> /day/well	Constrains	Comments
K1/20.08.1982 - 01.06.1986 (abandoned) K1/01.01.1987 (reproduction) - 01.02.2036 K2/15.11.1982 - 01.02.2006 K3/15.02.1983 - 01.02.2006 K9/01.08.1986 - 01.06.1988 (abandoned) + K1/01.03.2006 - 01.03.2036 K2/01.03.2006 - 01.03.2036 K3/01.03.2006 - 01.03.2036	K5/01.03.2006 - 01.03.2036 K9/01.03.2006 - 01.03.2036	6000 6000	<ul style="list-style-type: none"> <li>• Minimum Surface Oil Production Rate for all producing wells were 1 m<sup>3</sup>/day</li> <li>• Well bottomhole flowing pressure for all producing wells were kept at 10000 kPa (1450 psi) after 01.03.2006.</li> <li>• CO<sub>2</sub> was injected at 17500 kPa (2537 psi) (close to initial reservoir pressure).</li> <li>• The wells were shut when pressure reaches to 20000 kPa (2900 psi).</li> <li>• <b>(GOR) constraint was 500 m<sup>3</sup>/m<sup>3</sup>.</b></li> </ul>	
Run 4c: CO <sub>2</sub> EOR/SEQ.				
Wells in Production/Date	Wells in Injection/Date	CO <sub>2</sub> Injection Rate, m <sup>3</sup> /day/well	Constrains	Comments
K1/20.08.1982 - 01.06.1986 (abandoned) K1/01.01.1987 (reproduction) - 01.02.2036 K2/15.11.1982 - 01.02.2006 K3/15.02.1983 - 01.02.2006 K9/01.08.1986 - 01.06.1988 (abandoned) + K1/01.03.2006 - 01.03.2036 K2/01.03.2006 - 01.03.2036 K3/01.03.2006 - 01.03.2036	K5/01.03.2006 - 01.03.2036 K9/01.03.2006 - 01.03.2036	6000 6000	<ul style="list-style-type: none"> <li>• Minimum Surface Oil Production Rate for all producing wells were 1 m<sup>3</sup>/day</li> <li>• Well bottomhole flowing pressure for all producing wells were kept at 10000 kPa (1450 psi) after 01.03.2006.</li> <li>• CO<sub>2</sub> was injected at 17500 kPa (2537 psi) (close to initial reservoir pressure).</li> <li>• The wells were shut when pressure reaches to 20000 kPa (2900 psi).</li> <li>• <b>(GOR) constraint was 100 m<sup>3</sup>/m<sup>3</sup>.</b></li> </ul>	

Table 6.4 (continued)

Run 5a: CO <sub>2</sub> EOR/SEQ.				
Wells in Production/Date	Wells in Injection/Date	CO <sub>2</sub> Injection Rate, m <sup>3</sup> /day/well	Constrains	Comments
K1/20.08.1982 - 01.06.1986 (abandoned) K1/01.01.1987 (reproduction) - 01.02.2036 K2/15.11.1982 - 01.02.2006 K3/15.02.1983 - 01.02.2006 K9/01.08.1986 - 01.06.1988 (abandoned) + K2/01.03.2006 - 01.03.2036 K3/01.03.2006 - 01.03.2036	K1/01.03.2006 - 01.03.2026 KN1/01.03.2006 - 01.03.2026	6000 6000	<ul style="list-style-type: none"> <li>• Minimum Surface Oil Production Rate for all producing wells were 1 m<sup>3</sup>/day</li> <li>• Well bottomhole flowing pressure for all producing wells were kept at 10000 kPa (1450 psi) after 01.03.2006.</li> <li>• CO<sub>2</sub> was injected at 17500 kPa (2537 psi) (close to initial reservoir pressure).</li> <li>• The wells were shut when pressure reaches to 20000 kPa (2900 psi).</li> <li>• (GOR) constraint was 500 m<sup>3</sup>/m<sup>3</sup>.</li> </ul>	<ul style="list-style-type: none"> <li>• CO<sub>2</sub> was injected from the corners of the reservoir (KN1 is a new well).</li> <li>• CO<sub>2</sub> injection was started immediately after TPAO production.</li> <li>• 20 years of CO<sub>2</sub> sequestration.</li> </ul>
Run 5b: CO <sub>2</sub> EOR/SEQ.				
Wells in Production/Date	Wells in Injection/Date	CO <sub>2</sub> Injection Rate, m <sup>3</sup> /day/well	Constrains	Comments
K1/20.08.1982 - 01.06.1986 (abandoned) K1/01.01.1987 (reproduction) - 01.02.2036 K2/15.11.1982 - 01.02.2006 K3/15.02.1983 - 01.02.2006 K9/01.08.1986 - 01.06.1988 (abandoned) + K2/01.03.2006 - 01.03.2036 K3/01.03.2006 - 01.03.2036	K1/01.03.2011 - 01.03.2031 KN1/01.03.2011 - 01.03.2031	6000 6000	<ul style="list-style-type: none"> <li>• Minimum Surface Oil Production Rate for all producing wells were 1 m<sup>3</sup>/day</li> <li>• Well bottomhole flowing pressure for all producing wells were kept at 10000 kPa (1450 psi) after 01.03.2006.</li> <li>• CO<sub>2</sub> was injected at 17500 kPa (2537 psi) (close to initial reservoir pressure).</li> <li>• The wells were shut when pressure reaches to 20000 kPa (2900 psi).</li> <li>• (GOR) constraint was 500 m<sup>3</sup>/m<sup>3</sup>.</li> </ul>	<ul style="list-style-type: none"> <li>• CO<sub>2</sub> injection was started after 5 years of oil production.</li> </ul>
Run 5c: CO <sub>2</sub> EOR/SEQ.				
Wells in Production/Date	Wells in Injection/Date	CO <sub>2</sub> Injection Rate, m <sup>3</sup> /day/well	Constrains	Comments
K1/20.08.1982 - 01.06.1986 (abandoned) K1/01.01.1987 (reproduction) - 01.02.2036 K2/15.11.1982 - 01.02.2006 K3/15.02.1983 - 01.02.2006 K9/01.08.1986 - 01.06.1988 (abandoned) + K2/01.03.2006 - 01.03.2036 K3/01.03.2006 - 01.03.2036	K1/01.03.2016 - 01.03.2036 KN1/01.03.2016 - 01.03.2036	6000 6000	<ul style="list-style-type: none"> <li>• Minimum Surface Oil Production Rate for all producing wells 1 m<sup>3</sup>/day</li> <li>• Well bottomhole flowing pressure for all producing wells 10000 kPa( 1450 psi)</li> <li>• Injection Pressure 17500 kPa (close to initial reservoir pressure)</li> <li>• Shut the wells when pressure reaches to 20000 kPa.</li> <li>• Shut the production wells when gas oil ratio(GOR) reaches 500 m<sup>3</sup>/m<sup>3</sup></li> </ul>	<ul style="list-style-type: none"> <li>• CO<sub>2</sub> injection was started after 10 years oil production.</li> </ul>

**Table 6.4(continued)**

Run 6: Field Development&CO <sub>2</sub> EOR/SEQ				
Wells in Production/Date	Wells in Injection/Date	CO <sub>2</sub> Injection Rate, m <sup>3</sup> /day/well	Constrains	Comments
K1/20.08.1982 - 01.06.1986 (abandoned)	K1/01.03.2016 - 01.03.2036	6000	<ul style="list-style-type: none"> <li>• Minimum Surface Oil Production Rate for all producing wells were 1 m<sup>3</sup>/day</li> <li>• Well bottomhole flowing pressure for all producing wells were kept at 10000 kPa (1450 psi) after 01.03.2006.</li> <li>• CO<sub>2</sub> was injected at 17500 kPa (2537 psi) (close to initial reservoir pressure).</li> <li>• The wells were shut when pressure reaches to 20000 kPa (2900 psi).</li> <li>• (GOR) constraint was 500 m<sup>3</sup>/m<sup>3</sup>.</li> </ul>	<ul style="list-style-type: none"> <li>• CO<sub>2</sub> injection was started after 10 years of oil production.</li> <li>• New injection and production wells were drilled on the other side of the fault.</li> </ul>
K1/01.01.1987 (reproduction) - 01.02.2036	KN1/01.03.2016 - 01.03.2036	6000		
K2/15.11.1982 - 01.02.2006	KN3/01.03.2016 - 01.03.2036	6000		
K3/15.02.1983 - 01.02.2006				
K9/01.08.1986 - 01.06.1988 (abandoned)				
+				
K1/01.03.2006 - 01.03.2016				
K2/01.03.2006 - 01.03.2036				
K3/01.03.2006 - 01.03.2036				
K9/01.03.2006 - 01.03.2036				
K5/01.03.2006 - 01.03.2036				
KN1/01.03.2006 - 01.03.2016				
KN2/01.03.2006 - 01.03.2036				

### 6.4.1 Run 1: History Matching

History matching process was used to verify simulation data with the field data. Oil rate and cumulative water production data were matched simultaneously using the oil rate (Figure 6.11) as the controlling parameter. Figure 6.12 shows the final results of the history-matching for the field and simulated data. Oil water relative permeability data (Figure 6.6) was obtained at the end of history matching study by a trial-and-error process.

During the history matching, the simulator calculated the bottom hole flowing pressure at each well (Figure 6.13) that was necessary to produce the given oil production rate, and then used this bottom hole pressure to calculate the water production at each well. Since the simulator was able to predict the cumulative water production within a reasonable degree of accuracy, the corresponding flowing bottom hole pressure at the end history matching were thought to be acceptable. Thus, an average value of well bottom hole pressure was taken as 10000 kPa (1450 psi) for further simulation runs.

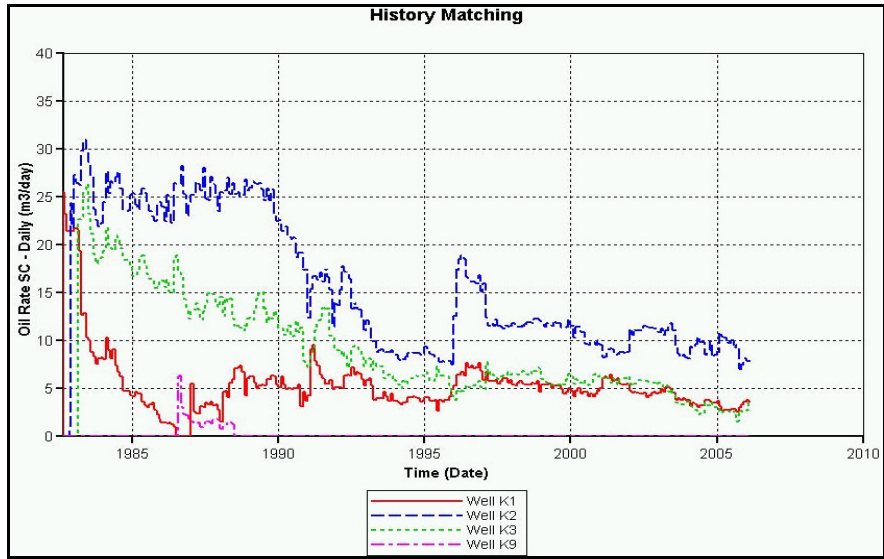


Figure 6.11 Oil production rates of the wells, Run 1, history matching

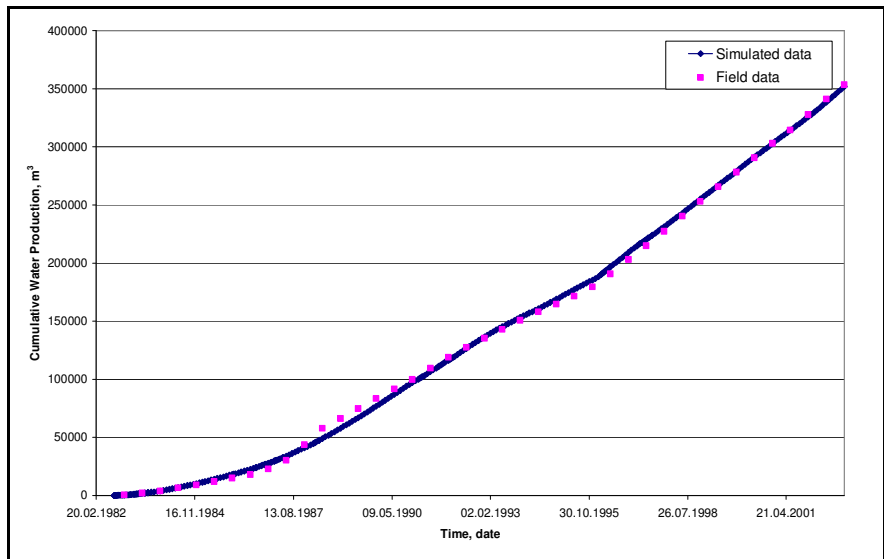
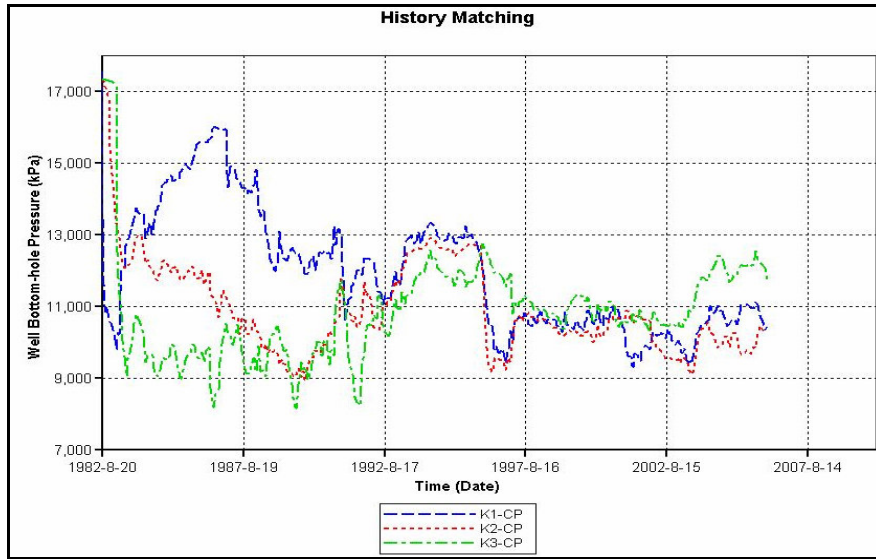


Figure 6.12 Cumulative water production comparison between the field data and simulator results, Run 1, history matching



**Figure 6.13 Well bottom-hole pressures of the wells, Run 1, history matching**

Figure 6.14 gives the outcomes of the history matching study in terms of field cumulative oil and water productions and reservoir pressure after depletion. The primary depletion was from 17375 kPa (2520 psi) to 12000 kPa (1740 psi) (pressure of grid block 26,7,2) during 24 years, with a cumulative production of 258791 sm<sup>3</sup> (1,6 MMSTB). The oil recovery is 23% of OOIP.

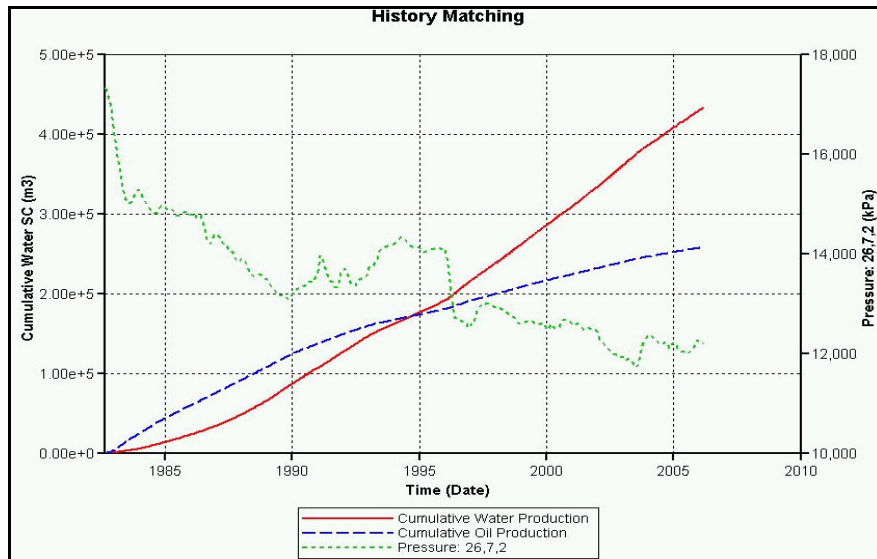


Figure 6.14 Field production summary after primary depletion, Run 1, history matching

#### 6.4.2 Run 2: Field Production Continued (Base Run)

In Run 2, TPAO oil production was continued from 3 wells (Figure 6.15) after 2006 till 2036 without any CO<sub>2</sub> injection. Well bottom-hole pressure was taken as 10000 kPa and minimum oil rate constraint was taken as 1 m<sup>3</sup>/day (6 barrel/day) in the wells. Figures 6.16 through 6.18 present the results for this run. Well K1 was closed in 2021 since the oil rate reached to the minimum rate constraint defined. The cumulative oil production for Run 2 was 340176 sm<sup>3</sup> with a total oil recovery of 31% of OOIP for 30 years of oil production. The results of Run 2 will be used for making comparison with the results of other simulation runs.

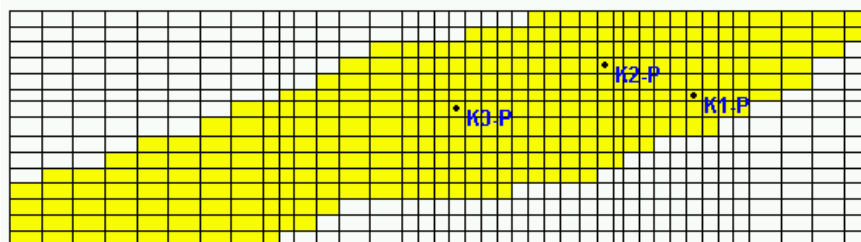


Figure 6.15 Location of production wells, Run2, field production continued

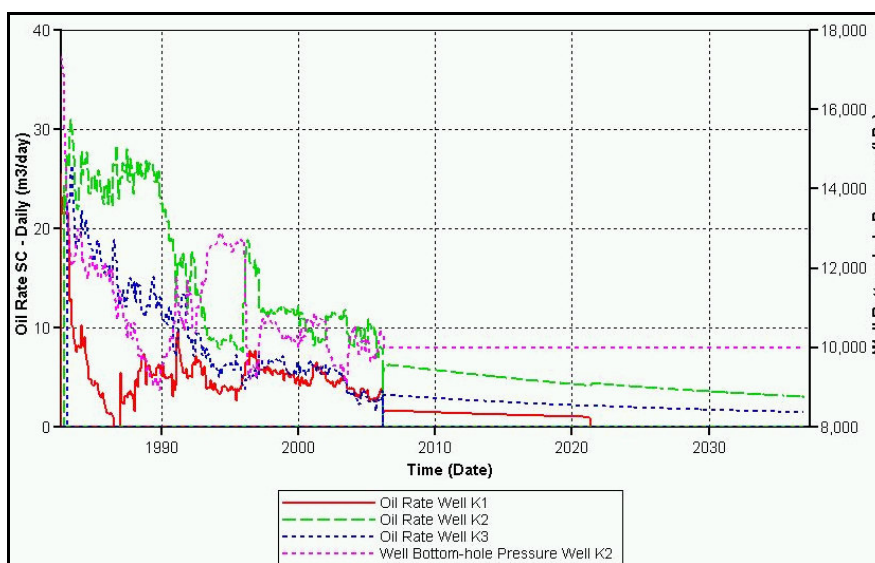


Figure 6.16 Oil production rates of the wells, Run 2, field production continued

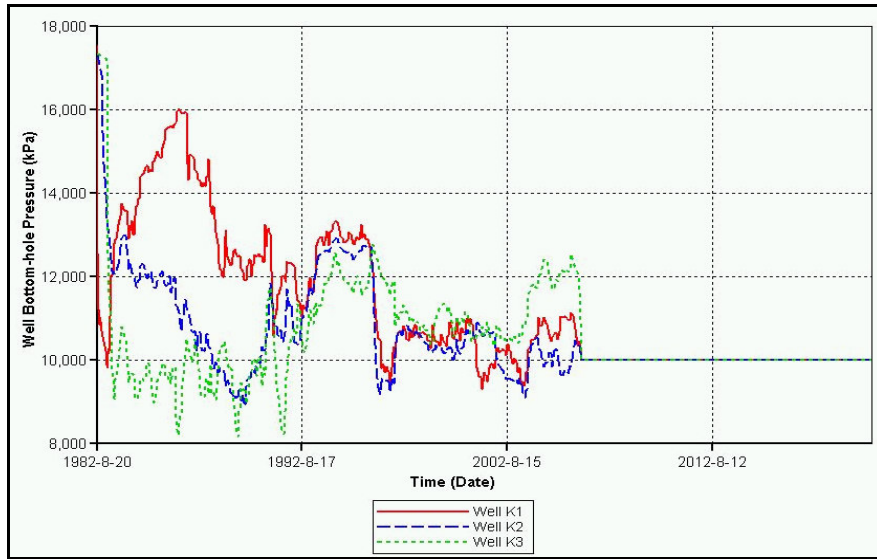


Figure 6.17 Well bottom-hole pressures of the wells, Run 2, field production continued

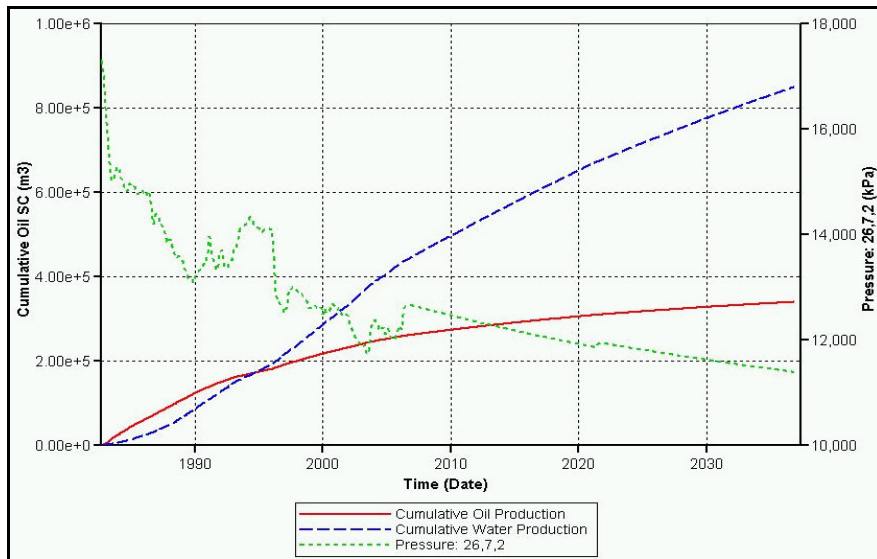


Figure 6.18 Field production summary, Run 2, field production continued

### **6.4.3 Run 3: CO<sub>2</sub> Sequestration (SEQ.)**

This scenario considered only the injection of CO<sub>2</sub> injection into all wells. In other words, oil production was not allowed from the wells. CO<sub>2</sub> injection was implemented in 2006, immediately after primary oil depletion. CO<sub>2</sub> was injected into 5 wells, 3 of which (K1, K2, and K3) were currently producing, and 2 of which (K5 and K9) were abandoned due to economical reasons (Figure 6.19). Maximum CO<sub>2</sub> injection rate was found out to be 6000 m<sup>3</sup>/day/well based on series of simulation runs. CO<sub>2</sub> was injected at supercritical state, at a pressure of 17500 kPa and temperature of 64 °C, close to initial reservoir conditions. The maximum average reservoir pressure constraint was assumed as 20000 kPa (approximately 15% more of initial reservoir pressure) to make sure that the formation was not fractured during CO<sub>2</sub> injection.

Results are given in Figures 6.20 and 6.21. CO<sub>2</sub> injection was planned for a period of 30 years, but the simulation was terminated after 8 months since the reservoir pressure reached to 20000 kPa. Cumulative CO<sub>2</sub> injection into the reservoir was 300 MMSCF for a period of 8 months. CO<sub>2</sub> emission from an average power plant (500 MW) is 250 MMSCF/day. Thus, it was decided to focus on oil recovery while CO<sub>2</sub> was sequestered within the reservoir.

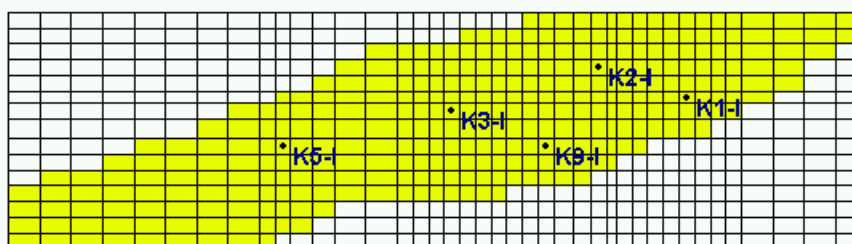


Figure 6.19 Location of injection wells, Run3, CO2 SEQ.

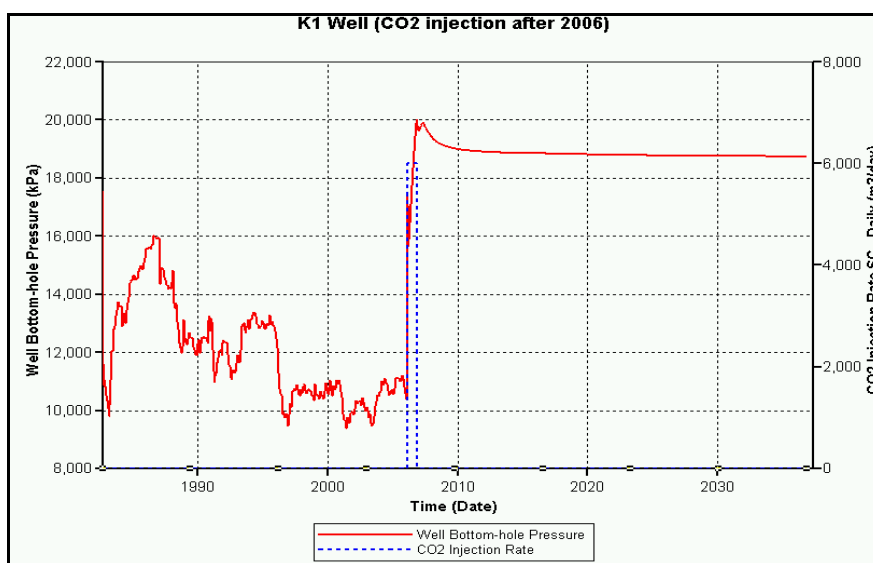


Figure 6.20 Well bottom hole pressure and CO<sub>2</sub> injection rate of Well K1, Run 3, CO<sub>2</sub> SEQ.

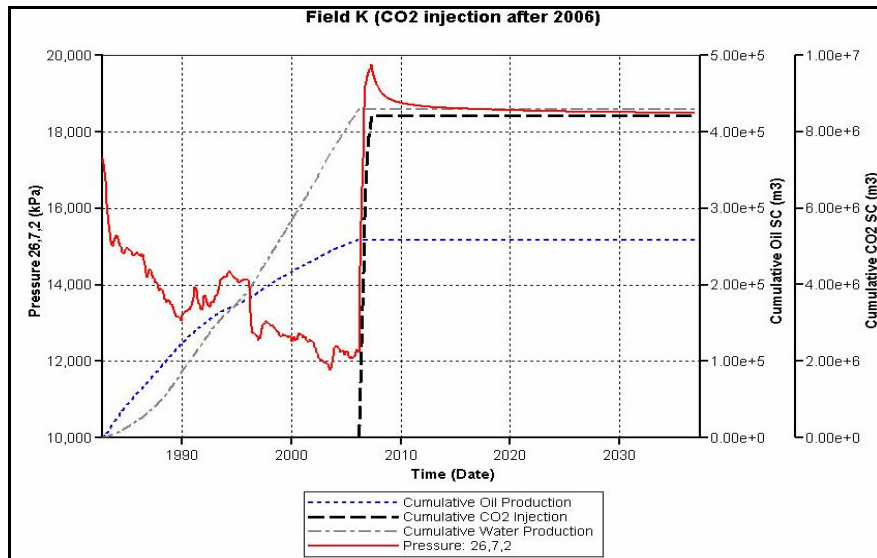
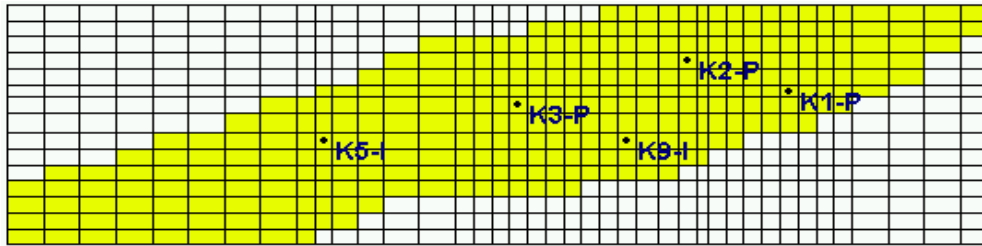


Figure 6.21 Field injection summary, Run 3, CO<sub>2</sub> SEQ.

#### 6.4.4 Run 4: CO<sub>2</sub> EOR/SEQ.

In this scenario oil recovery was studied during CO<sub>2</sub> injection. That gas oil ratio (GOR) was the controlling parameter whose effect on CO<sub>2</sub> EOR/SEQ performance was studied. Three cases, Run 4a, 4b and 4c were performed with different GOR constraints on production wells to find the best production and injection performance. In all cases, CO<sub>2</sub> injection was implemented in 2006 for a period of 30 years into the abandoned wells, K5 and K9, with the same rates as in Run 3. Oil was produced from K1, K2 and K3 wells (Figure 6.22).



**Figure 6.22 Location of injection and production wells, Run4, CO2 EOR/SEQ.**

Figures 6.23 through 6.31 present the outcomes for Run 4. Table 6.5 compares the cumulative water, oil and gas (CO<sub>2</sub>) production, and cumulative CO<sub>2</sub> injection for all cases for 30 years of CO<sub>2</sub> injection. The best case for oil recovery in this scenario was Run 4a in which no gas oil ratio constraint was defined for production wells. The cumulative oil production for Run 4a was 436371 sm<sup>3</sup> with a total oil recovery of 39% of OOIP. But, 82% of injected CO<sub>2</sub> were produced and decided to be recycled. Thus, high CO<sub>2</sub> and water production were problems at the well site such that installing of gas recycling and water treatment units could be uneconomical.

On the other hand, gas production was the least for Run 4c in which GOR constraint is defined as 100 m<sup>3</sup>/m<sup>3</sup> in production wells. Compared to Run 4a, only 1% of injected gas was produced on the well site, but the oil recovery of 26% of OOIP was lower compared to Run 4a. Moreover, simulation time was diminished, since the production wells were closed due to GOR constraint that was reached very quickly. Run 4b gave better results in terms of oil recovery and CO<sub>2</sub> sequestration. The cumulative oil production for Run 4b was 342524 sm<sup>3</sup> with a total oil recovery of 31% of OOIP and approximately 73% of the injected CO<sub>2</sub> was stored in the reservoir.

**Table 6.5 Comparison of simulations, Run 4, CO<sub>2</sub> EOR/SEQ.**

Run 4	Cum. Oil Prod.		Oil Recovery	Cum. CO <sub>2</sub> Inj.		Cum. CO <sub>2</sub> Prod.		CO <sub>2</sub> Prod/Inj
	sm <sup>3</sup>	STB	%OOIP	sm <sup>3</sup>	SCF	sm <sup>3</sup>	SCF	%
Case 4a (No GOR constraint)	436,371	2,744,773	39	1,31E+08	4,64E+09	1,08E+08	3,82E+09	82
Case 4b (GOR=500 m <sup>3</sup> /m <sup>3</sup> )	342,524	2,154,476	31	7,23E+07	2,55E+09	1,93E+07	6,83E+08	27
Case 4c (GOR=100 m <sup>3</sup> /m <sup>3</sup> )	287,837	1,810,494	26	3,70E+07	1,31E+09	4,09E+05	1,45E+07	1

The breakthrough of CO<sub>2</sub> was occurred at the production well K2 in less than 0.2 pore volumes (PV) of CO<sub>2</sub> injected. This result depends strongly on the heterogeneous distribution of the reservoir permeability. At breakthrough, the cumulative oil recovery was obtained as 25% of OOIP.

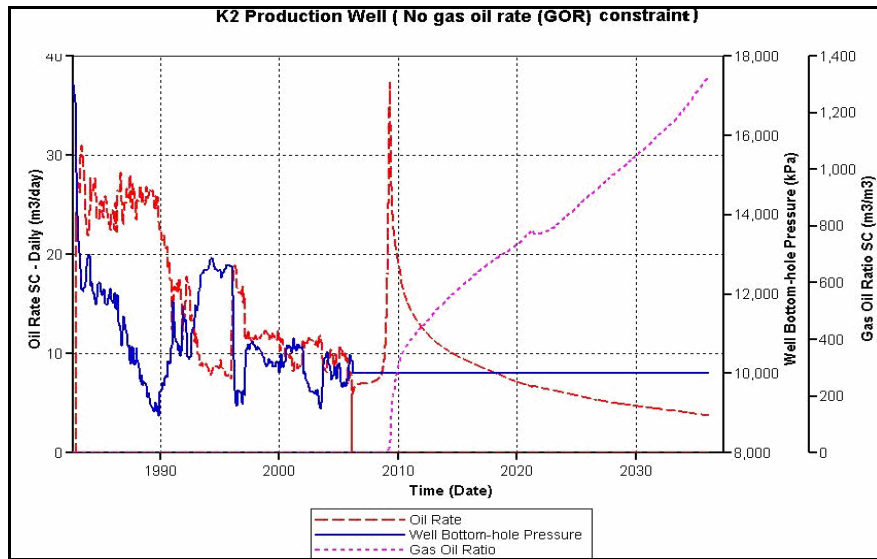


**Figure 6.23 Oil production rate of the well K2, Run 4a, CO<sub>2</sub>/EOR SEQ.**

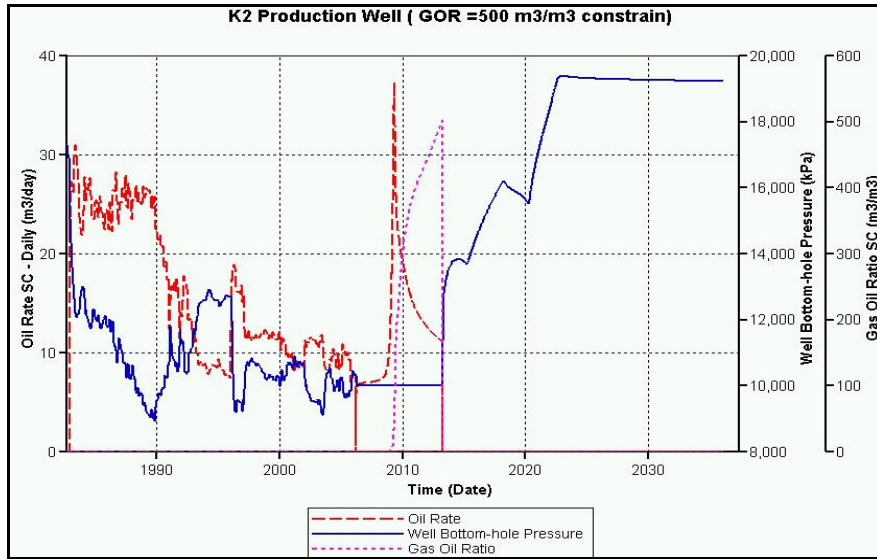


Figure 6.24 Oil production rate of the well K2, Run 4b, CO<sub>2</sub>/EOR SEQ.

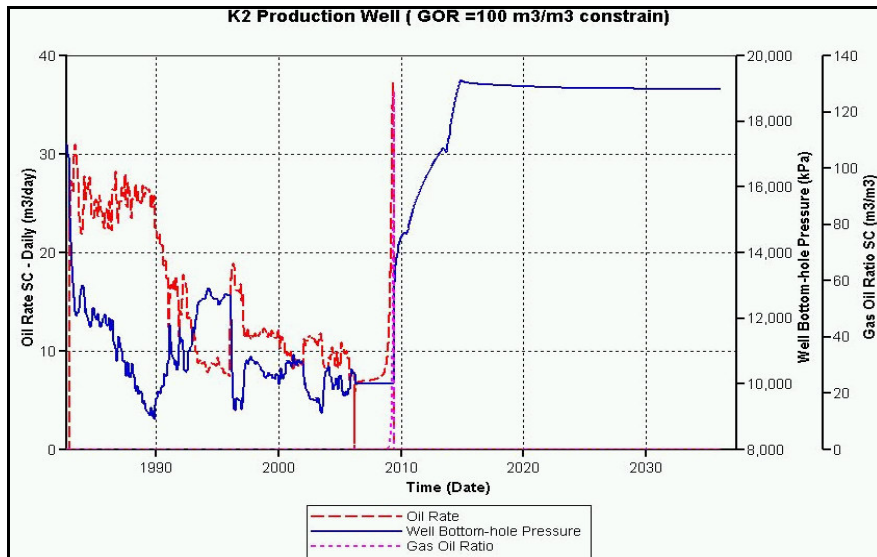


Figure 6.25 Oil production rate of the well K2, Run 4c, CO<sub>2</sub>/EOR SEQ.

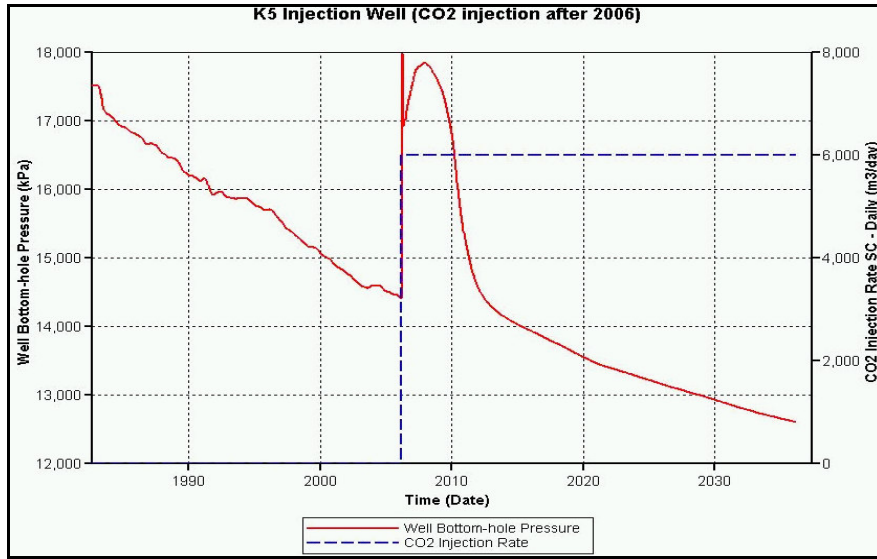


Figure 6.26 Well bottom hole pressure and CO<sub>2</sub> injection rate of Well K5, Run 4a, CO<sub>2</sub> EOR/SEQ.

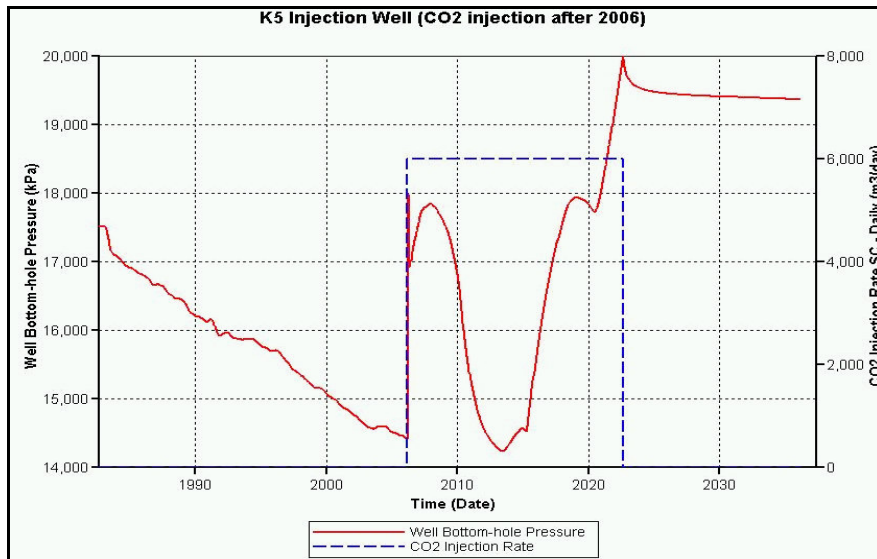


Figure 6.27 Well bottom hole pressure and CO<sub>2</sub> injection rate of Well K5, Run 4b, CO<sub>2</sub> EOR/SEQ.

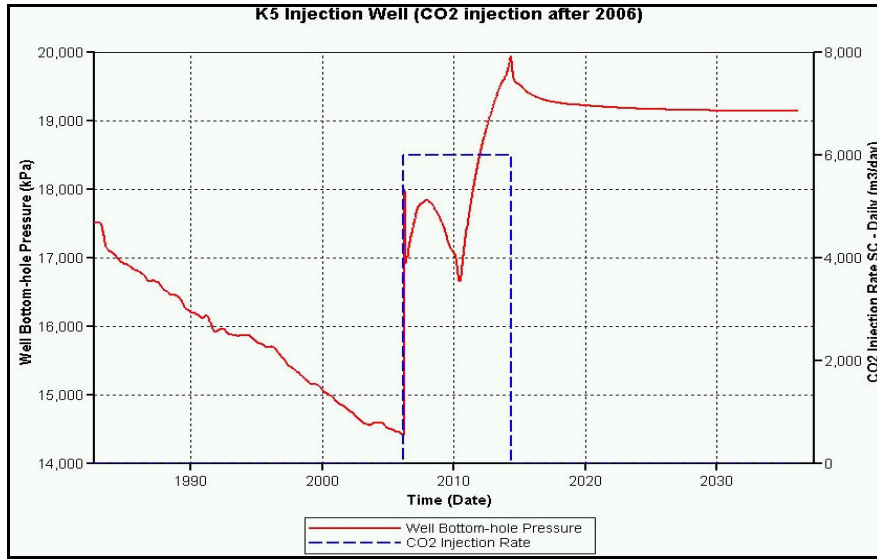


Figure 6.28 Well bottom hole pressure and CO<sub>2</sub> injection rate of Well K5, Run 4c, CO<sub>2</sub> EOR/SEQ.

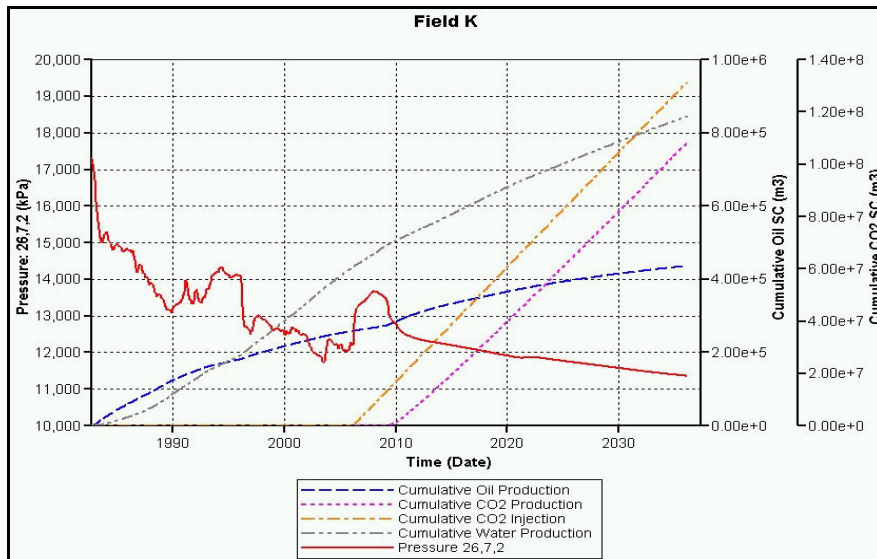


Figure 6.29 Field injection and production summary, Run 4a, CO<sub>2</sub> EOR/SEQ.

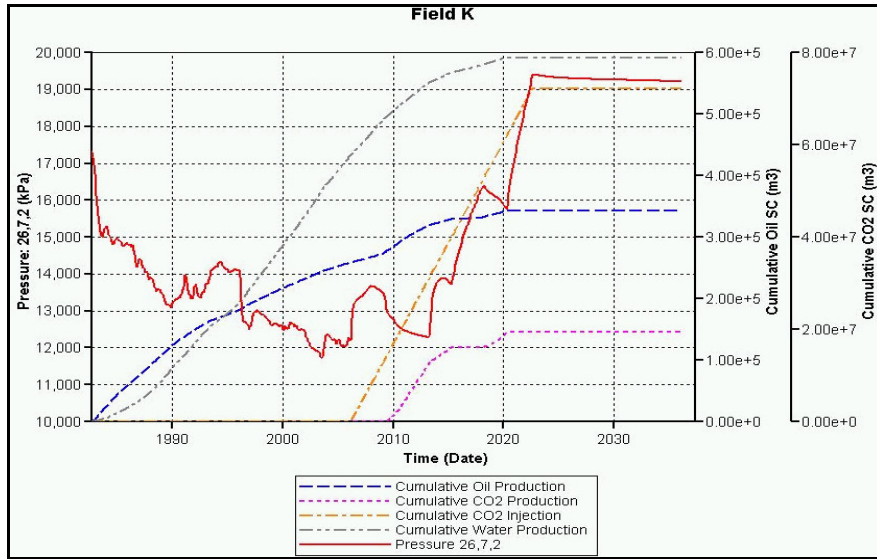


Figure 6.30 Field injection and production summary, Run 4b, CO<sub>2</sub> EOR/SEQ.

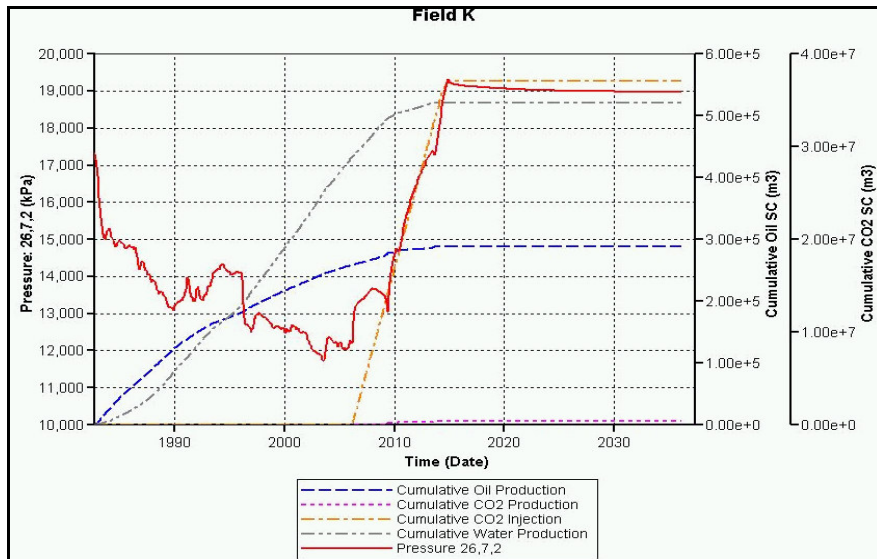


Figure 6.31 Field injection and production summary, Run 4c, CO<sub>2</sub> EOR/SEQ.

#### **6.4.5 Run 5: CO<sub>2</sub> EOR/SEQ**

The parameters of run 5 are similar to that of Run 4 except the location of production and injection wells that were redefined. Run 5 has three cases which have different starting dates for CO<sub>2</sub> injection between 2006 and 2036.

In this scenario, the producing K1 well was converted to injection well and a new well KN1 was drilled for CO<sub>2</sub> injection at the southwest of field K. K2 and K3 wells were still producing (Figure 6.32). CO<sub>2</sub> was injected at the rate of 6000 m<sup>3</sup>/day/well for 20 years. The GOR constraint was taken as 500 m<sup>3</sup>/m<sup>3</sup> for all production wells as in previous runs. CO<sub>2</sub> injection was started in 2006, 2011 and 2016 for runs 5a, 5b and 5c, respectively.

The results of simulation runs are presented in Tables 6.6 and 6.7 and Figures 6.33 through 6.43. It was observed that early injection of CO<sub>2</sub>, in 2006 for Run 5a, did not change the oil recovery (31.5 % of OOIP) significantly while producing 20 % of injected CO<sub>2</sub>. The cumulative water production was around 0.5 x10<sup>6</sup> m<sup>3</sup>.

In run 5c, CO<sub>2</sub> was injected in 2016 that was 20 years before the end of simulation. Although the amount of injected CO<sub>2</sub> was nearly same compared to the values of runs 5a and 5b, the oil recovery was 33.1% of OOIP and CO<sub>2</sub> production to injection ratio was 17%. Thus relatively higher amount of injected CO<sub>2</sub> was kept within the reservoir. CO<sub>2</sub> might contact with water and dissolve in it; as a result more CO<sub>2</sub> can be stored within the reservoir.

When CO<sub>2</sub> injection was started, the cumulative water production was about 0.4 x10<sup>6</sup> m<sup>3</sup> in 2006 for Run 5a and it was 0.6 x10<sup>6</sup> m<sup>3</sup> in 2016 for run 5c. The cumulative water production for Run 5c was around 0.7 x10<sup>6</sup> m<sup>3</sup>

which is higher than the value of Run 5a ( $0.55 \times 10^6 \text{ m}^3$ ) at the end of simulation runs. This might be the activity of aquifer system, during production period, which is connected to the bottom of the reservoir.

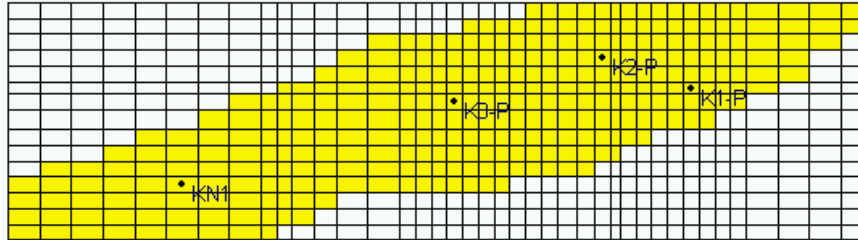


Figure 6.32 Location of injection and production wells, Run5, CO2 EOR/SEQ.

Table 6.6 Comparison of simulations, Run 5, CO<sub>2</sub> EOR/SEQ.

CO <sub>2</sub> injection period	Run 5a (Injection in 2006)		Run 5b (Injection in 2011)		Run 5c (Injection in 2016)	
	Oil recovery %OOIP	CO <sub>2</sub> Produced/injected %	Oil recovery %OOIP	CO <sub>2</sub> Produced/injected %	Oil recovery %OOIP	CO <sub>2</sub> Produced/injected %
0	23.3		24.8		26.1	
15	31.5	26	32.3	23	33.1	22
20	31.5	20	32.3	18	33.1	17

Table 6.7 Cumulative oil and gas (CO<sub>2</sub>) productions, Run5, CO<sub>2</sub> EOR/SEQ

CO <sub>2</sub> injection period	Run 5a (Injection in 2006)		Run 5b (Injection in 2011)		Run 5c (Injection in 2016)	
	Cum. Oil Prod. m <sup>3</sup>	Cum. Gas Prod. m <sup>3</sup>	Cum. Oil Prod. m <sup>3</sup>	Cum. Gas Prod. m <sup>3</sup>	Cum. Oil Prod. m <sup>3</sup>	Cum. Gas Prod. m <sup>3</sup>
0	258791		275841		290994	
15	350896	1.70E+07	359228	1.49E+07	368815	1.41E+07
20	350896	1.70E+07	359228	1.49E+07	368815	1.41E+07

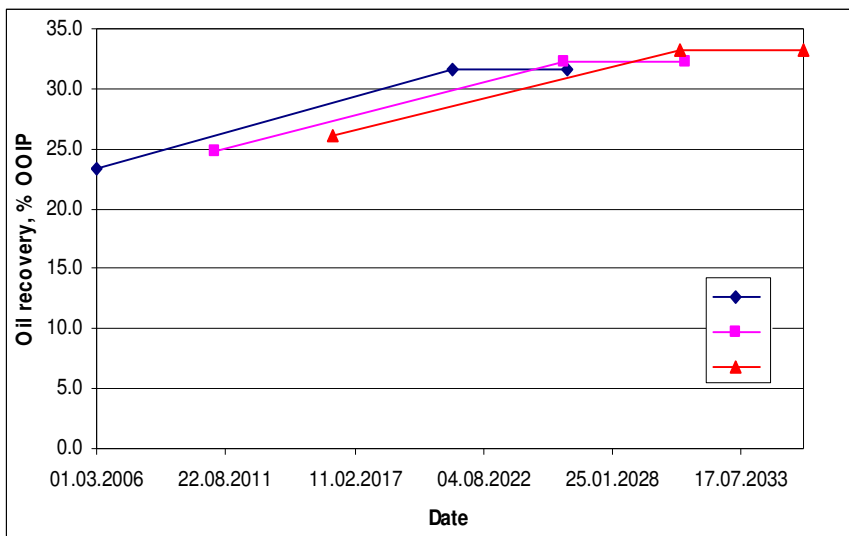


Figure 6.33 Oil recoveries vs. date, Run 5, CO<sub>2</sub> EOR/SEQ.

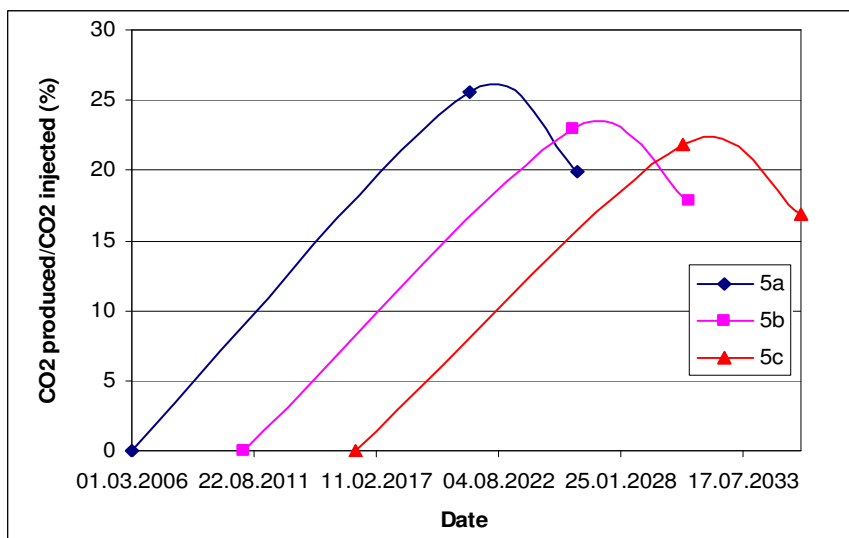


Figure 6.34 CO<sub>2</sub> produced/CO<sub>2</sub> injected vs. date, Run 5, CO<sub>2</sub> EOR/SEQ.

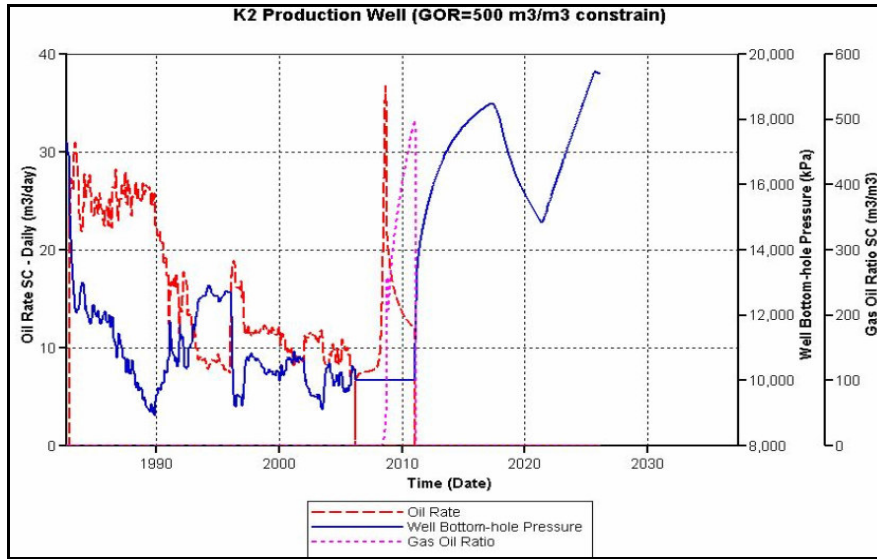


Figure 6.35 Oil production rate of the well K2, Run 5a, CO<sub>2</sub>/EOR SEQ.

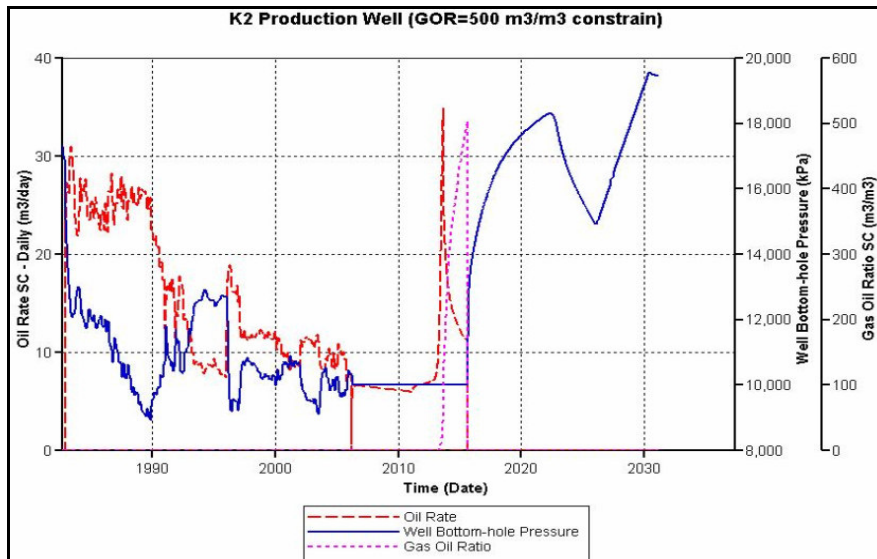


Figure 6.36 Oil production rate of the well K2, Run 5b, CO<sub>2</sub>/EOR SEQ.

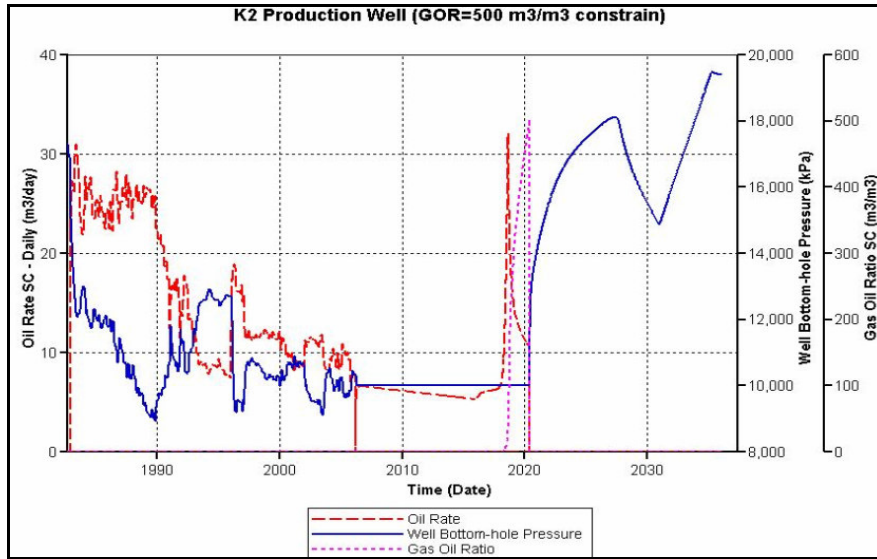


Figure 6.37 Oil production rate of the well K2, Run 5c, CO<sub>2</sub>/EOR SEQ.

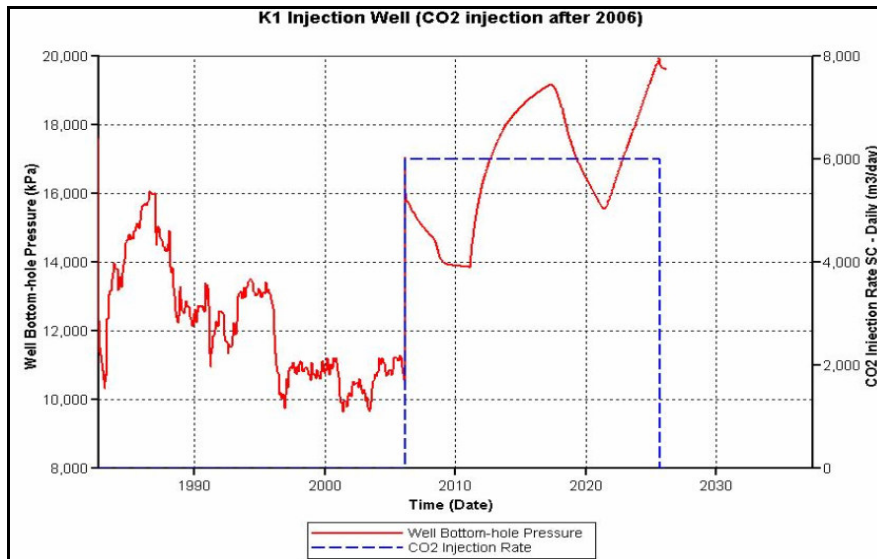


Figure 6.38 Well bottom hole pressure and CO<sub>2</sub> injection rate of Well K1, Run 5a, CO<sub>2</sub> EOR/SEQ.

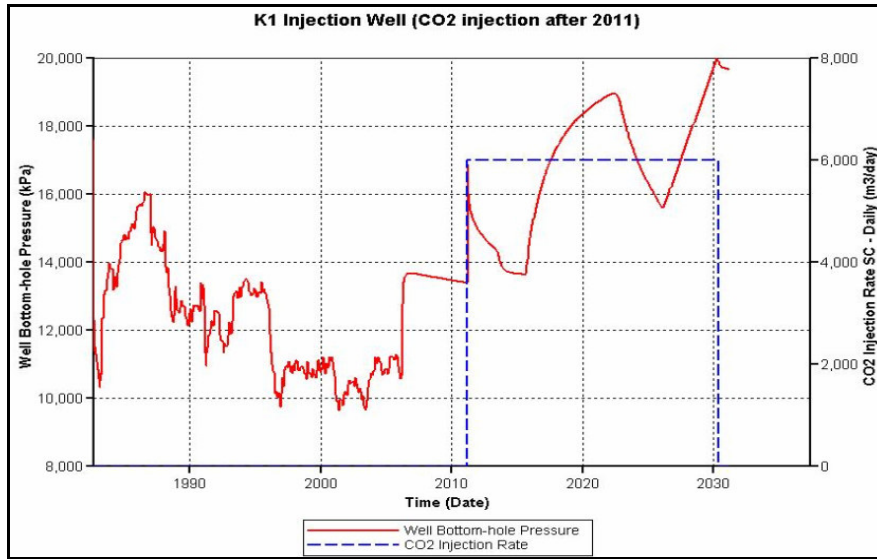


Figure 6.39 Well bottom hole pressure and CO<sub>2</sub> injection rate of Well K1, Run 5b, CO<sub>2</sub> EOR/SEQ.

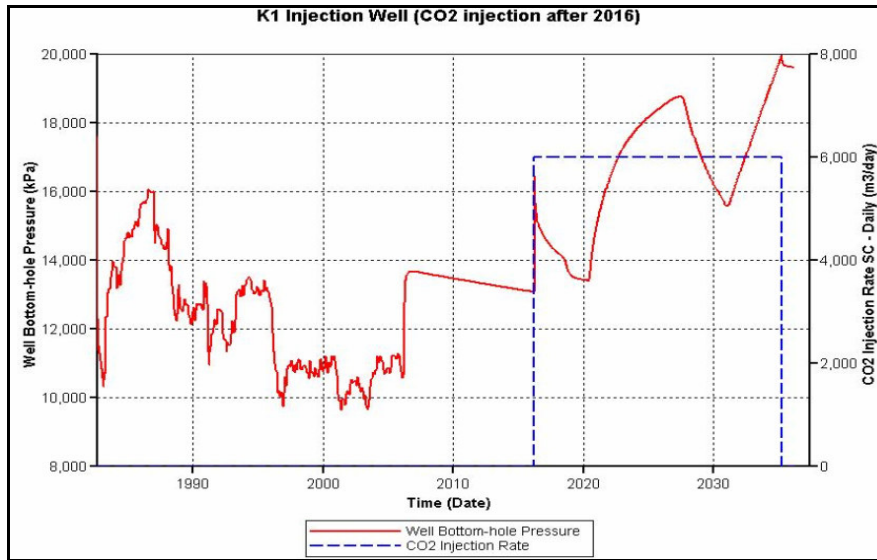


Figure 6.40 Well bottom hole pressure and CO<sub>2</sub> injection rate of Well K1, Run 5c, CO<sub>2</sub> EOR/SEQ.

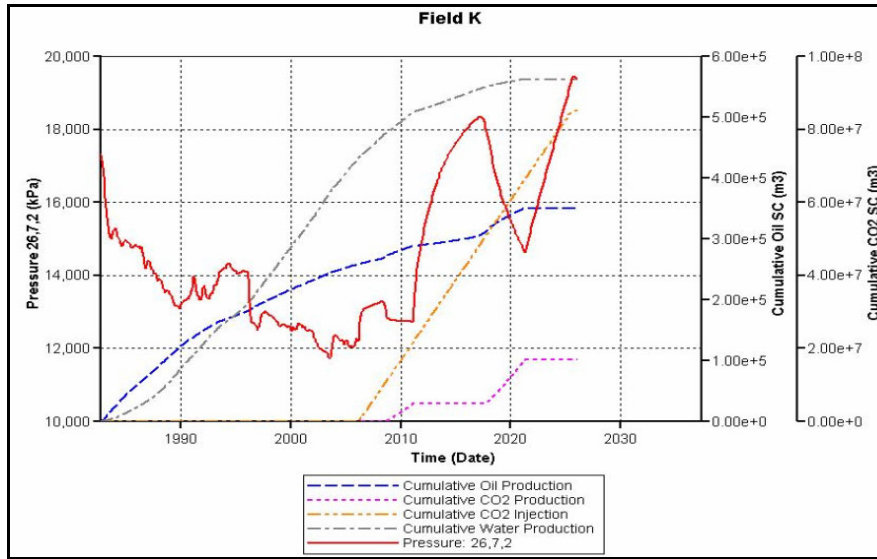


Figure 6.41 Field injection and production summary, Run5a, CO<sub>2</sub> EOR/SEQ.

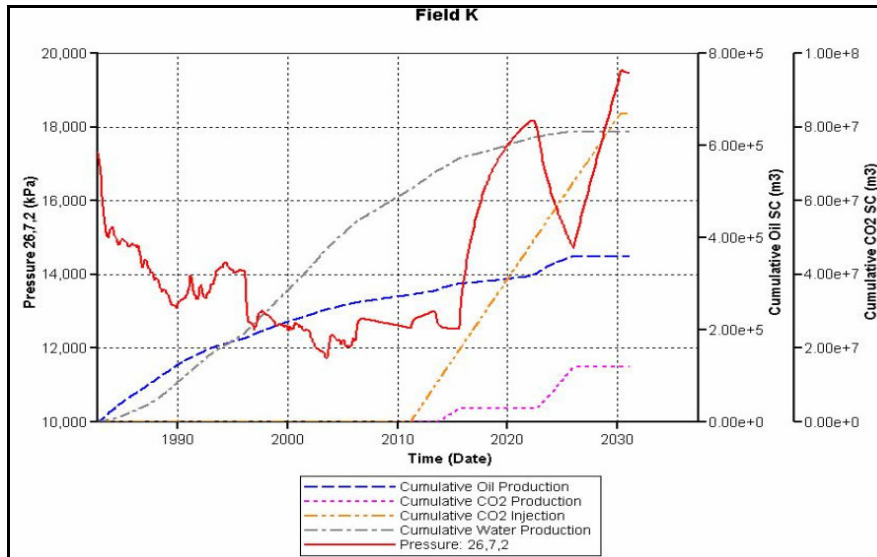


Figure 6.42 Field injection and production summary, Run5b, CO<sub>2</sub> EOR/SEQ.

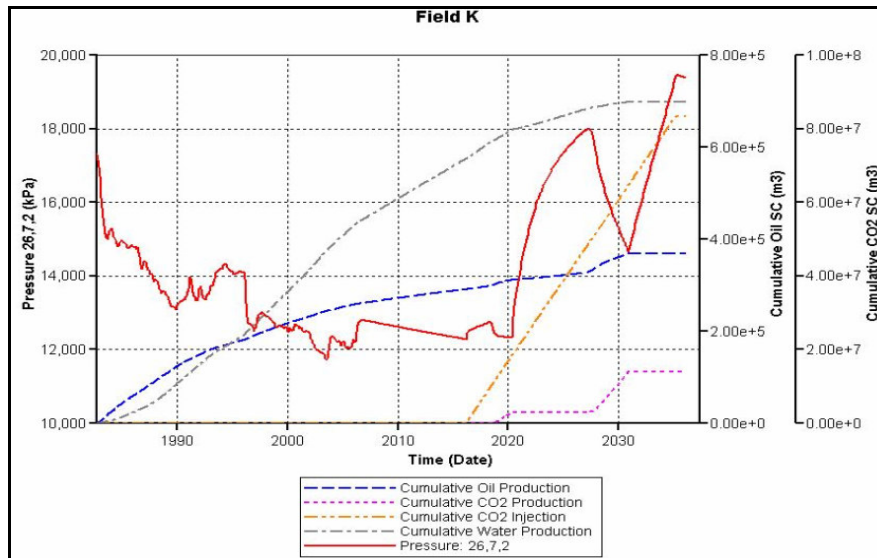


Figure 6.43 Field injection and production summary, Run5c, CO<sub>2</sub> EOR/SEQ.

#### 6.4.6 Run 6 Field Development & CO<sub>2</sub> EOR/SEQ

After simulating the scenario in Runs 4 and 5, it was decided to create Run 6 for increasing oil production and storing CO<sub>2</sub>. Thus GOR constraint was taken as 500 m<sup>3</sup>/m<sup>3</sup>. Three new wells (KN1, KN2 and KN3) were drilled. Locations of the existing and new wells are shown in Figure 6.44. In this Run, to get maximum oil recovery and increase amount of stored CO<sub>2</sub>, the locations of injection and production wells were redefined. Another new injection well (KN3) was drilled on the other side of the fault, and CO<sub>2</sub> injection was started at the corners of the reservoir after 2016.

In 2006, new production wells KN1 and KN2 were put on production in addition to existing K1, K2, K3 and abandoned K5 and K9 wells. Oil production was continued till 2016. After 2016, K1 and KN1 wells were converted to injection wells and new injection well KN3 was opened for injection at the north of the fault.

The results of Run 6 are given in Figures 6.45 through 6.49. Table 6.8 summarizes the results of simulation in terms of cumulative oil production, cumulative CO<sub>2</sub> injection and production. Oil recovery was obtained as 43 % of OOIP. This was the maximum recovery obtained among all other runs.

The difference between the injected and produced CO<sub>2</sub> was calculated as 8.4x10<sup>6</sup> sm<sup>3</sup> for Run 3, 23.2x10<sup>6</sup> sm<sup>3</sup> for Run 4a, 52.9x10<sup>6</sup> sm<sup>3</sup> for Run 4b, 36.6x10<sup>6</sup> sm<sup>3</sup> for Run 4c, 68.2x10<sup>6</sup> sm<sup>3</sup> for Run 5a, 68.8x10<sup>6</sup> sm<sup>3</sup> for Run 5b, 69.3x10<sup>6</sup> sm<sup>3</sup> for Run 5c and 92.3x10<sup>6</sup> sm<sup>3</sup> for Run 6. The results of Run 6 revealed the importance of optimizing oil recovery and stored amount of CO<sub>2</sub> with a proper field development by selecting appropriate locations and numbers for the injection and production wells.

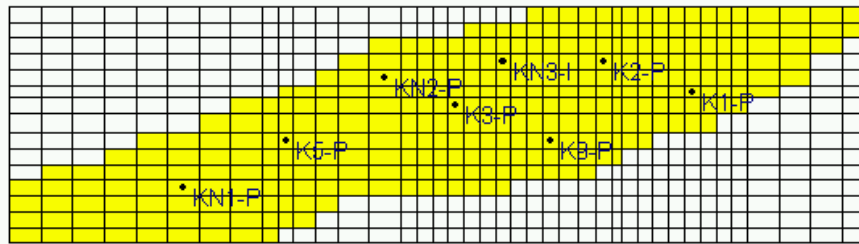


Figure 6.44 Location of injection and production wells, Run6, CO<sub>2</sub> EOR/SEQ.

Table 6.8 Comparison of simulation, Run 6, field development & CO<sub>2</sub>/EOR SEQ.

Cum. Oil Prod.		Oil Recovery	Cum. CO <sub>2</sub> Inj.		Cum. CO <sub>2</sub> Prod.		CO <sub>2</sub> Prod/Inj
sm <sup>3</sup>	STB	%OOIP	sm <sup>3</sup>	SCF	sm <sup>3</sup>	SCF	%
483,244	3,039,605	43	1.22E+08	4.30E+09	2.95E+07	1.04E+09	24

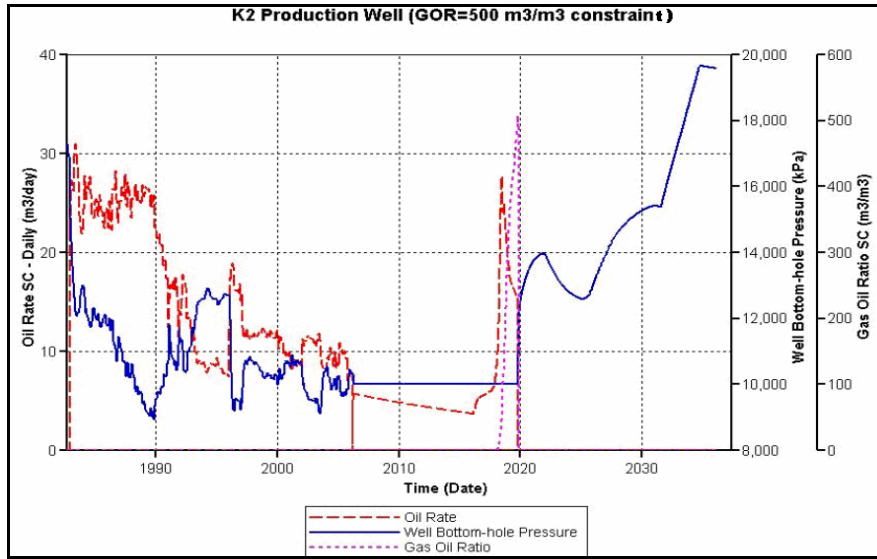


Figure 6.45 Oil production rate of the well K2, Run 6, field development & CO<sub>2</sub>/EOR SEQ.

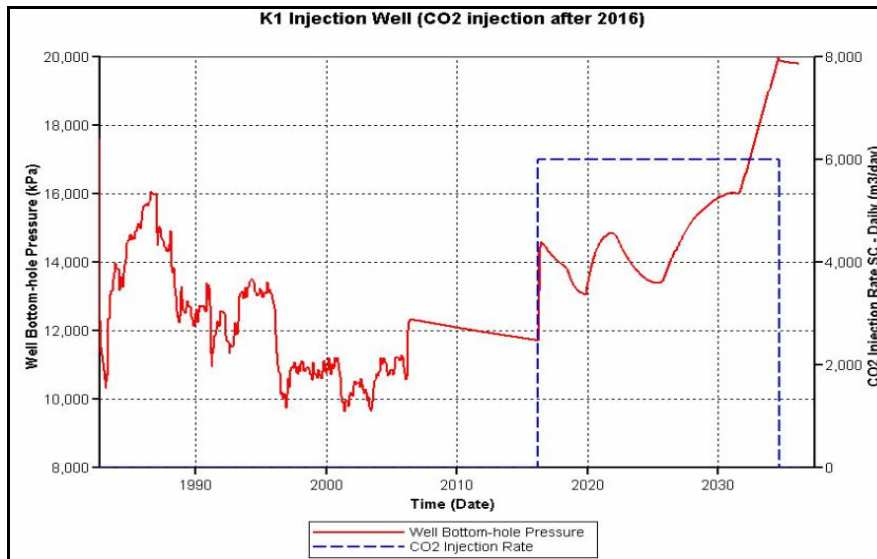


Figure 6.46 Well bottom hole pressure and CO<sub>2</sub> injection rate of Well K1, Run 6, field development & CO<sub>2</sub> EOR/SEQ.

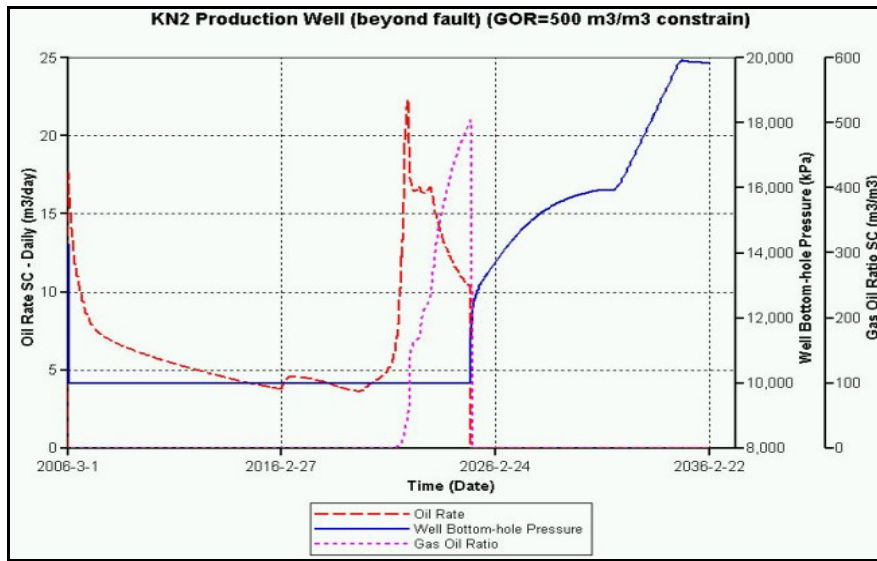


Figure 6.47 Oil production rate of the well KN2, Run 6, field development & CO<sub>2</sub>/EOR SEQ.

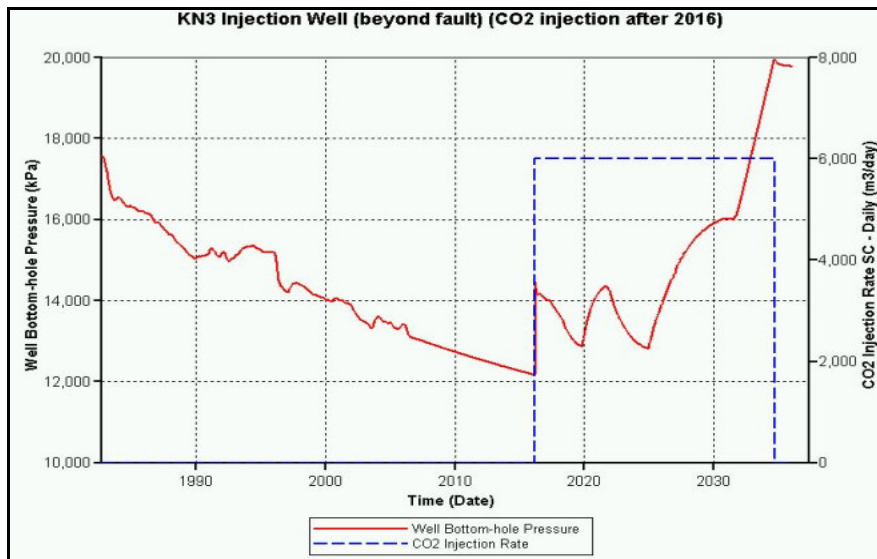


Figure 6.48 Well bottom hole pressure and CO<sub>2</sub> injection rate of Well KN3, Run 6, field development & CO<sub>2</sub> EOR/SEQ.

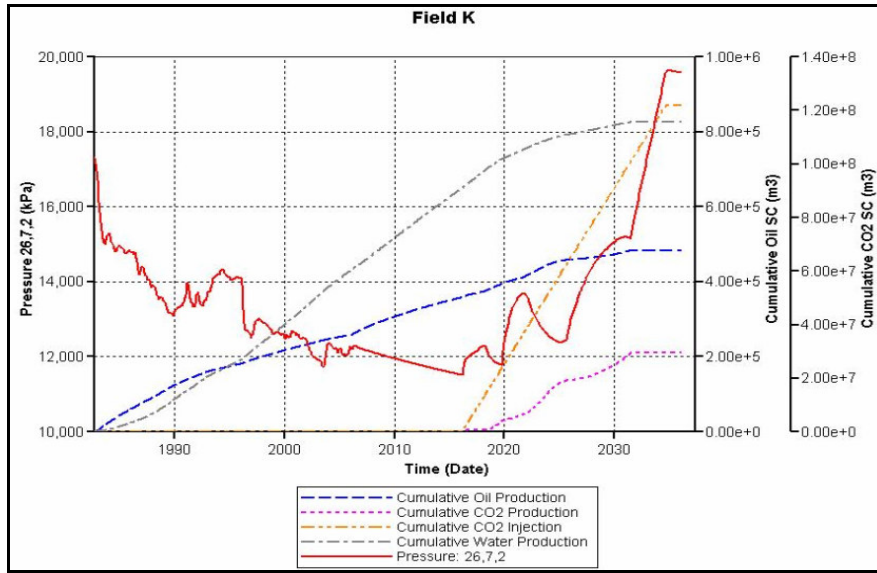
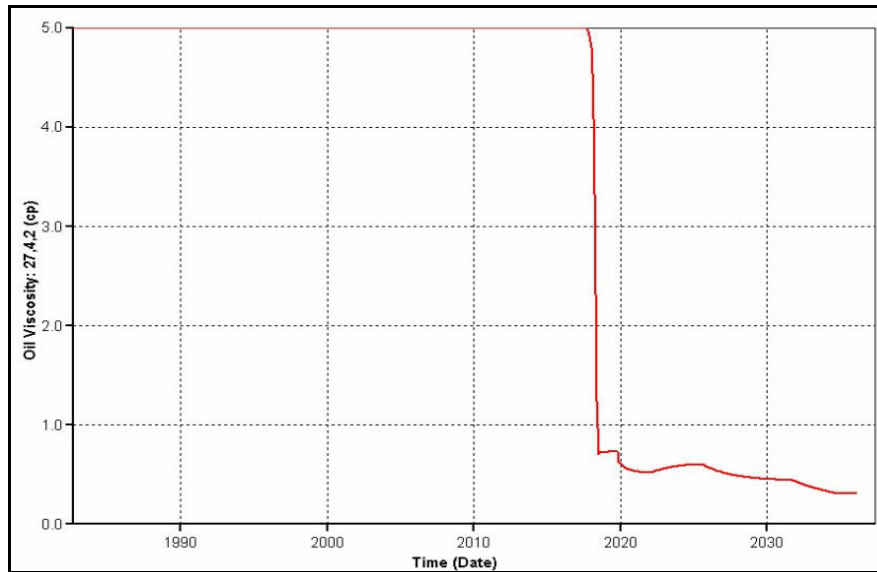


Figure 6.49 Field injection and production summary, Run 6, field development & CO<sub>2</sub>/EOR SEQ.

Figure 6.50 represents the change in oil viscosity after CO<sub>2</sub> injection. It was obvious that oil viscosity significantly was decreased by a factor of ten which improved the oil mobility as a result the oil recovery was increased.



**Figure 6.50 Change in oil viscosity after CO<sub>2</sub> injection, Run 6 field development & CO<sub>2</sub>/EOR SEQ.**

Figures 6.51 and 6.52 reveal that CO<sub>2</sub> propagation is upward due to buoyancy and gravitational effects. Thus as CO<sub>2</sub> migrated to the upper zones of the formation, it dissolved more in oil and water which resulted in the development of CO<sub>2</sub> sink at the top of the formation. At this point cap rock integrity could be critical. Although it was beyond the scope of this study, cap rock integrity could be studied for the continuation of this work.

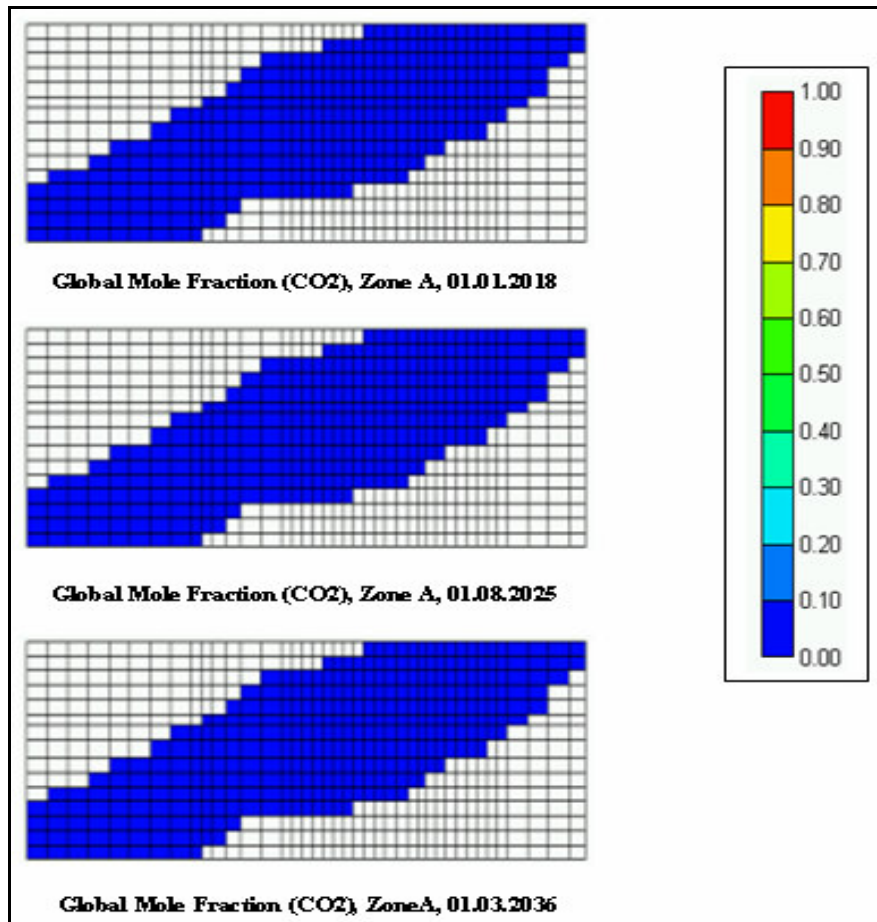


Figure 6.51 CO<sub>2</sub> propagation in Zone A, Run 6, field development & CO<sub>2</sub>/EOR SEQ.

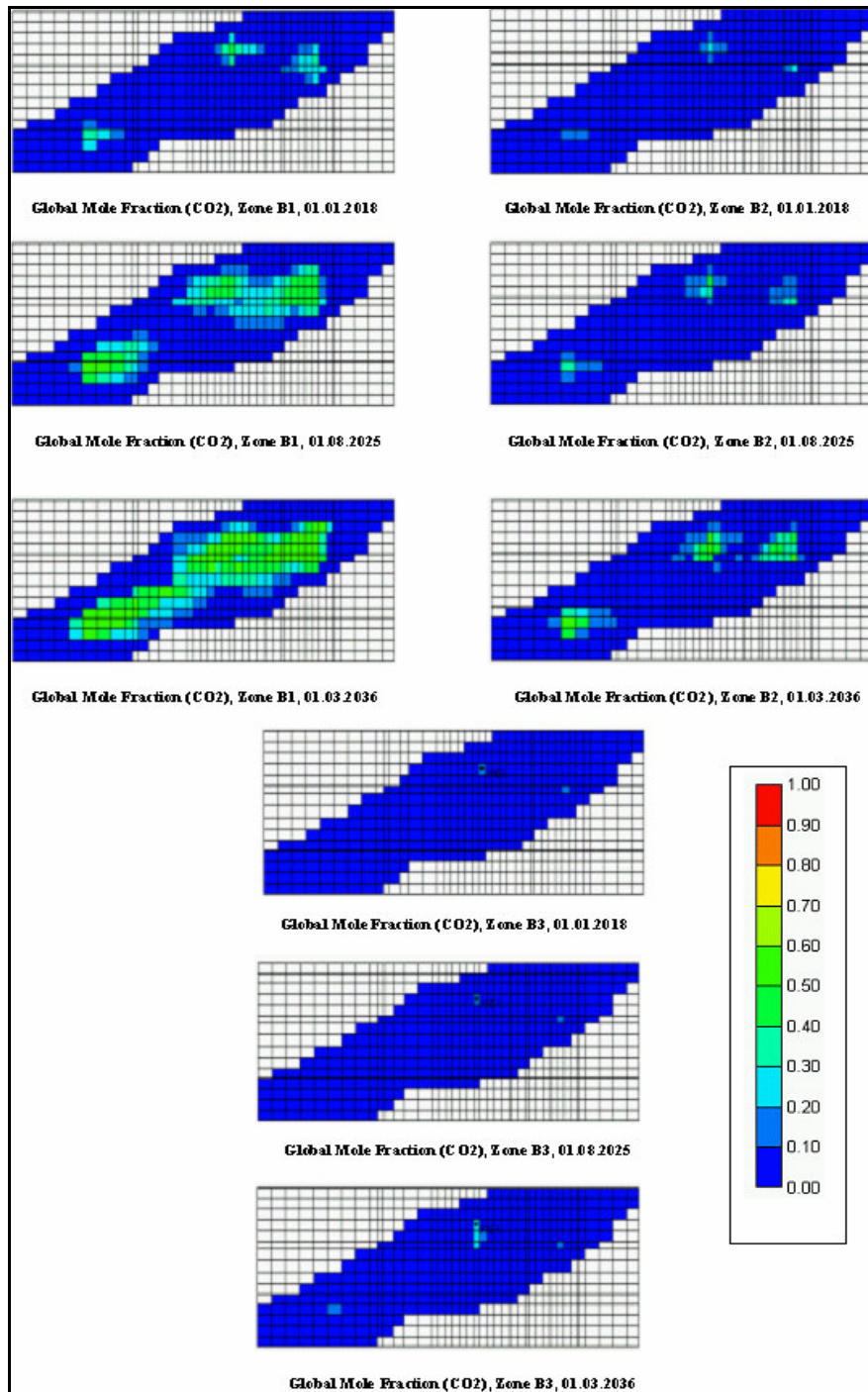


Figure 6.52 CO<sub>2</sub> propagation in layers of Zone B, Run 6, field development & CO<sub>2</sub>/EOR SEQ.

## CHAPTER 7

### CONCLUSIONS

In CO<sub>2</sub> EOR technique, the main purpose is to maximize oil recovery with the minimum injected amount of CO<sub>2</sub>, while a maximum amount of CO<sub>2</sub> is aimed to store in a sequestration process. Thus, enhancing oil recovery in a sequestration is an optimization process that requires careful analysis.

From this point of view, different scenarios were developed to maximize the amount of CO<sub>2</sub> stored while increasing the recovery of oil at the same time. The compositional simulator CMG/STARS software was used to study CO<sub>2</sub> storage and flooding potential of an oil reservoir located in southeast of Turkey. History matching study was utilized to verify simulation results with field data.

The following conclusions were drawn;

1. Monte Carlo simulation was used to estimate OOIP, probabilistically with the parameters having some sort of uncertainty. The OIIP was estimated as  $7 \times 10^6$  stb that was very close to  $7.5 \times 10^6$  stb given by TPAO and  $7.3 \times 10^6$  stb acquired from CMG.
2. CO<sub>2</sub> emission from an average power plant (500 MW) is 250 MMSCF/day. Cumulative CO<sub>2</sub> injection into the reservoir was 300 MMSCF (Run 3) for a period of 8 months from 5 wells. 20% additional oil recovery of OOIP was obtained by starting to CO<sub>2</sub> injection (Run 6) after 2006. Thus, Field K was decided to be not suitable for CO<sub>2</sub>

storage but appropriate for enhanced oil recovery while CO<sub>2</sub> was injected into the reservoir.

3. When no GOR constraint was defined (Run 4a), the oil recovery was found as 39% of OOIP, but 82% of injected CO<sub>2</sub> were produced. Thus, high CO<sub>2</sub> and water production may induce problems such as corrosion and hydrate formation in the well and increase the cost of process with the need of installing gas recycling and water treatment units.
4. When CO<sub>2</sub> was injected in earlier times (run 5a), the oil recovery was not higher than that of late CO<sub>2</sub> injection runs (Runs 5b and 5c). But relatively higher amount of injected CO<sub>2</sub> was kept within the reservoir for the late CO<sub>2</sub> injection runs. More water encroachment was occurred between the period of production and injection, as a result more CO<sub>2</sub> might be dissolved in oil and water.
5. After implementing CO<sub>2</sub> injection into the wells, CO<sub>2</sub> migrated to the upper zones of the formation; it dissolved more in oil and water which resulted in the development of CO<sub>2</sub> sink at the top of the formation (Zone B1) and hydrodynamically trapped at the bottom of impermeable rock (Zone A).
6. When CO<sub>2</sub> was injected, the oil viscosity was decreased by a factor of ten which improved the oil mobility; as a result, the oil recovery was enhanced.

7. Well defined production and injection scenario (Run 6) was critical issue for the optimization of CO<sub>2</sub> EOR/Sequestration process such that field development strategy by selecting appropriate conditions and locations for the injection and production wells increased the oil recovery and the stored amount of CO<sub>2</sub>.

## REFERENCES

1. Houghton, J.T., Filho, L.G.M., Callander, B. A., Harris, N., Kattenberg, A. and Maskell, K.: "Climate Change 1995: The Science of Climate Change", Cambridge University Press, 1996.
2. Jones, P. D. and Briffa, K. B.: "Global Surface Air Temperature Variations during the Twentieth Century, Part I: Spatial, Temporal and Seasonal Details", *The Holocene* 2, 1992, 165–179.
3. Sengul M.: "CO<sub>2</sub> Sequestration - A Safe Transition Technology", paper SPE 98617, presented at SPE International Health, Safety & Environment Conference, Abu Dhabi, UAE, 2-4 April 2006.
4. McCarthy J.J., Canziani, O.F., Leary, N.A., Dokken D.J., White K.S.: "IPCC 2001b, Climate Change 2001: Impacts, Adaptation and Vulnerability, Contribution of Working Group II to the Third Assessment Report of the Intergovernmental Panel on Climate Change", Cambridge University Press, 2001.
5. United Nations Environment Programme and the Climate Change Secretariat (UNFCCC): "Climate Change Information Kit", July 2002, Available at [http:// unfccc.int](http://unfccc.int) (accessed April, 2006).
6. van 't Veld, K. and Plantinga A.: "Carbon Sequestration or Abatement? The Effect of Rising Carbon Prices on the Optimal Portfolio of Greenhouse-gas Mitigation Strategies", *Journal of Environmental Economics and Management*, Vol. 50, Issue 1, 2005.

7. GCEP Technical Report 2003-2004: "Geologic CO<sub>2</sub> Sequestration Project Results", 2004, Available at <http://gcep.stanford.edu> (accessed April, 2006).
8. Houghton, J.T., Ding, Y., Griggs, D.J. Noguera, M., van der Linden, P.J. and Dai, X.: "Climate Change 2001: The Scientific Basis", Cambridge University Press, 2001, Available at <http://www.ipcc-wg.org/index.html> (accessed April, 2006).
9. Fact sheet US Delegation to the 3<sup>rd</sup> Conference of the Parties: "Six greenhouse gases", United Nations Committee on Climate Change, Kyoto, December 5, 1997.
10. International Energy Agency(IEA) 2000: "CO<sub>2</sub> Emissions from Fuel Combustion 1971–1998", Paris, 2000.
11. Galeotti, M. and Lanza, A.: "Richer and Cleaner: A study on Carbon Dioxide Emissions in Developing Countries". Energy Policy, Vol. 27, 1999.
12. Robertson K., Loza-Balbuena I. and Ford-Robertson J.: "Monitoring and Economic Factors Affecting the Economic Viability of Afforestation for Carbon Sequestration Projects, Environmental Science & Policy, Vol. 7, 2004.
13. Akçasoy, K., Önder, F. and Güven, S.: "Statistical Evaluation of Greenhouse Gas Emissions of Turkey Between the Years of 1970 and 2010," State Institute of Statistics, Environmental Statistics Division, Ankara, Turkey.
14. Başbuğ, B.: "Modeling of Carbon Dioxide Sequestration in a Deep Saline Aquifer", M. Sc. Department of Petroleum and Natural Gas Engineering, Middle East Technical University, Ankara, Turkey, July 2005.

15. Nguyen, D.N.: "Carbon Dioxide Geological Sequestration: Technical and Economic Reviews", paper SPE 81199, presented at the SPE/EPA/DOE Exploration and Production Environmental Conference held in San Antonio, Texas, USA, 10-12 March 2003.

16. Gallo, Y.L., Couillens, P. and Manai, T.: "CO<sub>2</sub> Sequestration in Depleted Oil and Gas Reservoirs", paper SPE 74104, presented at the SPE International Conference on Health and Safety and Environment in Oil and Gas Exploration and Production, Kuala Lumpur, Malaysia, 20-22 March 2002.

17. Carbon Sequestration Research and Development, Office of Fossil Energy U.S. Department of Energy, December 1999, Available at [http://www.ornl.gov/carbon\\_sequestration](http://www.ornl.gov/carbon_sequestration) (accessed April, 2006).

18. Shafeen, A., Douglas, P., Croiset, E. and Chatzis, I.: "CO<sub>2</sub> sequestration in Ontario, Canada. Part II: cost estimation", Energy Conversion and Management, Volume 45, 2004.

19. Ambrogi, S.: "Shipping CO<sub>2</sub> Could Help Norway Hit Kyoto Target" , Reuters UK April 24, 2002, Available at <http://www.planetark.org/newsid/15643/story.htm> (accessed April, 2006).

20. Grimston M. C., Karakoussis V., Fouquet R., van der Vorst R., Pearson P. and Leach M.: "The European and Potential of Carbon Dioxide Sequestration in Tackling Climate Change", Climate Policy 1, 2001.

21. Hendriks, C.A. and Block, K.: "Underground Storage of Carbon Dioxide", Energy Conversion and Management, Volume 34, 1993.

22. Auerbach, D., J. Caulfield, E. Adams and H. Herzog.: "Impacts of Ocean CO<sub>2</sub> Disposal on Marine Life: A toxicological Assessment Integrating Constant-concentration Laboratory Assay Data with Variable-concentration Field Exposure", *Environ. Model. Assess.*, 1997.
23. Dusseault, M. B., Bachu S. and Davison B.C: "Carbon Dioxide Sequestration Potential in Salt Solution Caverns in Alberta, Canada", Solution Mining Research Institute, Fall 2001 Technical Meeting, New Mexico, USA, October 8-9-10, 2001.
24. Parson, E.A., and Keith, D.W., Fossil Fuels without CO<sub>2</sub> Emissions, *Science* 282, 1053-1054, 1998.
25. Gale, J.: "Geological Storage of CO<sub>2</sub>: What's Known, Where are the Gaps, and What More Needs to be Done", *Greenhouse Gas Control Technologies*, Volume I, 2003.
26. Franklin, M. and Orr, Jr. "Storage of Carbon Dioxide in Geologic Formations", Distinguished Author Series, September 2004.
27. Krumhansl, J. L., Stauffer, P. H., Lichtner, P. C., And Warpinski, N. R.: "Geological Sequestration of CO<sub>2</sub> in a Depleted Oil Reservoir", paper SPE 75256, presented at the SPE/DOE Improved Oil Recovery Symposium, Tulsa, Oklahoma, USA, 13-17 April 2002.
28. International Energy Agency Greenhouse Gas R&D Programme 1998: "Enhanced Coal Bed Methane Recovery with CO<sub>2</sub> Sequestration, Cheltenham, 1998.
29. Ohga, K., Gale J. and Kay Y.: "Fundamental Tests on Carbon Dioxide Sequestration into Coal Seams", *Greenhouse Gas Control Technologies* Volume I, 2003.

30. Herzog, H. and Golomb, D.: "Carbon Capture and Storage from Fossil Fuel Use", contribution to Encyclopedia of Energy, 2004.
31. Damen, K., Faaij A., van Bergen, F., Gale, J. and Lysen, E.: "Identification of Early Opportunities for CO<sub>2</sub> Sequestration—Worldwide Screening for CO<sub>2</sub>-EOR and CO<sub>2</sub>-ECBM projects", Energy, Volume 30, 2005.
32. Stalkup Jr., F. I.: "Miscible Displacement", SPE Monograph Volume 8, New York, 1984.
33. Kavscek, A.R. and Cakici, M.D.: "Geologic Storage of Carbon Dioxide and Enhanced Oil recovery: II. Cooptimization of Storage and Recovery", Energy Conversion and Management, Volume 46, 2005.
34. Holm, L. W. and Josendal, V. A.: "Mechanisms of Oil Displacement by Carbon Dioxide", J. Pet. Tech., Dec. 1974.
35. Cronquist, C.: "Carbon Dioxide Dynamic Miscibility with Light Reservoir Oils, presented at the 4th Annual U.S. DOE Symposium, Tulsa, 28-30 August, 1978.
36. Holloway, S.: "Underground Sequestration of Carbon Dioxide—A Viable Greenhouse Gas Mitigation Option", Energy, Volume 30, 2005.
37. Bennaceur, K. Et al.: "CO<sub>2</sub> Capture and Storage – A Solution Within", Schlumberger Oilfield Review, 2004.
38. Bachu, S.: "Screening and Ranking Sedimentary Basins for Sequestration of CO<sub>2</sub> in Geological Media in Response to Climate Change, Environmental Geology, 44, 2003.

39. Metz, B., Davidson O., de Coninck, H., Loos M. and Meyer L.: "IPCC Special Report on Carbon Dioxide Capture and Storage", Cambridge University Press, NY, USA, 2005.
40. Tzimas, E., Georgakaki, A., Garcia Cortes, C. and Peteves, S.D.: "Enhanced Oil Recovery using Carbon Dioxide in the European Energy System", European Commission Directorate General Joint Research Centre DG JRC, 2005.
41. Data Provided by TPAO Production Group, (written permission for the use of data), May 2006.
42. STARS 2005.10 User's Guide, CMG Computer Modelling Group, Calgary, Canada, 2005.
43. Surfer by Golden Software. Inc., <http://www.goldensoftware.com>, accessed at May 2006.
44. Saphir by Kappa Software, <http://www.kappaeng.com>, accessed at May 2006.
45. @Risk by Palisade Corporation, <http://www.palisade.com>, accessed at May 2006.
46. Fanchi, J.R.: "Principles of Applied Reservoir Simulation", Gulf Publishing Company, Houston, TX, 2001.
47. Johnson, D. E., Pile, K.E.: "Well Logging in Nontechnical Language", PennWell Publusing, Tulsa, Oklahoma, 2002.
48. Pittman, Edward D., "Porosity, Diagenesis and Productive Capability of Sandstone Reservoirs", SEPM Special Publication No. 26, 159-173 March 1979.

49. Lasater, J.A.: "Bubble Point Pressure Correlation", Trans. AIME, 213, 1958.

50. Mungan, N., and Johansen, R.T.: "Fundamental Aspects of Carbon Dioxide Flooding", World Oil, August, 1981.

# APPENDIX A

## A.1 Drill Stem Test (DST) Results

Table A.1 DST Input Data (1946-1963 m)

$t_p = 86.7$  min.  
 $q = 783$  bpd  
 $\mu = 5$  cp  
 $B_o = 1.03$  rb/b  
 $h_{net} = 29.52$  ft

Period	Time	Pressure	Period	Time	Pressure
	hour	psig		hour	psig
1. Flow	0,000	182	2. Flow	1,794	446
	0,120	242		1,963	457
	0,241	286		2,131	503
	0,361	312		2,300	548
	0,482	348		2,468	593
	0,602	384		2,637	636
1. Shut in	0,721	2024	2. Shut in	2,810	2096
	0,840	2181		2,984	2221
	0,960	2259		3,157	2284
	1,079	2308		3,331	2324
	1,198	2339		3,504	2347
	1,317	2363		3,677	2368
	1,436	2381		3,851	2383
	1,556	2396		4,024	2396
	1,675	2407		4,198	2405
1,794	2416	4,371	2412		

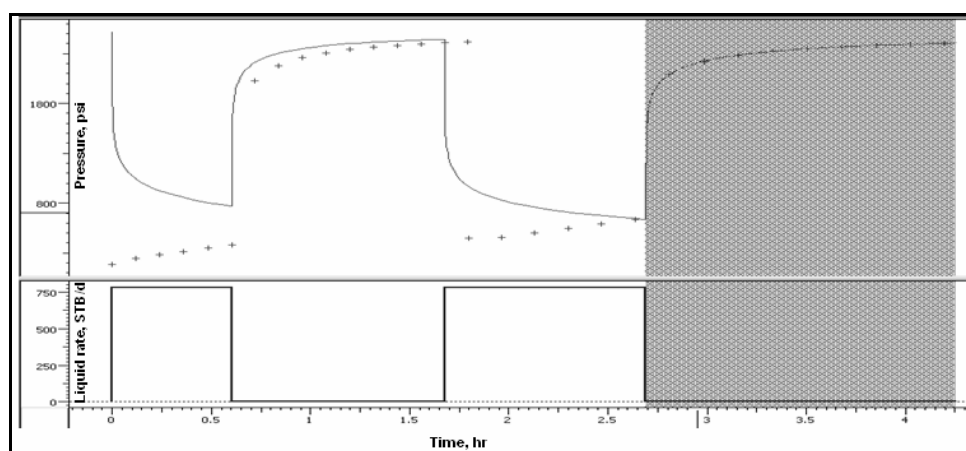


Figure A.1 History plot from DST data

**Table A.2 Results from DST data by SAPHIR program**

Name	Value	Unit
Selected Model		
Model Option	Standart Model	
Well	Storage+Skin	
Reservoir	Homogenous	
Boundary	Infinite	
Results		
C	2.23E-12	bbl/psi
Skin	0.381	---
Pi	2518.95	psi
k.h	1660	md.ft
k	56.2	md
Rinv	76	ft
Test.Vol.	27128.3	barrels

## A.2 Estimating Minimum Miscibility Pressure (MMP)

MMP is highly dependent on the oil composition, pressure and temperature. Light oil with an API gravity of 32° has a molecular weight of 200 (Figure A.2) and MMP for CO<sub>2</sub> was obtained as 2150 psi from Figure A.3. Reservoir temperature is 148 °F.

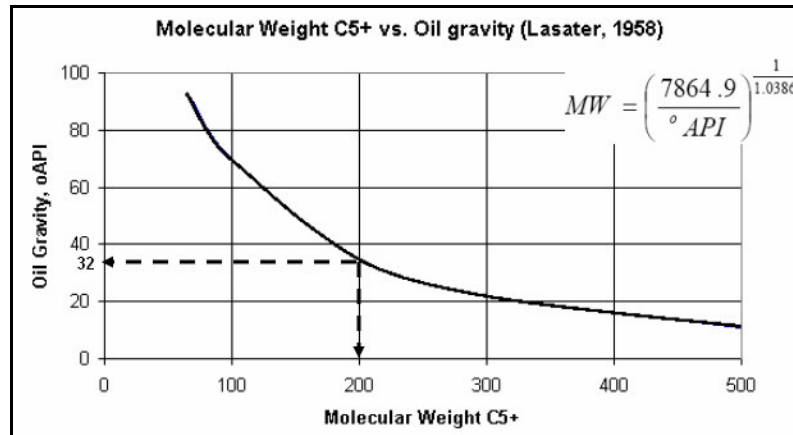


Figure A.2 Molecular weight vs. Oil gravity [49]

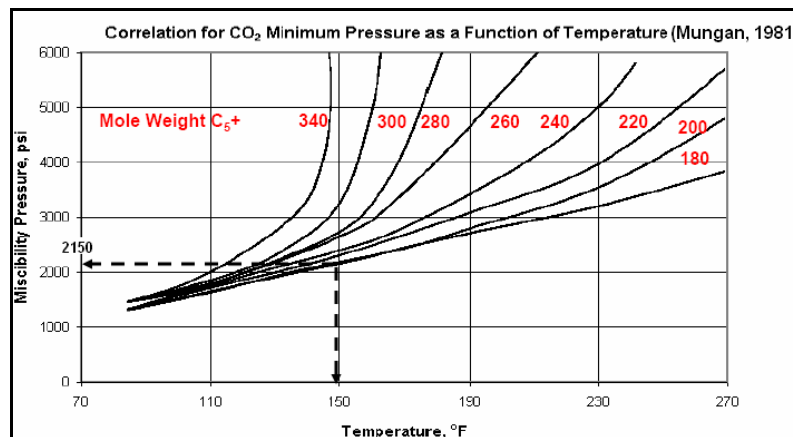


Figure A.3 Minimum miscibility pressure vs. temperature [50]

MMP was also calculated by using equation 2.1 [35]. It was found as 1986 psi. This is lower than 2150 psi. If the molecular weight was 214.4 and mole fractions of CH<sub>4</sub> and N<sub>2</sub> was zero, the MMP could be calculated as 2150 psi or if the molecular weight was 200 and mole fractions of CH<sub>4</sub> and N<sub>2</sub> was 10 percent, the MMP could be calculated as 2150 psi. The reason might be the presence of CH<sub>4</sub> and N<sub>2</sub> fractions and the change in molecular weight of C<sub>5+</sub> fractions. Therefore these values should be well known data for estimating MMP with equation 2.1.

### A.3 Well Logging Interpretation Results

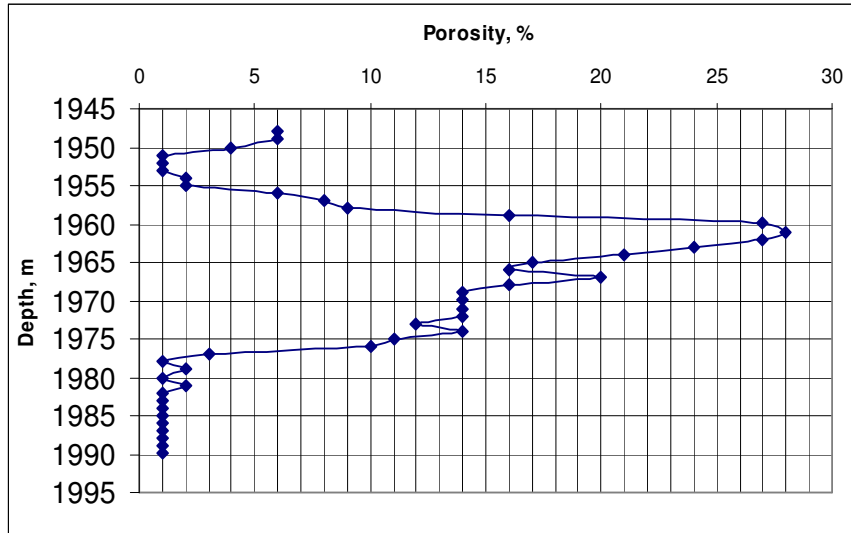


Figure A.4 Well K1 porosity vs. depth



Figure A.5 Well K1 water saturation vs. depth

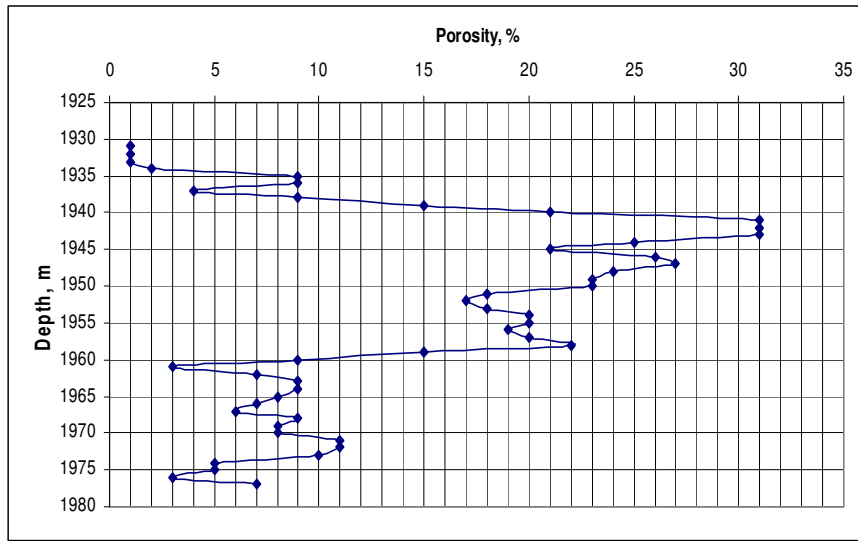


Figure A.6 Well K2 porosity vs. depth

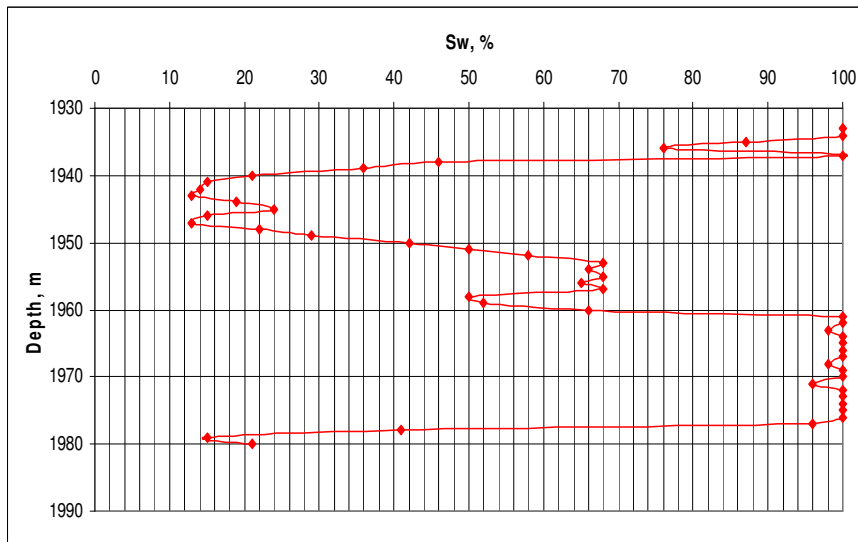


Figure A.7 Well K2 water saturation vs. depth

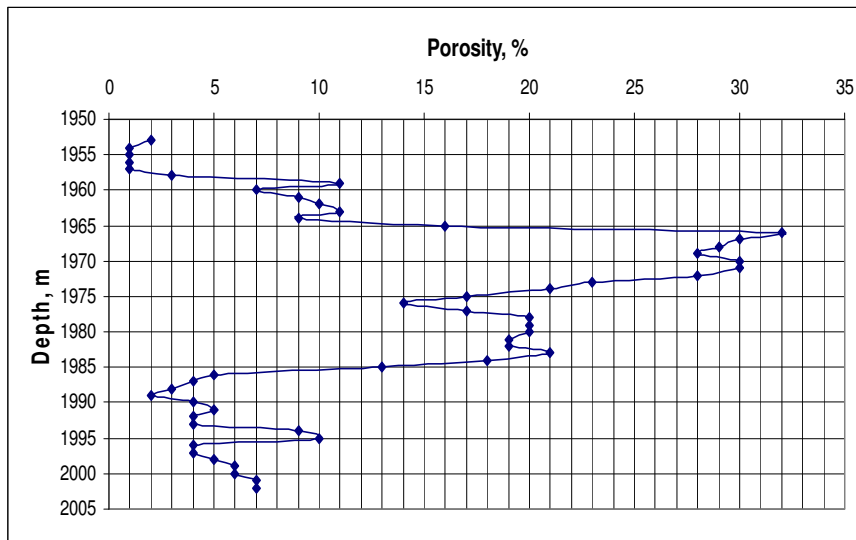


Figure A.8 Well K3 porosity vs. depth

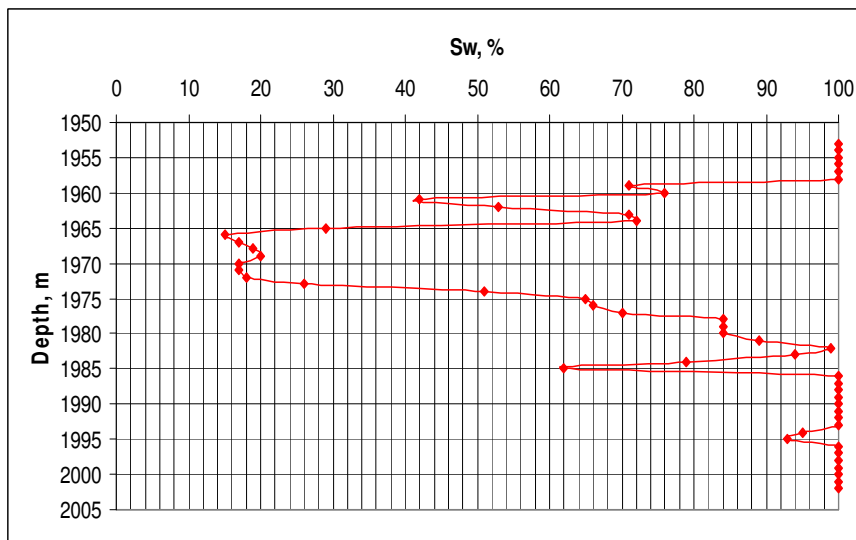


Figure A.9 Well K3 water saturation vs. depth

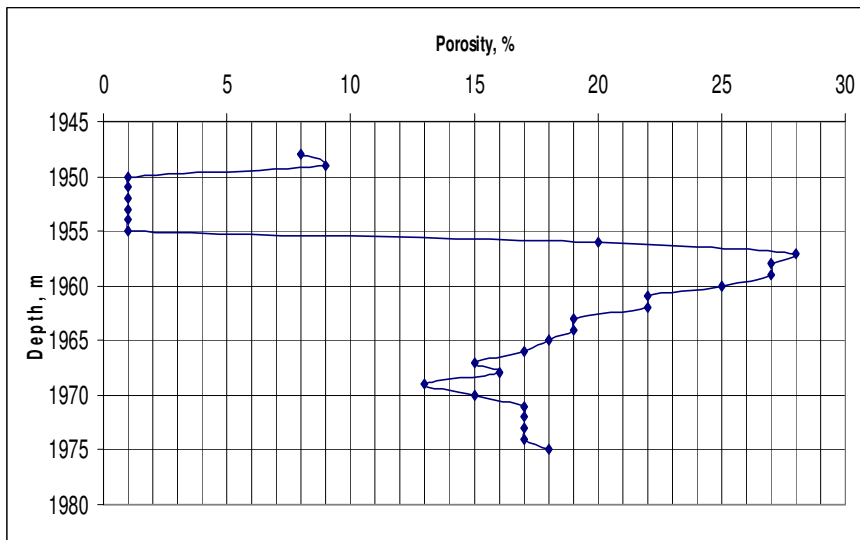


Figure A.10 Well K9 porosity vs. depth

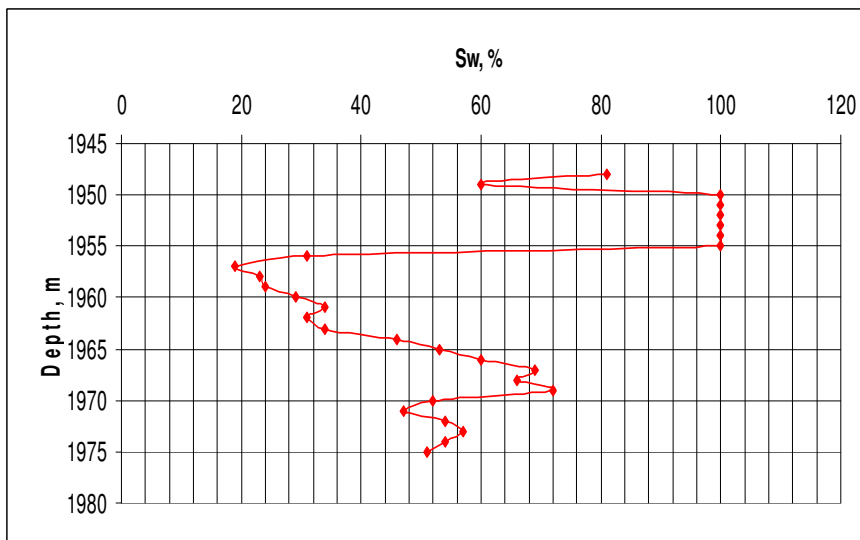


Figure A.11 Well K9 water saturation vs. depth

# APPENDIX B

## B.1 Monte Carlo Simulation Results

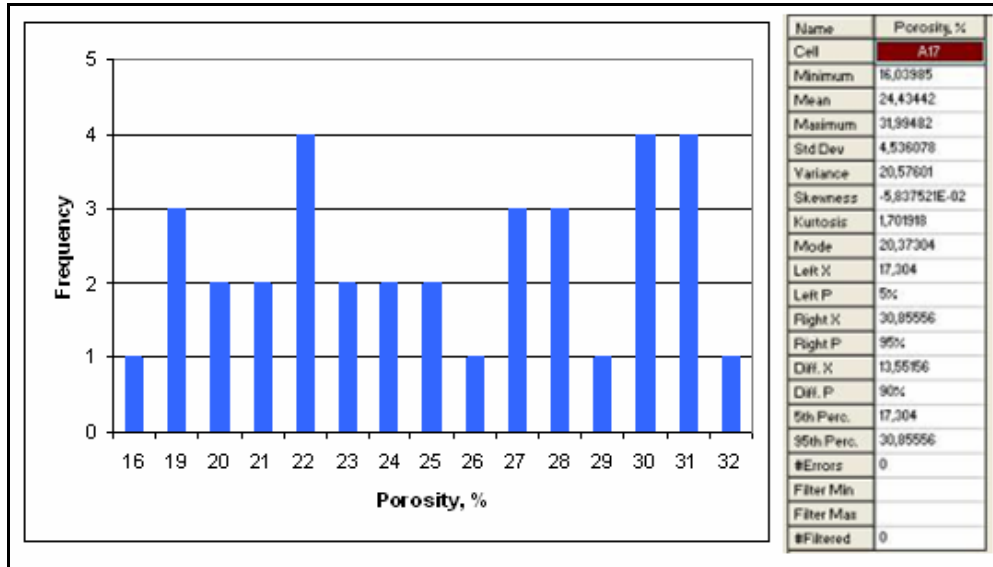


Figure B.1 Porosity histogram of zone B

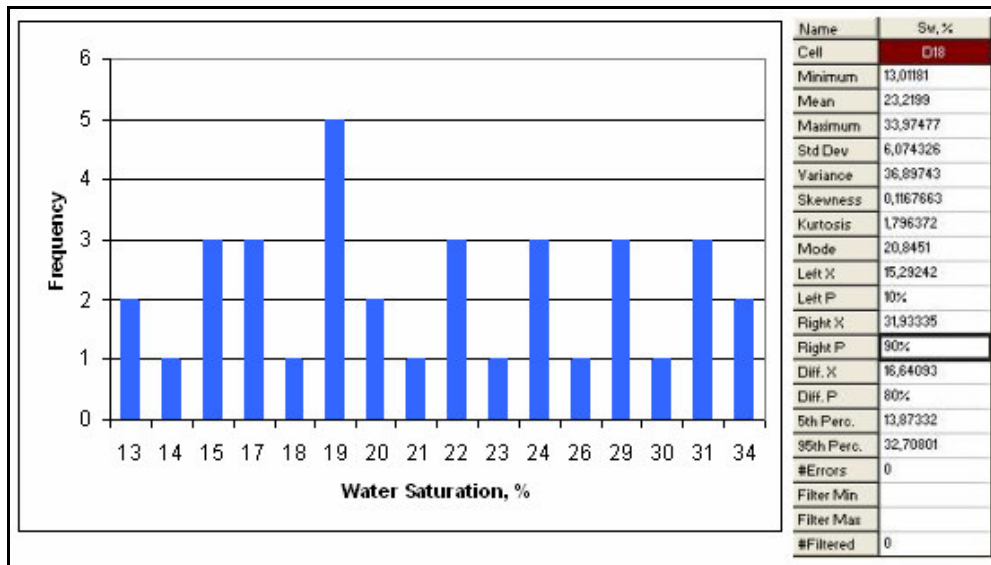


Figure B.2 Water saturation histogram of zone B

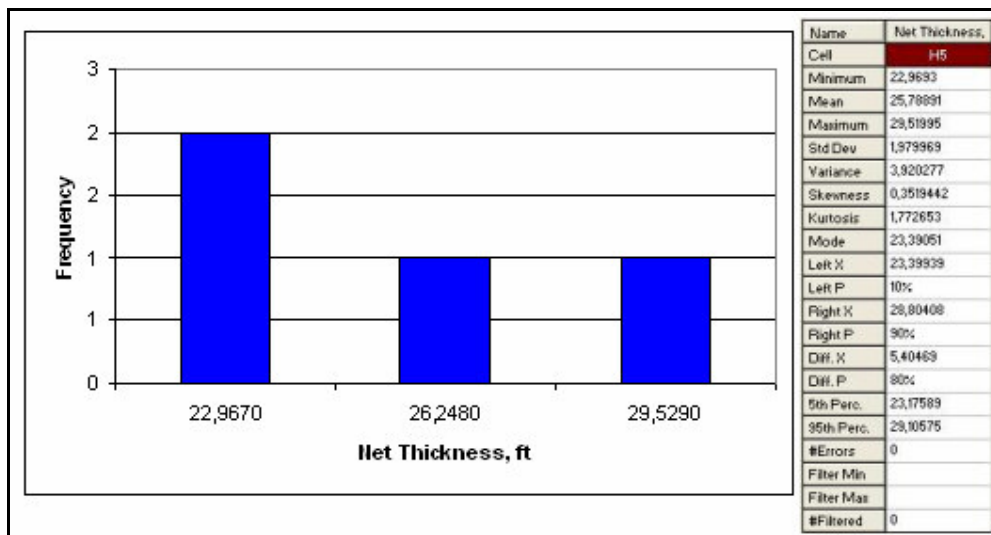


Figure B.3 Net thickness histogram of zone B

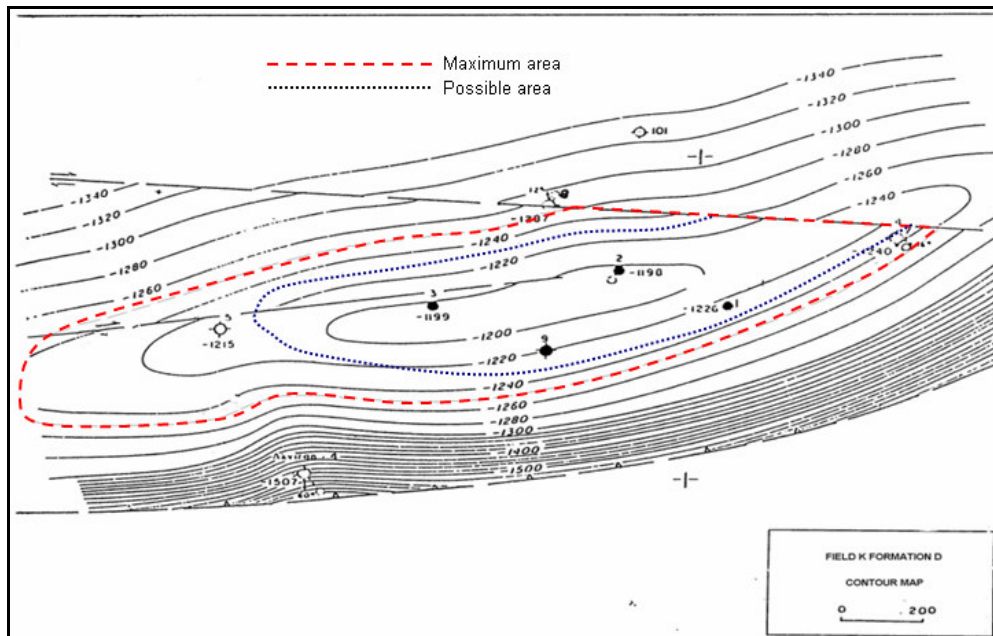


Figure B.4 Maximum and possible area of the field K

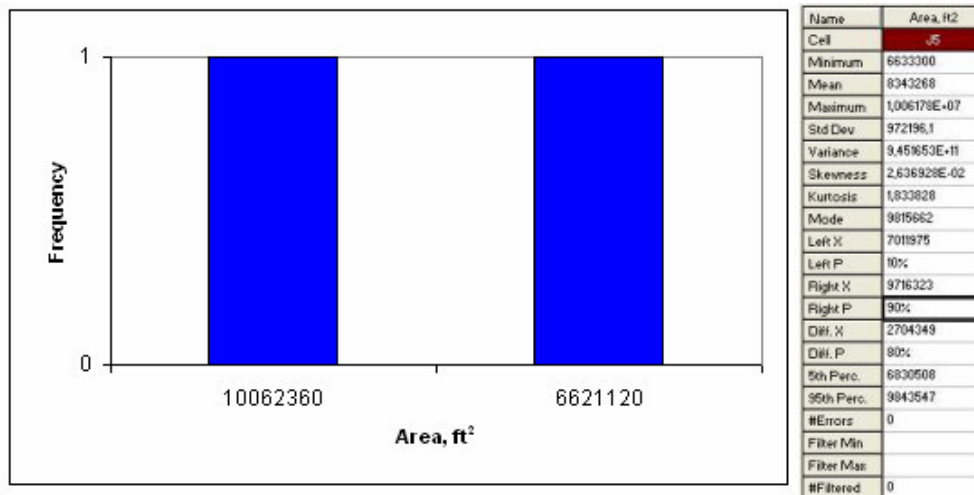


Figure B.5 Area histogram of the field (maximum and minimum)

**Table B.1 Summary statistics of Monte Carlo simulation**

	Name	Cell	Minimum	Mean	Maximum	s1	p1	s2	p2	s2-s1	p2-p1	Errors
Output 1	OOIP	M1	3306861	6988965	1,240533E+07	4811369	10%	9435680	90%	4624312	80%	0
Input 1	Net Thickness, ft	H5	22,9693	25,78891	29,51995	23,39939	10%	28,80408	90%	5,40469	80%	0
Input 2	Area, ft <sup>2</sup>	J5	6633300	8343268	1,006178E+07	7011975	10%	9716323	90%	2704349	80%	0
Input 3	Porosity, %	A17	16,03985	24,43442	31,99482	18,06642	10%	30,42575	90%	12,35932	80%	0
Input 4	Sw, %	D18	13,01181	23,2199	33,97477	15,29242	10%	31,93335	90%	16,64093	80%	0